Integrated geophysics for mapping of quick-clay landslide-prone areas in Norway.

Guillaume Sauvin

March 21, 2014

Series of dissertations submitted to the
Faculty of Mathematics and Natural Sciences, University of Oslo
No. 1473

ISSN 1501-7710

Cover: Inger Sandved Anfinsen.
Printed in Norway: AIT Oslo AS.

Produced in co-operation with Akademika Publishing.
The thesis is produced by Akademika Publishing merely in connection with the thesis defence. Kindly direct all inquiries regarding the thesis to the copyright holder or the unit which grants the doctorate.

Contents

Preface

On the initiative of Dr. Isabelle Lecomte at NORSAR, we co-wrote this Ph.D. project and asked for financial support to four different contributors: the Norwegian Public Roads Administration, the Norwegian National Railway Administration, the Norwegian Water Resources and Energy Directorate and the International Centre for Geohazards. Following the acceptance of the project by the University of Oslo, the Ph.D. project officially started in Januray 2011. The working title of my project was relatively wide "*Integrated geophysics for mapping and monitoring of landslide-prone valley and coastal grounds in Norway*" and while progressing, the field of investigation narrowed down to landslide related to quick clay mainly. That is why we change the title for "*Integrated geophysics for mapping of quick-clay landslide-prone areas in Norway*".

This thesis presents a three-year long research study focused on geophysical investigation of highly sensitive or "quick" clay landslide prone area. Four papers including the principal results from the work accomplished during the PhD studies are presented herein and listed below. As the investigation of landslide prone area requires a close collaboration between many fields of geosciences, the research work includes a wide range of topics such as geology, geophysics and geotechnics. The aim of this thesis is to investigate the potential of geophysical methods for mapping quick-clay landslide prone site.

Summary

Quick clay is a known hazard in formerly-glaciated coastal areas in e.g., Scandinavia and Canada, and hence significant efforts are being taken to map their occurrence and extent. Quick-clay landslide prone areas are usually investigated only by geotechnical means, but recently, considerable efforts by a number of researchers have been made to investigate areas of sensitive clay using a range of geophysical techniques. Although the majority of this work has focused on measurements of electrical resistivity, other geophysical techniques (electromagnetic and seismic) have also received attention in the literature. Although it was recognized that some intrusive geotechnical investigations will always be necessary, the objective of these studies was to develop techniques to maximize the use of non-intrusive geophysical surveys.

As a result of intensive research in the past thirty years, particularly in Norway, Sweden and eastern Canada, the effects of post-depositional physical and chemical processes on the engineering properties of soft clays are now fairly well understood. The importance of geological and physico-chemical factors in the interpretation and analysis of such geotechnical problems as landslides and the settlement of structures has been clearly recognized. Therefore, following a thorough review of the physical properties of quick clays, we evaluated the potential of geophysics for quick-clay investigation in order to find a suitable, integrated and multi-disciplinary approach to improve our possibilities to accurately identify its occurrence and map its extent both vertically and laterally.

Using a number of case study, we demonstrate how geophysics can contribute to better investigate sites prone to quick-clay landsliding and advantageously complement geotechnical localized 1D soundings by providing detailed stratigraphic and quantitative information in 2D and 3D. Since geophysics does not directly provide the necessary parameters for quick-clay characterization, one as to link geophysical parameters to geotechnical ones through, e.g., empirical correlations. We therefore also explored potential correlation between geotechnical and geophysical parameters.

Having different dataset to interpret, we perform data integration using data fusion by fuzzy logic or cluster analysis. Another alternative is to directly invert all of the available experimental data using a joint inversion algorithm. The resulting model can then be interpreted more easily and with more confidence since joint-inversion reduces the inversion uncertainty of each separate methods. The joint-inversion algorithm was developed in collaboration with Flora Garofalo, Ph.D. research fellow at Politecnico di Torino, Italy.

Finally, we show how the geological model resulting from geotechnical and geophysical data integration can be used for landslide site characterization and stability assessment.

Acknowledgements

I would like to thank my supervisors Isabelle Lecomte, Sara Bazin, Jean-Sébastien l'Heureux and Louise Hansen for their comprehensive guidance, inspiration, and support during this work. They not only guided me through my research but also helped and supported in every possible way to find my path ahead. I am also indebted to my non-official supervisor Maarten Vanneste for his regular advices, and all the interesting discussions we had. He was greatly interested in my work, and his insightful remarks were very helpful to come up with new ideas.

I am also very grateful to the sponsors of this Ph.D. thesis without which this project would not have came into being: the Norwegian Public Roads Administration (SVV), the Norwegian National Railway Administration (JBV), the Norwegian Water Resources and Energy Directorate (NVE) and International Centre for Geohazards (ICG).

I thank all of the ICG fellows for helpful discussions and diversions. This work would not have been possible without the friendly and exciting atmosphere at ICG. I am grateful to all NORSAR staff. Special thanks to Winnie Lindvik for her great support on practical matters. The author thanks Gedco, DGb and Sandmeier for providing academic licences of VISTA, OpendTect and Reflexw, respectively.

Special thanks to Nele Kristin Meyer, Nadège Langlet, Sylvain Tissot, Christian Maskrey, Håkon Akerholt, Tor Overskeid, Karine Petrus, Mesay Geletu Gebre, Gunther Druivenga and Berit Paulsen for their help in the field.

I am grateful to the University of Oslo, the Norwegian Geotechnical Institute (NGI) and NORSAR for providing the necessary field equipment.

I remain forever grateful to my families for their unconditional support and motivation. My fiancée Maud is the source of my strength that helped me to accomplish this work.

List of Publications

Refereed Journal/Book/Conference Publications

Manuscripts listed in reversed chronological order

Sauvin, G., Lecomte, I., Bazin, S., L'Heureux, J.-S., Vanneste, M., Solberg, I.-L., and Dalsegg, E., 2013. *Towards geophysical and geotechnical integration for quick clay mapping in Norway.* Special Issue, Near Surface Geophysics, EAGE, 11, 613-623, doi:10.3997/1873-0604.2012064.

Sauvin, G., Lecomte, I., Bazin, S., L'Heureux, J.-S., Vanneste, M., 2013. *Geophysical data integration for hazard assessment of quick-clay landslide-prone areas: the Hvittingfoss case study, Norway.* In *Landslides in Sensitive Clays: From Geosciences to Risk Management*, (eds. J.-S. L'Heureux et al.), Advances in Natural and Technological Hazards Research 36, doi:10.1007/978-94-007-7079-9_ 18, Springer Science+Business Media Dordrecht, pp. 236-246.

Sauvin, G., Lecomte, I., Bazin, S., L'Heureux, J.-S., Vanneste, M., 2012. *Geophysical investigations of quick-clay slide prone areas.* 8th European Meeting of Environmental and Engineering Geophysics, Paris, France. Extended Abstract, pp. 5. Won the AGAP best PhD extended abstract award.

Garofalo, F., **Sauvin, G.**, Socco, L.V., I. Lecomte, I. 2012. *Joint Inversion of Surface-wave Dispersion, P-wave Refraction and Apparent Resistivity Data.* 8th European Meeting of Environmental and Engineering Geophysics, Paris, France. Extended Abstract, pp. 5.

Sauvin, G., Lecomte, I., L'Heureux, J.-S., and Malehmir, A. 2012. *Quick-clay landslide-prone grounds in Norway and Sweden: a complex problem requiring a combined geophysical and geotechnical approach.* 74th EAGE Conference & Exhibition – Workshops: *Integrated Geosciences for Subsurface Instabilities, Offshore and Onshore*, Copenhagen, Denmark. Extended Abstract, pp. 5.

Sauvin, G., Bazin, S., Vanneste, M., Lecomte, I., and Pfaffhuber, A.A. 2011. *Towards joint inversion/interpretation for landslides-prone areas in Norway Integrating geophysics and geotechnique.* 17th European Meeting of Environmental and Engineering Geophysics, Leicester, UK. Extended Abstract, pp. 5.

Submitted publications

Sauvin, G., Lecomte, I., Bazin, S., Hansen, L., Vanneste, M., and L'Heureux, J.-S. Submitted. *On the integrated use of geophysics for quick-clay mapping: The Hvittingfoss case study, Norway.* Journal of Applied Geophysics.

Garofalo, F., **Sauvin, G.**, Socco, L.V., I. Lecomte, I. Submitted. *2D Laterally varying media solved by the joint inversion of seismic and electrical data.* Submitted. Geophysics.

Other publications

Donohue, S., Long, M., L'Heureux, J.-S., Solberg, I.-L., **Sauvin, G.**, Rømoen, M., Kalscheuer, T., Bastani, M., Persson, L., Lecomte, I., and O'Connor, P. 2013. *The use of geophysics for sensitive clay investigations.* Proceedings, First International Workshop on Landslides in Sensitive Clays, Laval, Québec, (Springer-Verlag).

Hansen, L., L'Heureux, J.-S., **Sauvin, G.**, Polom, U., Lecomte, I., Vanneste, M., Longva, O., and Krawczyk, C.M., 2013. *Effect of mass-wasting on the stratigraphic architecture of a fjord-valley fill: Correlation of onshore, shear-wave seismics and marine seismic data at Trondheim, Norway.* Sedimentary Geology, 289, 1-18.

L'Heureux, J.-S., Long, M., Vanneste, M., **Sauvin, G.**, Hansen, L., Polom, U., Lecomte, I., Dehls, J., and Janbu, N., 2013. *On the prediction of settlement from high-resolution shear-wave reflection seismic data: the Trondheim harbour case study, mid-Norway.* Engineering Geology, 167, 72-83.

L'Heureux, J.-S., Hansen, L., **Sauvin, G.**, Polom, U., Lecomte, I., Vanneste, M., 2012. *High-resolution sub-surface geo-characterization from shear-wave seismic reflection profiling: An example from the Trondheim harbour, mid-Norway.* 31st Nordic Geotechnical Meeting, Copenhagen.

Long, M., Donohue, S., L'Heureux, J.-S., Solberg, I.L., Rønning, J.-S., Limacher, R., O'Connor, P., **Sauvin, G.**, Rømoen, M., and Lecomte, I. 2012. *Relationship between electrical resistivity and basic geotechnical parameters for marine clays.* Canadian Geotechnical. Journal. 49, 1-11.

Lecomte, I., Juliussen, H., Støren, E.N., **Sauvin, G.**, Hamran, S.E., Petrakov, D., Lavrentiev, I., Kutuzov, S., and Tissot., S. 2012. *Geophysical Investigations of Unstable Mountain Slopes in Jotunheimen, Norway.* 8th European Meeting of Environmental and Engineering Geophysics, Paris, France. Extended Abstract, pp. 5.

L'Heureux, J.-S., Hansen, L., Longva, O., **Sauvin, G.**, and Vanneste. M. 2012. *A multidisciplinary study of near-shore landslides in the Trondheim harbour, mid Norway.* 74th EAGE Conference & Exhibition Copenhagen, Denmark. Extended Abstract, pp. 5.

Polom, U., Hansen, L., **Sauvin, G.**, L'Heureux, J.-S., Lecomte, I., Krawczyk, C., Vanneste, M., Longva, O. 2012. *High-resolution, SH-wave reflection seismics for characterization of onshore soil conditions in the Trondheim harbor, central Norway.* In *Advances in Near-Surface Seismology and Ground-Penetrating Radar* (eds. R.D. Miller, J.D. Bradford, K. Holliger), Geophysical Development Series No. 15, Society of Exploration Geophysicists (SEG), pp. 297-312.

Garofalo, F., **Sauvin, G.**, Socco, L.V., and Lecomte, I. 2013. *Joint inversion of apparent resistivity and seismic surface and body wave data.* Geophysical Research Abstracts. Vol. 15, EGU2013-4306. EGU General Assembly.

Juliussen, H., Støren, E.N., Lecomte, I., **Sauvin, G.**, Tissot, S., Hamran, S.E., Petrakov, D., Lavrentiev, I., and Kutuzov, S. 2012. *Coupling alpine lake sediments with slope deposits using a combined geophysical and sedimentological approach, Leirvatnet, Jotunheimen, southern Norway.* Geophysical Research Abstracts. Vol. 14, EGU2012-12333. EGU General Assembly.

List of acronyms

Symbol	Meaning
CPTU	Cone Penetration Testing with pore pressure measurement
EM	Electromagnetic
ERT	Electrical Resistivity Tomography
GPR	Ground Penetrating Radar
MASW	Multi-Channel Analysis of Surface Waves
RCPTU	CPTU with resistivity measurement
RPS	Rotary Pressure Sounding
SCPTU	CPTU with seismic measurement
SRT	Seismic Refraction Tomography
V_p	P-wave seismic velocity ($m \cdot s^{-1}$)
V_s	S-wave seismic velocity ($m \cdot s^{-1}$)
q_t	Corrected CPT tip resistance (Pa)
$q_t - \sigma_{v_0}$	Net CPT tip resistance (Pa)
s_{ur}	Undrained Remoulded shear Strength (Pa)
s_u	Undrained shear Strength (Pa)
S_t	Sensitivity
F	Force (N)
ρ	Density ($kg \cdot m^{-3}$)
G_{max}	Small-strain shear modulus (Pa)

Chapter 1

Introduction

Quick-clay landslides occur worldwide and threaten people as well as infrastructures. Recent events, e.g., in Canada and Norway (e.g., Finneidfjord in 1996 (Longva et al., 2003), Kattmarka in 2009 (Nordal et al., 2009) and St-Jude in 2010 (Locat et al., 2012)), show how disastrous such landslides can be and emphasize the need for proper understanding, characterization and assessment of landslide-prone areas. Landslide risk evaluation aims to determine the "*expected degree of loss due to a landslide and the expected number of live lost, people injured, damage to property and disruption of economic activity*" (Varnes, 1984). In mountainous countries such as Norway, human settlements and transport networks are mainly localised in valleys and along coasts as these lowlands are often fertile and inhabited. However, these rather-flat valley/coast environments may be prone to major landslides as is the case in Norway and Sweden with, e.g., disastrous quick-clay slides (Rankka et al., 2004; Furseth, 2006), and retrogressive submarine landslides encroaching land / backstepping onshore, involving weak layers that were deposited following past quick-clay slides onshore (Polom et al., 2012; Hansen et al., 2013; L'Heureux et al., 2013; Lecomte et al., 2008a,b). Even short roads or railroads closures of small sections within the transportation network, due to landslides, may result in significant economical losses (Dalziel and Nicholson, 2001). Moreover, Norwegian climate changes are bringing more precipitation – more frequent and more intense rainfall, milder winters, warmer summers, and increase in wind speed and storm frequency (Easterling et al., 2000). Higher groundwater levels will raise floods and increase erosion; more rain will increase the landslide hazard. The combination of these factors makes Norwegian valleys and coastal lowlands potential high landslide-risk zones and emphasizes the need for detailed quantitative hazard and risk assessments of such areas, in a multidisciplinary and integrated manner.

When a potential unstable site is identified through, e.g., geological and geomorphological mapping, the common site investigation approach is to carry out geotechnical investigations such as Rotary Pressure Sounding (RPS) and Cone Penetration Test with pore pressure measurements (CPTU) combined with sampling in boreholes. Such measurements are crucial, giving precious information about the soils/sediments and rocks, but are intrusive and often expensive. These intrusive methods typically result in spotlike 1D sub-surface characteristics at isolated locations spread across the site, without providing the possibility to extrapolate the data or address the spatial and vertical variability in

soil conditions. Geophysical investigation can help to better locate/map landslide-prone areas, and evaluate their extent. Geophysics can indeed map the ground in between and away from CPT/borehole sites, i.e., giving lateral information and better depth penetration. These methods are non-intrusive when carried out from the surface, sometime cheaper, and map several physical parameters, e.g., elastic, electrical, etc. However, geophysical techniques do not directly provide geological and geotechnical properties, so a minimum of ground-proofing is necessary (e.g., boreholes) in order to calibrate geophysical measurements against geological/geotechnical ones.

It is also crucial to use the proper geophysical methods depending of the type of material present in the studied site and one method (often related to one physical parameter) is not necessarily sufficient. As the actual site conditions are typically unknown, a multi-method approach is the way forward. Indeed, the trend in near-surface geophysics is nowadays to combine several methods to better constrain the interpretation (joint interpretation and inversion) and the corresponding physical parameters should guarantee a proper convergence of the inversion (Ghose, 2010). Besides integrating different geophysical methods, it is also important to attempt 3D imaging contra 2D. In complex/highly-varying grounds, a 2D acquisition does not provide a proper result due to 3D effects, hence an even stronger non-uniqueness of the result if only one method is used. Geophysics can also be used for monitoring, i.e., to follow the changes of selected parameters over time and may therefore further contribute to landslide hazard/risk assessment (e.g., Chambers et al. 2009). This is particularly true regarding the role of water in the ground, water being an important factor to assess for stability evaluation, and the subsequent use of so-called hydrogeophysics has seen an explosive evolution the last decade (Rubin and Hubbard, 2005).

Multidisciplinary studies on a regional/local scale have shown to be fruitful in understanding all kind of landslide processes around the world (Jongmans and Garambois, 2007), but have seldom been performed in Norway using geophysics "full power", in contrast to many countries in Europe. In Norway, the prospecting approaches have usually been method-driven, i.e., one single method that presumably addresses most satisfactorily a given exploration goal is employed first. Any additional method – if any – is then used separately depending on expectation (regarding accuracy, reliability, etc.) and resources (e.g., funding, expertise and time). This is, e.g., the case for recent works carried out on quick-clay sites in Norway by Solberg (2007); Solberg et al. (2008, 2012). As quick clay is characterized by higher resistivity values due to leaching of salt over time, Electrical Resistivity Tomography (ERT) is the method of choice, but the inversion results are far to be non-unique, even if partially calibrated with CPT measurements, and are very smooth. Very recent works by Long and Donohue (Long and Donohue, 2007, 2010) also use shear-wave velocity information for marine sediment characterization in Norway.

1.1 Background, possibilities and challenges

Even with detailed investigation and monitoring, it can be challenging to evaluate stability and assess the associated landslide risk. This is particularly the case for sites where

little precursors for incipient failure exist, e.g., quick-clay sites. Quick-clay landslides often develop very quickly and may result in total destruction or collapse (nothing left to measure afterwards). Reconnaissance methods, which mainly include remote-sensing and aerial techniques, geological and geo-morphological mapping, geophysical and geotechnical techniques, have to be adapted to the characteristics of the involved ground. According to Mc Cann and Foster (Mc Cann and Forster, 1990), a standard geotechnical appraisal of the stability of a landslide-prone area has to consider three issues: (1) the definition of the 3D geometry of the area with particular reference to failure surfaces or weak zones, (2) the definition of the hydrogeological regime, and (3) the detection and characterisation of the movement. However, specific combinations of these factors are associated with different degrees of landslide hazards and point (3) may not even be present, as with quick-clay sites.

Landslide-prone ground often differs in its internal architecture from the surrounding stable areas, both in terms of hydro-geological and geological properties. This difference may in turn lead to changes in physical and mechanical properties. The definition of the 3D shape of the unstable body requires the investigation down to the undisturbed rock or soil. As indicated in the introduction, the main advantages of geophysical techniques are that (1) they are flexible, relatively quick to deploy, even on rather difficult grounds, (2) they are non-invasive and give information on the internal structure of the soil or rock mass, and (3) they allow a large area to be investigated. On the other hand, their main drawbacks are: (1) the decreasing resolution with depth, (2) the non-uniqueness of the solution for a set of data and the resulting need for calibration and (3) the indirect information they yield (physical parameters instead of geological or geotechnical properties). However, it is worth noting that almost all the advantages of geophysical methods correspond to disadvantages of the geotechnical techniques, and vice-versa, emphasizing the complementarities between the two investigation techniques.

Geophysics can be first used in a short pilot study to 1) test the feasibility of the methods and 2) determine the optimal locations of geological/geotechnical boreholes, hence reducing the cost of the latter. After ground proofing, which is always necessary, geophysics can in a second stage be used in a more thorough manner to map the relevant properties, both laterally and vertically, and preferably in a quantitative manner to be of use for geotechnicians. Finally, both boreholes and geophysics can be re-used for monitoring of temporal parameter variations, if any, with again the former measurements for calibration and the latter for spatial variability.

Geophysical methods provide distributions of physical parameters at depth at one given surface location (1D), along a line (2D) or for a grid (3D). Besides more traditional "contrast" imaging as in reflection/refraction seismic and in Ground Penetrating Radar (GPR), geophysical inversion of, e.g., refracted waves or apparent resistivity, provides continuous imaging of the underground. Geophysical inversion is, however, a complex and non-linear problem and image interpretation has to be done with a critical mind, considering the already mentioned limitations of geophysical techniques and additional constraints linked to the inversion process.

In a joint-interpretation stage, merging several sets of results in an automated manner (e.g., fuzzy logic data integration, (Grandjean et al., 2006; Grandjean, 2012)), and not

just by visual comparison would greatly help the interpretation but. Even better, each method could help constraining the results of the other one during an inversion process, i.e., as a result of a so-called joint inversion (Ghünter and Rücker, 2010; Mota and Monteiro Santos, 2010). Finally, most of the existing images are 2D, whereas a landslide is a 3D phenomenon. A minimum and judicious strategy to tackle this problem is to perform 2D and 3D forward modelling to evaluate the robustness and reliability of the obtained image.

Instead of applying the different geophysical methods separately, there is a need to explore the possibility of conceiving an integrated approach designed to solve a specific exploration problem following, e.g., Ghose (2010). It may indeed be possible, under certain boundary conditions, to integrate different methods or disciplines based on the underlying physics to solve accurately and efficiently a near-surface characterization problem. This approach differs conceptually from multidisciplinary integration performed at the interpretation stage (data processed separately and then joint interpretation is performed) or from stochastic inversion (joint inversion of different datasets based on statistical or empirical correlation), as done in the recent years (Grandjean, 2012; Gallardo et al., 2012). These attempts to combine different methods to achieve a given goal have indeed been rather qualitative. Until now, such joint interpretation/inversion have not been applied to quick-clay areas and there is also a need to go back to the underlying physics in order to get a more quantitative understanding as proposed by Ghose (2010). Such physics-based integrations have been tried successfully for the integration of geophysical (seismic) and geotechnical (CPT) measurements (Ghose, 2004, 2006), integration of ultra-shallow seismic reflection (elastic wave) and GPR (high-frequency electromagnetic wave) (Ghose and Slob, 2006), integration of velocity and attenuation of different seismic wave types in saturated soils, and integration of the reflection coefficients of different seismic wave types in saturated soil (van Dalen et al., 2010).

1.2 Objectives

1. The development of 2D and 3D geophysical techniques has aroused a growing interest for assessing the potential landslide volume, characterizing the physical properties of the landslide material and locating the groundwater flows within and around the slide. The geophysical methods to apply depend on their adequacy to the problem to solve. Therefore, depending on the existence of geophysical boundaries, the penetration depth, the resolution and the signal-to-noise ratio, we intended to evaluate the benefits and limitations of the different geophysical or combination of different geophysical methods to detect/characterize/image the selected parameters in a defined type of environment.

    - On a theoretical basis and from previous geological/geotechnical landslide studies, determine the geophysical potential for landslide prone area investigation in terms of: imaging ability, resolution, depth penetration and costs.
    - Determine which geophysical methods to use according to geotechnical/geological

needs in order to locate/map/characterize a defined type of landslide (morphology, boundaries).

- Define the adapted geophysical survey strategy for landslide prone area investigation in Norway for prospection, imaging and monitoring, which is an important step for prevention and mitigation.

2. A successful near-surface geophysical application can indicate that a geophysical property varies laterally and/or vertically. It is an advantage if the measured geophysical property can be given absolute through internal calibration, boreholes, or samples. And it is even better if the geophysical response can actually be associated with geotechnical properties specifically required for the project. In several cases (Hunter et al., 2010; Long and Donohue, 2010), it has been possible to associate geophysical properties of soils with basic geotechnical parameters for a particular region and/or a particular geological unit. Empirical relationships correlating geophysical measurements with geotechnical properties of materials have been established for local geological properties. These relationships can be useful guides in geophysical or exploration geophysical mapping of landslide prone area.

   - Define relationships between geophysical and geotechnical measurements.
   - According to geotechnical stability calculation and modelling of landslides, evaluate potential geophysical inputs for more constrained computation and modelling

3. Unlike the oil and gas or mining industries, geophysics for engineering and environmental applications has not had the long-term financial investments to develop high-level technologies, until perhaps the last 20 years or so. Most techniques that have been used for investigating landslide-prone areas were borrowed and modified from other geophysical sectors. Nowadays, in several countries, a lot of activities are ongoing towards the use of geophysics for landslide-prone area investigations (Hack, 2000; Jongmans and Garambois, 2007; Hunter et al., 2010). Therefore, geophysical techniques and methods need to be adapted to near-surfaces objectives and developed to answer the problem defined above. A review of the available methods which may be applicable to our cases should be done and then, these methods should be adapted.

   - Enhance acquisition, processing, imaging and modelling for near-surface purposes. Geophysical inverse problems often suffer ambiguity and satisfactory results can only be obtained if additional information is incorporated in the inversion. A priori information can be structural information about known boundaries or information about the parameters or their limits. However, this is rarely done by the available inversion software packages (Ghünter and Rücker, 2010).
   - Develop data integration and joint-interpretation as well as joint-inversion.

4. Key to characterizing a ground-movement hazard is developing a set of criteria that are indicators or predictors of future instability. Recording data over time in order

to follow the evolution of the parameters governing the stability of an area will greatly enhance the understanding of landslide processes. Geophysical methods can be used to efficiently monitor ground property variations (e.g., Niesner 2010).

- Implement efficient cost effective geophysical monitoring tool adapted to the area of study.
- Monitor variations of geophysical parameters related to factors influencing slope stability and triggering factors (e.g., water flows).

5. To validate the developed geophysical methods, testing on real data is necessary. In the framework of this Ph.D., different test sites were selected in discussion with the partners.

   - Fieldwork.
   - Data processing and testing of the developed methods.

6. One of the goals of the proposed work was also to come up with practical recommendations for geophysics investigations of valley/coastal landslides in Norway, both for mapping and monitoring, i.e., easy-to-use guidelines. Such a tool can help increasing the success rate of geophysical surveys. Presently, the use of geophysical techniques for landslide-prone area investigations is less than at its full potential. This could be due to the fact that in quite a number of cases geophysics did not supply the information that was expected. The information may be too vague or/and more ambiguous than what geotechnicians and geologists are used to, and/or the performance of the geophysical technique can be poor due to the site characteristics (applying geophysical methods without satisfactory results for end-users is, in long term, bad for geophysics in general). Often these unsatisfactory results are due to a lack of evaluation of applicability of the geophysical techniques at specific site prior to the survey and also, to a bad use of the geophysical equipment and results.

1.3 Test sites

Several sites were considered to test and validate the developed methods. Together with the partners of this Ph.D. project, 5 sites were selected based on the geology, the availability of previous site investigation data as well as practical issues. These sites were: Vålen, Rissa, Trondheim, Hvittingfoss and Dragvoll (Fig. 1.1). Additionally, within the Geophysicist Without Borders (GWB) project, we also helped for the investigation of the Fråstad quick-clay site along the Gotä Älv river in Sweden.

Vålen As one of the quick-clay laboratory site of NGI, and because of its easy accessibility, the Vålen site was selected. NGI conducted a series of geotechnical measurements at the riverside, grass field and several geotechnical reports are available. Motivated by positive results obtained in a similar area (Pfaffhuber et al., 2010), ERT, and seismic measurements (Multi-channel Analysis of Surface Waves – MASW) were performed in the summer of 2010 to better constrain the soil conditions and the landslide hazard. One

of the objectives was to investigate the transition between the interpreted quick-clay layer and the surrounding low sensitive clay. The expected quick-clay layers were targeted to check their geophysical/geotechnical response to the different measurement techniques adopted.
Unfortunately, for practical reasons (conflict between NGI and the owner of the land) this site had to be abandoned in 2011.

Rissa The Rissa site is well-known for the 1978 quick-clay landslide that was captured on video (Gregersen, 1981; L'Heureux et al., 2012), and it has been a laboratory site for the Geological Survey of Norway (NGU) and the Norwegian University of Science and Technology (NTNU). In addition to the already numerous geotechnical measurements, and as part of a road construction project, NGU acquired a number of ERT profiles in 2010 and 2012. In 2012, we also acquired a number of GPR profiles and one MASW profile. The objectives at this site were to establish correlations between geotechnical and geophysical parameters and map the coarse-grained material deposited at the surface as well as the topography of the bedrock as it influences the presence of quick clay.
The road construction project was canceled as well as the laboratory measurements that were supposed to be done on bloc samples, because they were not collected.

Hvittingfoss The Hvittingfoss site has been investigated by NGI and mitigated against potential landsliding in 2008 (Moholdt, 2008). This site served as a "blind test site" since no geophysical measurements were conducted before. Interpretation of the geotechnical soundings indicated that the soils in the area are dominated by marine and fjord deposits, as well as alluvial deposits. In 2011, GPR, ERT, and P-wave seismic data were acquired, and in 2012, S-wave seismic data as well as a 3D GPR grid were also collected, in order to evaluate the potential of geophysics to detect quick clay beneath a thick fluvial deposit. RCPTU and SCPTU (CPTU with Resistivity and Seismic measurements, respectively) were also acquired to better constrain the correlation between geotechnical and geophysical parameters.

Trondheim Trondheim harbour is partly built as land-reclamation on the fjord delta. In this area, several historic submarine and near-shore landslides happened, revealing the need for a full understanding of the site. Numerous geotechnical measurements were conducted, and in 2008 a large S-wave seismic reflection data set was acquired. Detailed stratigraphy of the delta deposits was achieved and detection of the weak, up to 5 m thick clay layers was possible. This site was included in this Ph.D. as a coastal, non quick-clay landslide prone area. This study was pending the funding of a calibration borehole which never materialized, and therefore, only little attention was given to this site.

Dragvoll The Dragvoll site is located about 2 km south-east of Trondheim. Dragvoll's geology is rather simple, a superficial layer of peat covers a thick homogeneous clay deposits and that is why this site has been selected for the installation of salt injection wells as part of Tonje Eide Helle's Ph.D project (NTNU). The main aim is to monitor the

geotechnical parameters changes during salt diffusion. In this respect geophysical measurements (ERT, GPR, P- and S-wave seismic) were performed to evaluate its potential to capture the changes in sediment properties.

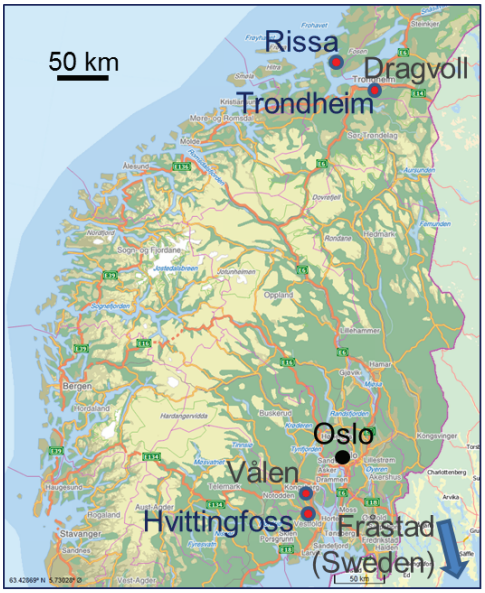

Figure 1.1: Map of Southern Norway showing the site locations.

1.4 Structure of the thesis

This thesis consists of 9 chapters including this introduction.

Chapter 2 reviews quick-clay formation processes and physical properties. From a theoretical basis, previous studies, and according to geotechnical needs, the potential of geophysics for quick-clay investigation is also discussed in this chapter. The first part of Paper I presents the main conclusions of this review.

Chapter 3 explains how geophysics can contribute to better improve site characterization of areas prone to quick-clay landsliding. Complementing the 1D geotechnical localized measurements with geophysical data allows for proper integration of stratigraphic and quantitative information in 2D to 3D. This is exemplified in case-study papers II and III.

Chapter 4 explores potential correlations between geotechnical and geophysical parameters. Since geophysics does not directly provide the necessary parameters for quick-clay characterization, one has to link geophysical parameters to geotechnical ones through, e.g., empirical correlations. Paper III presents some possible correlations.

Chapter 5 introduces data integration via cluster analysis, fuzzy logic, and joint inversion. One of the challenges in geophysics is to properly interpret the different output models (e.g., P- and S-wave velocity, resistivity). This is not an easy task with one given

parameter model, but it is even more difficult when several parameter models are available. One convenient way to ease the interpretation is to integrate the models using, e.g., data fusion by fuzzy logic. Another alternative is to directly invert all of the available experimental data using a joint inversion algorithm. The resulting model can then be interpreted more easily and with more confidence since joint-inversion reduces the inversion uncertainty of each separate methods. Paper IV presents a joint-inversion algorithm developed in collaboration with Flora Garofalo, Ph.D. research fellow at Politecnico di Torino, Italy.

Chapter 6 shows how the geological model resulting from geotechnical and geophysical data integration can be used for landslide site characterization and stability assessment. An example of the design of such a geological model for a given site is presented in paper III.

Chapter 7 presents the geophysical investigation and monitoring plans of the Dragvoll test site where salt wells have been set up as part of Tonje Eide Helle Ph.D. thesis which aims to monitor the geotechnical properties changes has salt migrates through the clay.

Chapter 8 presents the main scientific achievements of this Ph.D. project and **Chapter 9** concludes the thesis with final remarks and an outlook for future work.
Finally, all the papers are gathered at the end of the thesis.

Chapter 2

Quick-clay physical properties

Sensitivity (S_t), the ratio of the undisturbed soil shear strength (s_u) to its remoulded shear strength (s_{ur}), is a key concept (Skempton, 1953). For designation of a soil as "sensitive", S_t must be higher than 1. For designation as "quick clay", the most important criterion is that the post-failure strength must be so low (<0.5 or 0.4 kPa by fall cone test) that the thoroughly disturbed soil behaves as a liquid. A minimum sensitivity criterion is also commonly applied, with S_t exceeding 30; however, this definition is not universally accepted. According to Norwegian standards, quick clay is defined as a clay with a remoulded undrained shear strength below 0.5 kPa (NGF, 1975), whereas the current Swedish definition is slightly different: sensitivity has to be over 50 and remoulded shear strength lower than 0.4 kPa (Rankka et al., 2004).

Sensitive clays are present in both sub-aerial and sub-aqueous (marine or lake) settings, while quick clays are almost entirely restricted to sub-aerial settings, even though their accumulation and early consolidation stages occurred in sub-aqueous (generally submarine) environments. Models for explaining the development of quick clays must invoke mechanisms which will both increase the ratio between the undisturbed and remoulded shear strengths and provide for the decrease of the remoulded strength to less than 0.5 kPa. Mechanisms that tend to increase s_u include flocculation and cementation (Crawford, 1963; Conlon, 1966). On the other side, leaching (Rosenqvist, 1953, 1955; Bjerrum, 1954) and dispersing agents (Söderblom, 1966) lower s_{ur}.

Some of the factors are essential to the development of quick clays, while others cannot be considered essential, nevertheless, they do contribute to the problem of quick clays by increasing the sensitivity to higher values than caused by the essential factors alone. Because of certain fundamental differences, the marine and brackish water sediments must be considered separately from the fresh water sediments. Since Norway presents mainly quick clays originating from sea water, the following chapters focus on these types of clay.

2.1 Depositional factors

Quick clays developed in sediments that accumulated during the most recent late-glacial (Pleistocene epoch) and early post-glacial periods when the weight of the continental ice sheets had depressed the underlying land surface to a greater extent than ice accumulation

had lowered global sea level. The glaciers delivered debris, ranging in size from boulders to clay-sized rock flour, to the glacier/sea contact zone. Coarse material accumulated close to the glacial snout and the silt and clay particles were carried into the sea where they quickly flocculated into aggregates and settled to the sea floor. When ice sheets retreated, their melt waters continued to deliver fine particles to the sea, sand formed deltas at river mouths, and silt and clay particles were still carried seaward where flocculation and sediment accumulation continued.

Low activity minerals dominate – Low s_{ur} The most common clay minerals are, among others: illite, kaolinite, smectite and chlorite. Clay minerals result from the weathering of silicates, such as mica, amphibolites or feldspar. Clay minerals are built up from layers of plane network. The networks consist of aluminium hydroxide or magnesium hydroxide (Al/Mg(O/OH)) octahedrons and silica (SiO4 tetrahedrons), Fig. 2.1. A tetrahedral coordination means that a cathodic ion is surrounded by four oxygen ions, whereas an octahedral coordination means that a central cathodic ion is surrounded by six oxygen ions. A tetrahedral coordination has smaller cathodic ions, such as Si or Al, and octahedral coordination have larger ions, such as Mg, Fe, Mn, C, Na and K. The stability of the structure depends on how well the cathodic ion fits in between the oxygen ions. For example, the bonding between the different mineral layers in illite is very strong and the counter ions are normally not exchangeable, whereas in montmorillonite, the ions are exchangeable and the distance between the layers can thereby increase allowing the material to swell (Appelo and Postma, 2005).

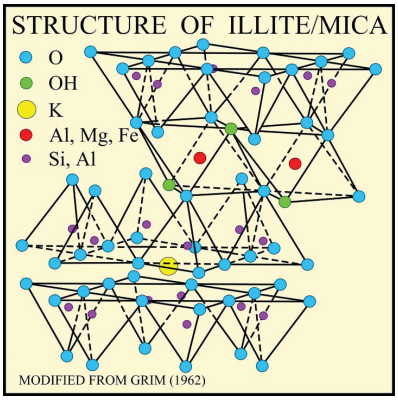

Figure 2.1: Cluster of crystals of the illite clay mineral. Courtesy of USGS

A precondition for the formation of quick clay is that the sediment is dominated by non-swelling mineral with low activity. The concept of *activity* of clay minerals was introduced by Skempton (1953). He studied the relation between plasticity index and clay content in clay. This relation was designated the *activity* of the clay, a_c, and is defined as the ratio of the plasticity index to the clay size fraction (percentage by weight of particles finer than 2 μm). Activity depends mainly on the ion exchange capacity and the specific

surface of the clay minerals, as well as on the content of organic colloids. Bjerrum (1954) compiled values of clay content and plasticity index for several Norwegian clays. He found that the activity of all these clays fell in the range $0.15 < a_c \leq 0.65$ and the clays were thus designated as low-active clays.

The presence of high activity swelling clay minerals, the liquid limits of which increase during leaching, inhibits or prevents the development of high sensitivities (Torrance, 1983). It is not clear what the relative roles of clay-sized primary silicates and low-activity clay minerals may be but it has been suggested that inactive clay-size particles of quartz and feldspar are essential to the development of high sensitivity (Smalley, 1971; Cabrera and Smalley, 1973; Bentley and Smalley, 1978; Moon, 1979). The low activity and the primary silicates of clay and colloidal size behave similarly in many respects, but the primary silicates are more susceptible to cementation. Thus it is suggested that the mineralogical requirement for quick-clay behaviour to develop is that low activity minerals must dominate in the sediment. The activity of quick-clay is normally less than 0.5 (Mitchell, 1976).

Flocculated structure – High s_u In systems containing both water and clay particles, there is continuous reaction between the two phases. As clay minerals have considerable ion exchange abilities, ions from the surrounding water may replace ions weakly bounded to clay particles. In the mineral cluster of all clay minerals, positive ions are always replaced by ions of lower valency. This gives a negatively charged surface on the long side of the minerals. In order to maintain a neutral charge, the surface attracts and bonds positive ions, such as: K^+, Na^+ or Ca^{2+}. This layer of counter ions around the particles is called the diffuse electrical double layer (Fig. 2.2). The extent of the double layer, which is a measure of the electrokinetic potential, depends on the ion concentration in the pore water (Fig. 2.2). The double layer is larger at low ion concentration (fresh water) and smaller at high ion concentration (salt water).

Clay particles in suspension influence each other with both repelling and attracting forces. Repelling forces occur when two particles have the same charge. The magnitude of the repelling force depends on the extent of the double layer. Repelling force is therefore largest at low ion concentration. At high ion concentration, repelling force cease to dominate and particles flocculate (Brand and Brenner, 1981; Mitchell, 1976), a process in which the single unstable particles in suspension in saline water tend to lump together, forming flocs or flakes (Rosenqvist, 1978; Quigley, 1980).

For the development of quick clay, it is generally agreed that the sediment must have a flocculated structure with a high void ratio. This structure is the normal state in fine-grained post-glacial sediments which have accumulated in marine or brackish water. In these environments, flocculation occurs rapidly and the silt and clay-sized particles settle together without any preferred orientation to form a flocculated high void ratio sediment. A similar, though not as random, flocculated structure develops under lacustrine conditions if the cation exchange sites are satisfied predominantly by divalent rather than monovalent cations, leading to denser and more uniform sedimentation (Pusch, 1973).

The clay particles of non-swelling minerals are sedimented in a flocculated state because the electrokinetic potential is low (small electrical double layers), either due to

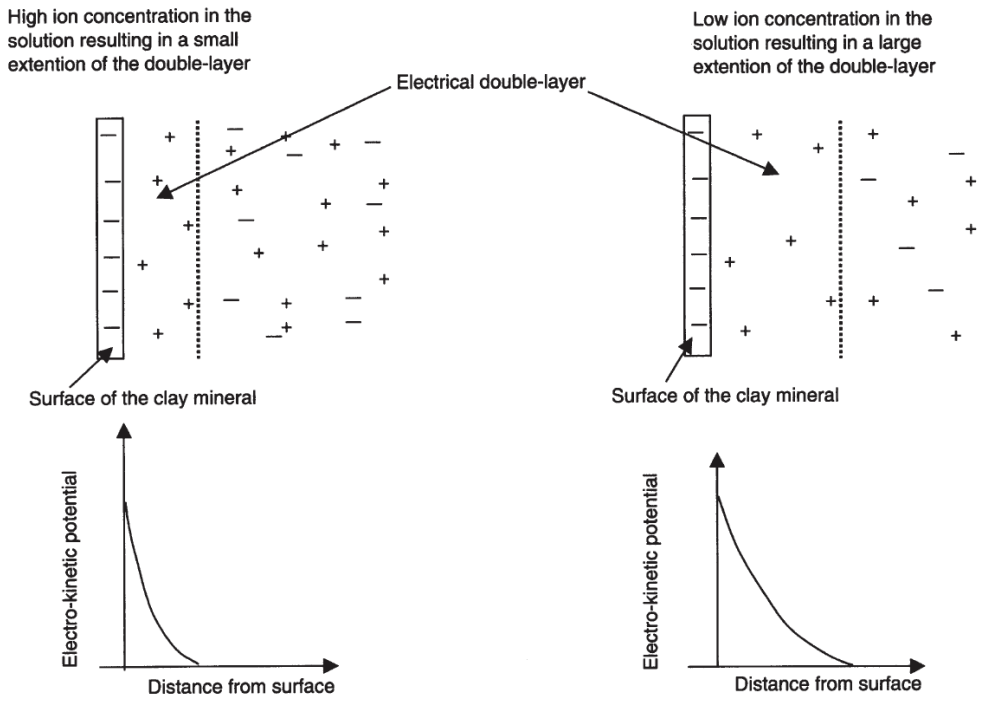

Figure 2.2: Electrical double layer extent depending on ion concentration in pore-water. After, Rankka et al. (2004).

salinity in the water (high cation concentration) or due to absorption of strongly held counter ions as Fe^{3+}, Al^{3+}, Ca^{2+} and Mg^{2+} (Pusch, 1966). Particles in a suspension abundant with positive ions will be connected, i.e. flocculated, which may lead to many different types of particle arrangements; plane to plane, edge to plane, edge to edge, or a combination. Depending on the concentration of positive ions in the pore-water, small to large number of particles will be connected. Therefore, flocs deposited in sea water are larger and denser than in clay deposited in fresh water (Pusch, 1973).

Electron photomicrograph show book-house and stepped-flocculated particle arrangements in medium sensitive to sensitive quick-clays. During consolidation, this fabric can carry effective stress at a void ratio higher than it would be possible if the particles and particle groups were arranged in an efficient, parallel array. When the clay is remoulded, the fabric is disrupted, effective stresses are reduced because of the tendency for the volume to decrease, and strength is less.

The microfabric of quick clay and that of adjacent zones of much less sensitive clay may be the same. The highly sensitive clays do not differ from the clays of low sensitivity with regard to the mineral composition or grain size distribution (Rosenqvist, 1946). Thus while an open flocculated fabric is necessary, it is not a sufficient condition for quick clay development.

2.2 Post depositional factors

As the ice sheets retreated farther and farther, isostatic uplift took place, i.e., the local land surface rebounded faster than sea level rose, eventually lifting more and more of the old sea bottom above sea level. With exposure to subaerial processes, a weathering crust formed in the surface zone. Movement of fresh water through the sediment, whether by infiltration and downward movement from the surface or by upward movement driven by artesian pressures originating in nearby uplands, gradually leached the high-salinity pore water from the sediment. The flocculated microstructure remained intact and kept the water content almost constant during leaching, but the material properties changed (Rosenqvist, 1953).

Leaching – Low s_{ur} Leaching is a process that removes substances such as dissolved salt ions from part of the soil profile.[1] It is a natural process in all temperate regions with marine clays that through the isostatic uplift of the land have been raised above sea level (Torrance, 1978). In principle, there are three different types of leaching process; (1) meteoric water (rain and snow melt) percolating through the deposit, (2) water seeping upwards through the deposit due to artesian pressure, and (3) diffusion of salts towards zones with lower ion concentrations. Combinations of these processes may also occur. The presence of percolating freshwater in silt and sand lenses is sufficient to remove salt from the clay without the requirement that the water flow through the pores of intact clay. Leaching may therefore decrease the original salt content in the pore water of a deposit.

Below the weathering crust, reduction in the salinity of marine clay by leaching is an essential step in the development of a quick clay. Although leaching causes little change in fabric (flocculated structure), the inter-particle forces may be changed. The large increase in inter-particle repulsion, which is responsible for the de-flocculation and dispersion of the clay on mechanical remoulding, results in part from the decrease in electrolyte concentration, which causes an increase in double layer thickness. Leaching also strongly affects the ability of the particles to re-flocculate after remoulding. This results in a decrease in undisturbed strength of up to 50%, and such a large reduction in remoulded strength that a quick clay may form (large relative decrease of s_{ur} compared to s_u). For the same reasons, leaching decreases the liquid limit of the low activity materials involved while the water content remains constant or decreases only a small amount. Changes in sensitivity, shear strength and consistency limits during leaching were studied by Bjerrum (1954) (Fig. 2.3).

The rate of the leaching process depends mainly on the hydraulic gradient and the hydraulic conductivity (Torrance, 1978). The presence of permeable layers, such as sand and silt layers, that are connected to surface water or other water conducting layers greatly enhances the possibility of leaching. The topography of the bedrock can also enhance leaching: if there is a local high in the surface of the bedrock underlying the soil,

[1] In everyday language, salt is usually taken to mean sodium chloride (NaCl), while salt in the context of chemistry refers to chemical compounds consisting of cations and anions, such as potassium hydrogen phosphate (KH_2PO_4). The compounds occur as free ions in a solution, for example Ca^{2+}, Mg^{2+}, Cl^-, Na^+, CO_3^{2-}, K^+, but form salts on drying.

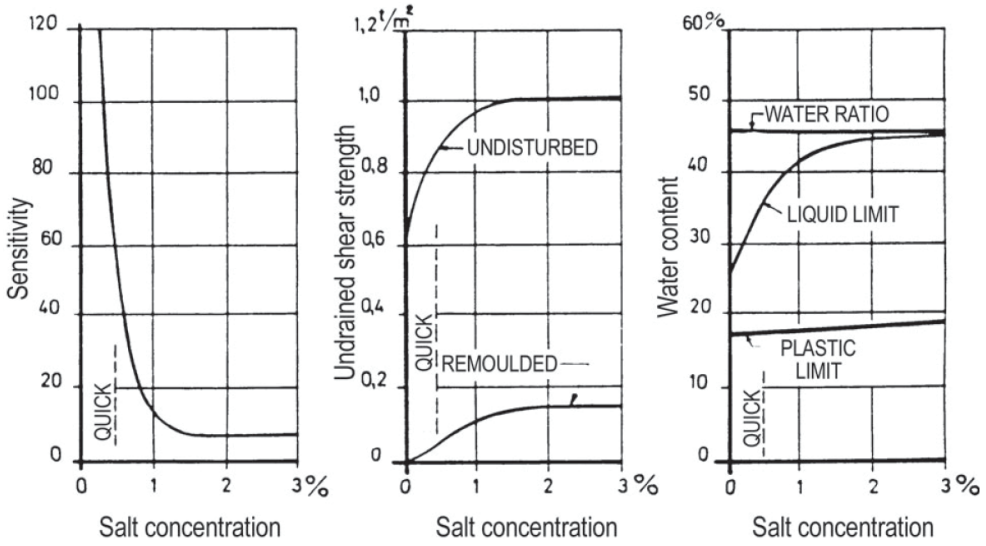

Figure 2.3: Changes in sensitivity, shear strength and consistency limits as functions of the salt concentration in pore water during leaching. After Bjerrum (1954).

the outflow of ground water may be concentrated to this point. A concentration of the outflow of water results in more extensive leaching and thus a greater possibility of quick clay formation at this point.

Although leaching of salt is necessary, it may not be sufficient for the development of quick clay. Research by Talme (1968); Söderblom (1969); Penner (1965), among others, has shown that a low salt content is a precondition for high sensitivity, but that this condition alone is not always sufficient. Thus, there are many clays deposited in sea water which today have low salt contents but are not quick or even highly sensitive. As an example, the salt content of Champlain clay in western Canada rarely exceeds 1 to 2 g/l, yet the sensitivities of different samples range from 10 to 1000. The reason for this large range is that the essential condition for development of a quick clay is an increase in inter-particle repulsions through expansion of the double layer.

The ion composition and the relative amounts of monovalent and divalent cations in the pore water has a controlling influence on equilibrium particle arrangements and therefore, affect the formation of quick clay. A large proportion of monovalent ions leads to large diffuse double layers around the clay particles (Söderblom, 1974). A larger extent of the double layer is required to achieve charge neutrality when the pore water contains monovalent ions compared to when it contains bivalent ions (provided that the same number of ions are present). Larger diffuse double layers imply larger repulsive forces between the particles. After remoulding, these forces will prevent flocculation of the clay particles. This reduces the remoulded shear strength and increases the sensitivity of the clay.

Depending on the bedrock composition, the ground water dominating ions will vary and so will the sensitivity. For example, water containing Ca^{2+} and Mg^{2+} as dominating

ions occurs in areas where the bedrock in the surrounding consist of limestone. Therefore, the pore water contains mainly bivalent ions and the quick clay will then typically not form.

Cementation – High s_u Many soils contain carbonates, iron oxide, alumina, and organic matter that may precipitate at inter-particle contacts and act as cementing agents. On disturbance, the cemented bonds are destroyed leading to a loss of strength. Cementation increases the undisturbed strength and thereby increases the sensitivity. The magnitude of the strength increase presumably depends on the nature and the amount of the cementing agents and the nature of the mineral particles. Several cementing agents have been proposed including carbonates, hydrous and anhydrous oxides of iron and aluminium, oxides of manganese and amorphous materials. Cementation alone will typically not produce a quick clay since the remoulded strength is not changed by the presence of the cementing compounds.

The time at which cementation occurs is important. The faster the cementation develops to the point where the sediment can carry the overburden without further consolidation, the higher the final void ratio will be and the greater the liquidity index after leaching. Thus, rapid cementation will increase the probability of a quick clay being developed. If cementation develops slowly, the final void ratio of the sediment will approximate that for the uncemented sediment under similar overburden and, while the sensitivity will increase because of the higher undisturbed strength, the probability of fluid behaviour upon remoulding will not be changed.

The main role of cementation is to increase the undisturbed strength. Only in rare cases where the undisturbed strength might otherwise be too low for the sensitivity to exceed 30 does Torrance (1983) believes that the cementation has been essential to quick clay development. Even in these cases it plays a secondary role to leaching.

Slow load increase – High s_u Slow load increase, the presence of only a low overburden, or the rapid development of cementation after sedimentation will increase the sensitivity compared with more heavily loaded or uncemented material. Slow load increase will minimize the amount of consolidation at the final overburden pressure. The slower the rate of load increase, the greater the time available for cementation, which inhibits further consolidation. The final void ratio will thus be higher than for more rapid load increase and the remoulded strength will be lower, thereby increasing the possibility for quick clay behaviour. As it allows for minimal consolidation and cementation, slow load increase augments the shear strength (and therefore the sensitivity) compared with more heavily loaded or uncemented material.

Minimal consolidation – Low s_{ur} The less post-depositional consolidation that occurs, the higher the water content and the greater is the probability that, after leaching, the water content will exceed the liquid limit, thereby producing a low remoulded strength. The amount of consolidation is minimized by the flocculated structure.

Dispersant – Low s_{ur} In brackish water sediments, the liquid limit decrease accompanying salt displacement may not be sufficient to produce quick clay. Introduction of dispersing agents, such as organic compounds, may decrease the liquid limit sufficiently for quick clay to develop. Small amounts of inorganic dispersants, would have the same effect. Dispersing substances break up bonds and separate particles. When organic substances act dispersively, they can bond bivalent ions (Ca^{2+}, Mg^{2+}) and change the ion composition in the pore water, which in turn can lead to an expansion of the diffuse double layer (Brand and Brenner, 1981). According to Söderblom (1974), the dispersing agents act in such way that they bond cations from a clay particle and thereby increase the negative charge of the particle surface. The double layers around the particles thereby expand. Among the inorganic dispersing agents are silicates, phosphates, sulphides and bicarbonates. Penner (1965) studied the effect of chemical dispersing agents on the remoulded shear strength of clay. Addition of sodium metaphosphate ($Na(HPO_3)_x$) results in increased sensitivity. Measurements of the electrokinetic potential showed that this parameter increased upon the addition of sodium metaphosphate. Penner (1965) proposed the explanation that particles which were held together by strong van der Waal forces were separated by remoulding. When adding sodium metaphosphate, the phosphate is absorbed on the mineral surfaces and thereby increase the repulsive forces between the clay particles. The repulsive forces are too high to allow the clay particles to be reconnected and the remoulded shear strength is thereby reduced.

Clays deposited in fresh water, and which have flocculated structures and low activity, may become quick due to the action of dispersing agents. This was shown indirectly by Söderblom (1974), who treated fresh water deposited clays with different dispersing substances and found very low remoulded shear strengths. The tests were performed in such a way that an artificial kaolin clay was remoulded and the remoulded shear strength measured. The dispersive agents was then added and remoulding and shear strength measurement of the specimen repeated. Söderblom (1974) also showed an example of a natural, quick, fresh water deposited clay beneath peat.

According to Söderblom (1974), organic agents affect clays in several ways from a chemical point of view. Certain organic agents can, apart from their ability to act dispersively, also act in a cementing way. They thereby provide a stable gel structure, which in certain cases can result in a heterogeneous macrostructure with fine fissures and increased permeability.

2.3 Synthesis and potential for geophysics

The original marine sediments with salt porewater, if thoroughly disturbed, would behave as a plastic solid/extremely viscous liquid, with its water content being approximately at its liquid limit. After leaching, the low-salinity sediment (at the same water content) behaves as a liquid when disturbed. The marine sediment with salt porewater was "sensitive clay"; the leached sediment has become "quick clay". Figure 2.4 summarized the principles of quick clay formation in a diagrammatic form.

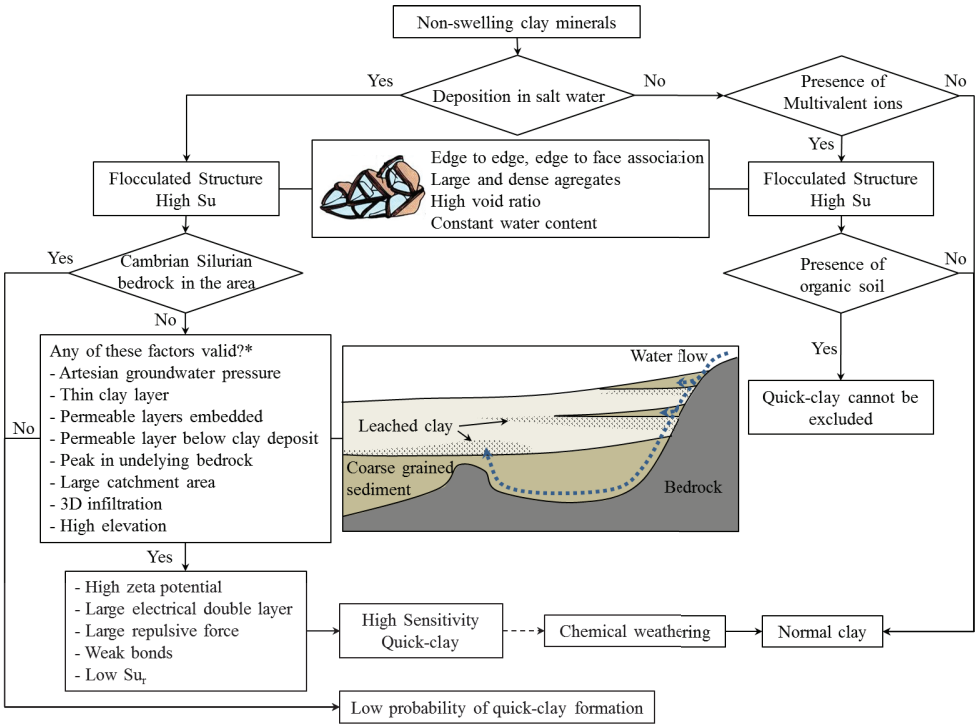

Figure 2.4: Schematic diagram of a quick-clay formation (Fig. 2 in Paper I). A schematic drawing of a flocculated clay particle along with the corresponding properties, as well as a schematic drawing of the preferential groundwater flows that leach the clay are included. *The more factors, the higher the probability of a quick-clay formation.

Geophysical potential The open flocculated structure required for the development of sensitive clay (with large, dense aggregates separated by large voids), could potentially be differentiated from more dispersed structures (with small and relatively porous aggregates separated by small voids) using geophysical parameters. Indeed, clay with flocculated structure has higher void ratio and lower density than the clay with dispersed structure, hence lower seismic velocities. Yet, the density difference between flocculated and dispersed structures might not be large enough to have a noticeable seismic velocity change in practice. In addition, the higher water content due to larger pores will affect the dielectric constant and resistivity depending on the water composition, hinting that resistivity methods may well provide the better proxy. However, as the microfabric of quick clay and that of adjacent zones of much less sensitive clay may be the same, geophysical detection of flocculated structures is not enough. An open flocculated fabric is necessary, but it is not a sufficient condition for quick clay development.

Dealing only with marine clays in our study (left-hand side of Fig. 2.4), being able to know whether or not the clay has been leached from its salt would therefore greatly improve the mapping of sensitive clays. Since the leaching processes in marine clay sed-

iments depend upon hydraulic gradient and time, at a specific location, it is virtually impossible to tell whether or not there is leached sensitive clay in the ground without drilling. Nevertheless, a good knowledge of the groundwater flow system is necessary to locate the preferential leaching of marine clays and map the potentially quick-clay areas. Using geophysical measurements, the stratigraphy and a variety of physical properties within the subsurface can be mapped in detail and thus, the potential groundwater flow paths can be located. The presence of permeable layers, such as sand and silt layers, which are connected to surface water or other water conducting layers, greatly enhances the possibility of leaching. The topography of the bedrock can also affect leaching: if there is a local high in the surface of the bedrock underlying the soil, the outflow of groundwater may be concentrated towards this point (Fig. 2.4). A concentration of the outflow of water results in more extensive leaching and thus a greater possibility of quick-clay formation at this point. Moreover, the amount of leaching (salt concentration in pore water) could possibly be imaged using the dielectric constant geophysical parameter (Solberg et al., 2012) and the weak bonding of clay particles could potentially lead to an S-wave velocity decrease in leached clays (Donohue et al., 2010).

Chapter 3

Geophysics for quick-clay investigation

As illustrated previously, even though geophysical investigation do not directly provide parameters to characterize quick clays, it can be used to improve the probability to find quick clays at a given site. One of the primary information geophysical methods can provide is the stratigraphy of the subsurface. All geophysical methods give an image of the ground, including stratigraphic information, but, depending on the targeted geophysical parameter, they do not necessarily provide the same image. Depending on the nature of the subsurface and the type of method used, the resolution varies. Methods based on geophysical parameters variation at boundaries, such as GPR or seismic refraction, usually provide the best geometrical image of the subsurface. Methods giving a smooth model of the subsurface, such as electrical or seismic tomography, also provide key stratigraphic information that might not be retrieved from contrast-based methods. This is due to the fact that a given method responds to a given set of physical parameters of the subsurface (e.g. elastic or electrical), but this specific parameter set might not reflect the actual changes in the stratigraphy. That is why, even for stratigraphy, a combination of different methods provides the best results.

For investigation of areas prone to quick-clay landslides, the stratigraphy of the subsurface plays a major role. The geometrical arrangement of the sediment layers, the topography of the bedrock, in 2D and possibly in 3D, are key information. Once the stratigraphy of the subsurface is known and we dispose of a detailed geological model, it needs to be populated with the physical parameters of interest for the characterization of a quick-clay site (Karlsrud et al., 1985). As mentioned in Chapter 2, quick-clay physical properties are usually described by geotechnical parameters. Nevertheless, geophysical investigation provides information on the elastic and electrical properties of the subsurface, which is also of interest when studying quick clay. Because of the nature of geophysical measurements, one needs to take into careful consideration critical steps that are acquisition, processing, and, whenever possible, modelling.[1]

[1]It is in fact always possible to do modelling and indeed, highly recommended, but unfortunately seldomly done. Note also that inversion is intrinsically doing modelling.

3.1 Prospecting and imaging

Acquisition Proper planning of an acquisition is always a necessity, first according to the target of interest (size, depth, expected/searched properties, etc.), which should then in principle guide the choice of the methods (if one is so lucky as to have access to different ones), and then choose the acquisition parameters according to the former requirements (location, sampling, time window, etc.). If a priori information is available at the site to be investigated, one can then perform modelling prior to acquisition, as to better define the acquisition parameters (e.g., resistivity modelling based on stratigraphy interpreted from previous geotechnical measurements at Hvittingfoss, papers II, and III).

Processing Processing is the next crucial step in geophysical data analysis. For each method, although demanding and time consuming, careful targeted processing is necessary to obtain good results. GPR and seismic reflection processing as well as fine tuning of inversion parameters for ERT, SRT (Seismic Refraction Tomography) and MASW need to be done with good care.

3.2 Resistivity

Resistivity, measured in $\Omega \cdot m$, is the inverse of conductivity. It is a bulk physical property of materials that describes how difficult it is to pass an electrical current through the material. Clay materials, metallic oxides, and sulphide minerals are the only common sedimentary materials that can carry significant electrical current through the material itself. As such, the resistivity of most near surface sedimentary materials is primarily controlled by the quantity and chemistry of the pore fluids within the material. Any particular material can have a broad range of resistivity responses that is dependent on the level of saturation, the concentration of ions, the presence of organic fluids, faulting, jointing, weathering, etc.

Within the frame of this thesis, solely ERT and RCPTU methods have been used to evaluate the resistivity of the medium. ERT is a geophysical method used to determine the subsurface's resistivity distribution by making measurements on the ground surface. The general principles that ERT is based on have been in use by geophysicists for almost a century. Recent advances to field equipment and data processing procedures have made rapid 2D surveys routine and 3D surveys possible. Old-style 1D resistivity surveys are still common and are useful on many occasions, but encounter interpretation problems in areas of complex 2D or 3D geology. ERT interpretations, supported by borehole data or alternate geophysical data, represent the geometry and lithology and/or hydrology of subsurface geologic formations.

Stratigraphy Because the resistivity model is the results of an inversion process (tomography), it has some inherent limitations. One of them is that it lacks resolution at depth and the resulting model only presents smooth resistivity variations. Therefore, stratigraphic interpretation from ERT results alone is limited. Nonetheless, thanks to the large resistivity difference between dry crust, coarse material, bedrock, and the wet

clay-rich sediments in the studied sites, it is possible to identify these bodies and better constrain the stratigraphic interpretation (Papers I, II, and III).

Resistivity - quantitative information Because the quick clay fundamental property is its pore water ion concentration and composition, it makes resistivity measurement the geophysical method of choice. Resistivity models from ERT, when constrained by resistivity values from RCPTU, possibly enable to differentiate leached clay from clay that has not been leached (Rankka et al., 2004; Solberg et al., 2008, 2012). Indeed, leached clay has a lower pore water ion concentration compare to a non-leached clay. This lower ion concentration affects the resistivity measurement and higher resistivity values are expected for leached clays. However, due to solution non-uniqueness and interpretation ambiguities, differentiating leached clay from non-leached clay based on resistivity models alone is challenging. Variation in grain size distribution and/or water content might very well induce the same resistivity changes (Papers I, II, and III).

3.3 *P*- and *S*-wave seismic

Seismic measurements are well-known from their use in hydrocarbon exploration, but can also be applied for mapping shallower structures. Seismic waves are generated by a seismic source (e.g., sledge hammer, vibrator) on the surface and they travel through the sub-surface. Within the frame of this thesis, both *P*- and *S*-wave have been acquired and both seismic reflection and refraction were used for stratigraphic interpretation and velocity estimation. Surface-wave analysis was also conducted but only used to derive *S*-wave velocity profiles.

Stratigraphy *P*-wave SRT was performed, and as for ERT, the resulting *P*-wave velocity model has low resolution at depth and relatively smooth variation which only allows identification of the main features or deposits (e.g., dry crust, sand, saturated clay, bedrock). *S*-wave SRT could have been used too, but for practical reasons, we only used the *S*-wave seismic dataset for reflection imaging.

At the Hvittingfoss test site, continuous reflections were identified within the *P*-wave seismic refraction dataset and a reflection section was therefore derived. Since the reflection section provides information on the location of impedance (velocity times density) contrasts of the subsurface, it gives good stratigraphic information (Papers I and II), but the *P*-wave resolution is too low (minimal vertical resolution of 2.6 m) to perform detailed stratigraphic interpretation within the sediment lying above bedrock.

S-wave seismic reflection measurements were also conducted at Hvittingfoss. The high-resolution of the *S*-wave seismic data (with a minimal vertical resolution of 0.4 m) allows for a detailed geological interpretation in depth and detailed features can be extracted within some units (Fig. 3.1; Paper III). Similar investigations were conducted at other landslide prone areas, such as the Trondheim harbour (Polom et al., 2012; Hansen et al., 2013; L'Heureux et al., 2013) and Göta Älv river (Polom et al., 2013; Krawczyk et al., 2013; Extended abstract II), and similar very-high-resolution reflection profiles allowed for establishing a detailed stratigraphic model.

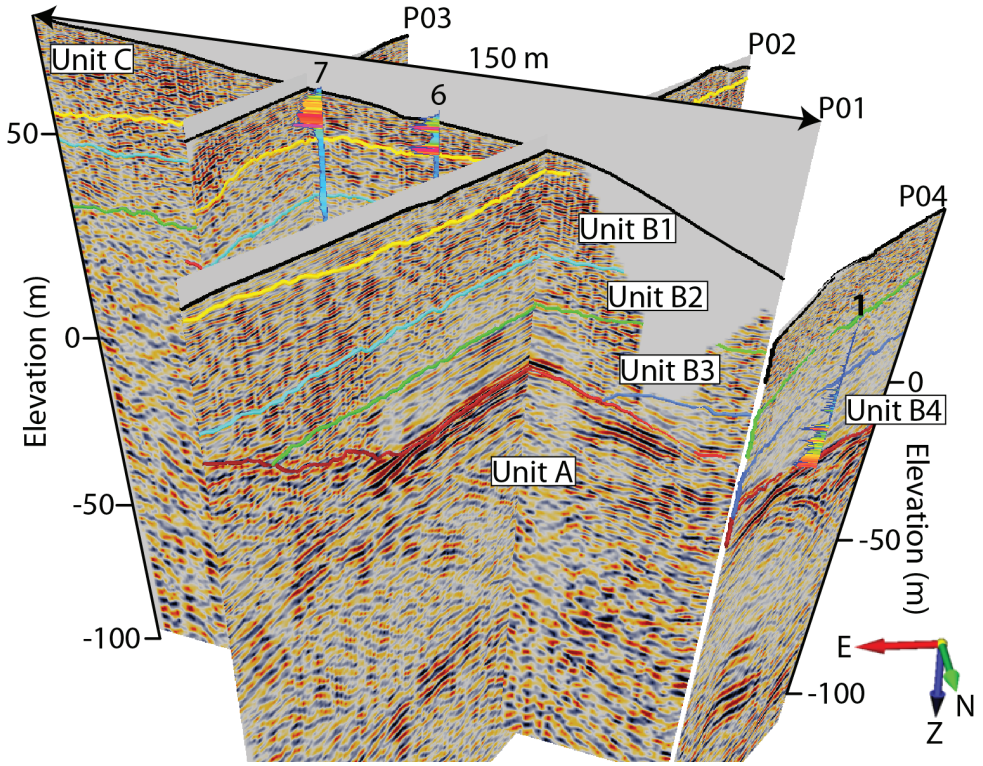

Figure 3.1: Pseudo 3D view of depth-converted S-wave seismic reflection profiles and the drilling resistance of rotary pressure soundings 1, 6, and 7 from Hvittingfoss test site. The interpreted top of units are also displayed. See paper III

.

***P*- and *S*-wave seismic – quantitative information** These methods are important not only for structural information, e.g., in delineating sedimentary structures, but also for physical characterization of layers. P-wave velocity (V_p) extracted from SRT, apart from medium type discrimination, gives information on the water saturation among others.

The S-wave velocity (V_s), derived from MASW or seismic reflection velocity analysis, gives information on the matrix of the medium alone since S-waves do not propagate in fluids. As mentioned earlier, quick clay differentiates from lower sensitive clay mainly by the ion concentration in the pore water. The low ion concentration in the quick-clay pore water also leads to weak bonding of clay particles, which in turn, could potentially lead to an S-wave velocity decrease (Donohue et al., 2010; Papers I and III). Within the frame of this Ph.D., only one of the investigated sites, Vålen (Paper I) allowed for the distinction between leached and non-leached clay. Within the clay deposit, a lower V_s can indeed be observed where the clay has been leached. Nevertheless, the velocity decrease is small, about 20 m/s, and therefore, one should be careful when interpreting the velocity model, because it might fall within the error of the method (Extended Abstract I).

3.4 Ground-penetrating radar

GPR is a geophysical method that uses electromagnetic (EM) waves in the microwave band (10 MHz - 3 GHz) to image the subsurface. This method uses the EM waves transmitted from an antenna, reflected at a dielectric contrast in the subsurface and received at another antenna. The principles involved are similar to reflection seismology, except that electromagnetic energy is used instead of seismic energy, and reflections appear at boundaries with different dielectric constants instead of seismic impedances.

The depth range of GPR is limited by the electrical conductivity of the ground, the transmitted centre frequency and the radiated power. As conductivity increases, the penetration depth decreases. The reason is that the electromagnetic energy is more quickly dissipated into heat, causing a loss in signal strength at depth. Good depth penetration is achieved in dry sandy soils or massive dry materials such as granite, and limestone. In moist and/or clay-rich sediments and sediments with high electrical conductivity, penetration is sometimes only a few centimetres. Therefore, GPR is rarely considered as a suitable method for quick-clay site investigations. Nevertheless, our experience shows that each site is specific and may show significant lateral variations, with upper resistive layers (coarse grained materials or dry clay-rich sediments) well imaged by GPR. Such zones are then better constrained for later inversion of the properties at greater depth such as resistivity (see, e.g., Hvittingfoss (Papers I, II, III), Rissa (Paper I, Extended abstract II), Finneidfjord (Lecomte et al., 2008a,b) and at a smaller depth scale at the Swedish site (Extanded abstract II). Moreover, GPR acquisition is quick and easy, and 3D images of the subsurface can also be achieved.

Stratigraphy Even though GPR does not have the sufficient depth penetration to image clay deposits, we found out that it can be used to map in details the coarse-grained cover, especially at the Hvittingfoss site. The detailed stratigraphy of the upper part of the subsurface retrieved from GPR measurements thus allows for a better definition of the geological model and therefore, a better understanding of the geological prerequisites that might have played a role in the formation of quick clay (Papers I, II, and III).

In a presence of a sand/gravel cover, as in Hvittingfoss case study (Papers II, and III), a detailed 3D image of the fluvial deposit has been retrieved from GPR grid measurements. This high-resolution stratigraphic model allows for a good understanding of the depositional history, and an improved mapping of the interface between fluviodeltaic and marine deposits(Fig. 3.2). We refer the reader to Paper III for a detailed presentation of the acquisition and processing of the GPR cube. Interpretation is provided in Paper III as well as in Figure 3.3.

Attenuation In general, the clay deposits are not homogeneous; grain size distribution and conductivity can vary depending on, e.g., the degree of leaching or the presence of coarser-grained material embedded. In this respect, variation in GPR attenuation can also be used to identify potential variations in the upper part of a clay deposit (Paper III).

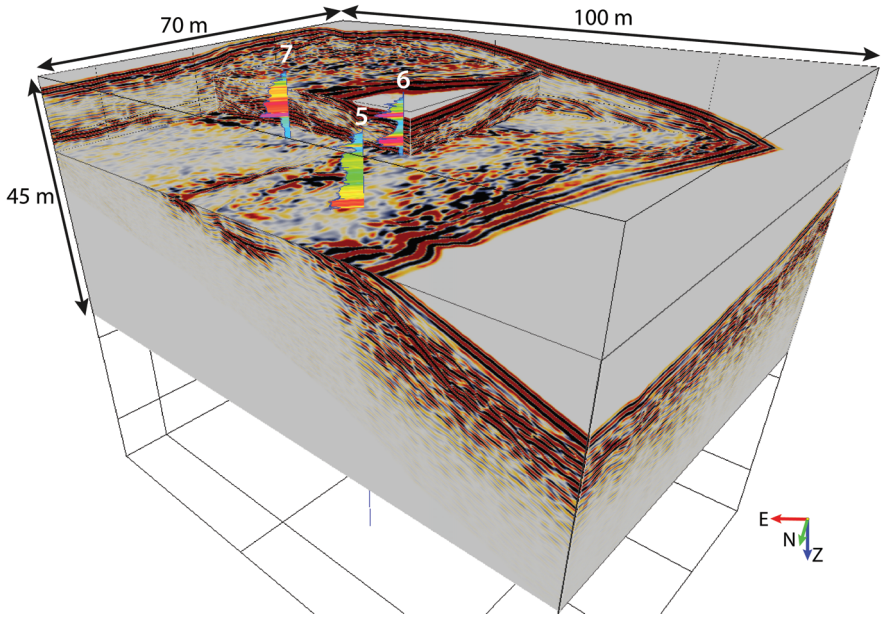

Figure 3.2: Depth-converted GPR cube from Hvittingfoss test site. The fluviodeltaic deposit is well resolved and the transition to marine clay-rich sediment well defined, as supported by geotechnical soundings. Drilling resistance values from RPS 5, 6, and 7 are also depicted.

3.5 Integration

If different types of data are available at a given site, it is of critical importance to integrate the data, even just for stratigraphic interpretation. *P*-wave seismic refraction and reflection allows for clear detection of the bedrock, and, combined with *S*-wave seismic reflection, detailed stratigraphic interpretation can be achieved all the way down to the bedrock. In the shallow part, GPR and ERT profiles give detailed structural information on the coarse material cover, and the dry crust, if any (Fig.3.3).

Additionally, wherever available, geotechnical data provides the necessary ground proofing for accurate geophysical data processing and interpretation (Fig.3.3). The resulting detailed and consistent stratigraphic model provides the necessary information to understand the sedimentation history, and, in some cases, it also gives an idea of the preferential groundwater flow. Bedrock topography, large catchment area and permeable layers can be imaged, indicating the degree of leaching the clay may have undergone (Papers I, II, and III). Similarly, the stratigraphy retrieved from integrated geophysical and geotechnical data interpretation allows to map the thickness of the different clay layers at a given site. The thinner the clay layers, the more likely they could have been leached.

All together, geophysical data calibrated with geotechnical soundings allow for the construction of a consistent stratigraphic model that can then be populated with geophysical/geotechnical parameters of interest. Resistivity, V_p and V_s models can then be used to build a complete geological model.

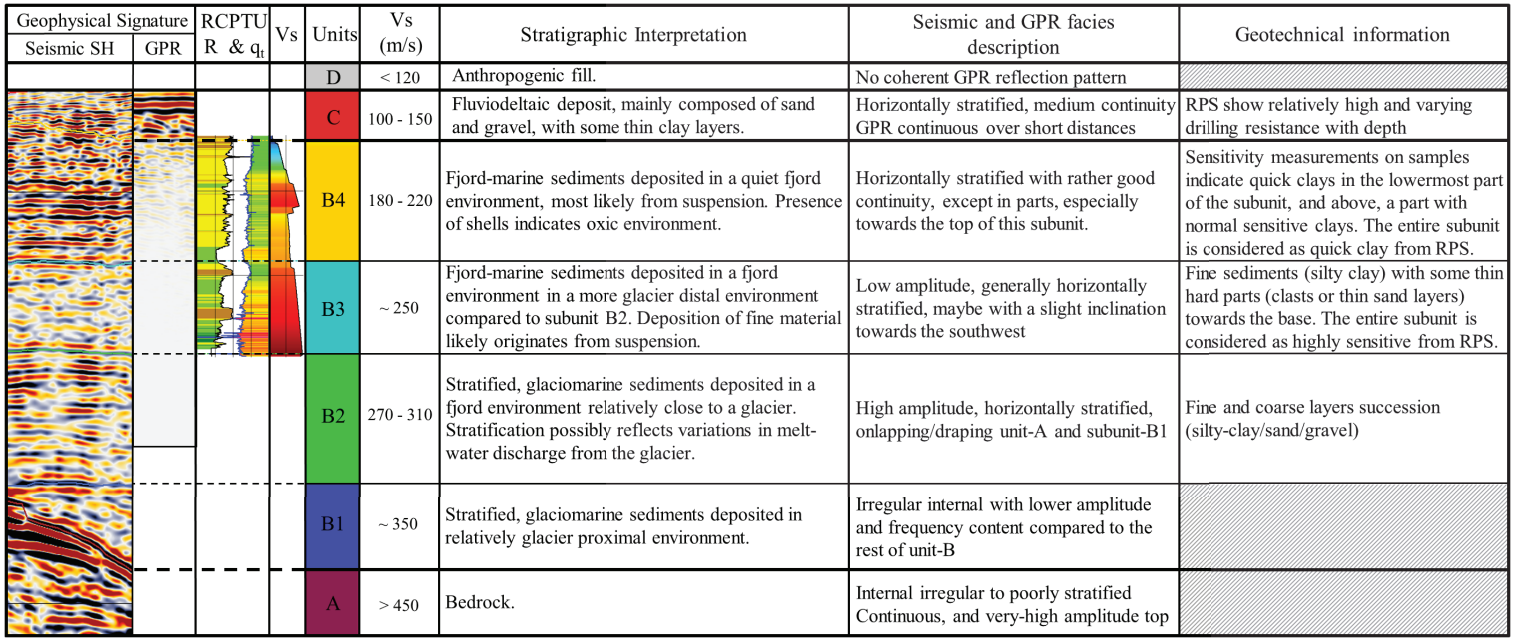

Figure 3.3: Example of stratigraphic interpretation from Hvittingfoss test site based on the S-wave seismic reflection and GPR data (Paper III). Correlation with resistivity and corrected tip resistance values from RCPTU, as well as S-wave interval velocity derived from seismic reflection velocity analysis is also presented. The geotechnical information are also given wherever available.

Chapter 4

Geophysical and geotechnical parameter correlation

Parameters of interest for quick-clay investigation, e.g., density, plasticity index, clay fraction, undrained undisturbed and undrained remoulded shear strength, as well as sensitivity cannot be directly extracted from geophysical measurements, and therefore, empirical relationships have to be made to link the geophysical parameters to the physical/chemical parameters of interest. It is also of interest to derive correlation between geophysical and geotechnical parameters when it comes to stability assessment. These relationships can then be used to populate the geological model derived from geophysical and geotechnical data integration.

4.1 Resistivity

From previous studies (Long et al., 2012), good relationships between resistivity and pore-water salt content have been presented (Fig. 4.1), as well as resistivity and clay content or plasticity. However, no simple relationship exists between s_{ur} or S_t and resistivity since it ignores detailed particle size distribution, mineralogy, ionic content, role of dispersing agents, etc. According to (Torrance, 1983), salt concentration has to be below 2 g/l for a clay to be considered "quick". Therefore, resistivity profile inverted from ERT measurement can possibly be used as a necessary criterion for highly sensitive clay, based on salt content. As an example, we used the relationship between the resistivity and the salt concentration S_c derived from various Norwegian quick-clay sites by (Long et al., 2012) (Fig. 4.1), to evaluate the salt content at Hvittingfoss and Vålen test sites from ERT measurements (Fig, 4.2). Interpretation of geophysical and geotechnical data indicate the presence of both leached and unleached clay at Vålen. Below the high-resistive dry crust, a layer of leached clay can be found in the South-Eastern part of the profile. Below this layer and in the North-Western end of the profile, a layer of unleached clay is present (blue patch in Fig. **??**). At the Hvittingfoss test site, only leached clay is present below the coarse material cover (Fig. **??**).

As remoulded shear strength is directly related to the salt content of the pore fluid, (Long et al., 2012) showed a strong link between resistivity and s_{ur} (from fall cone). In addition,

leaching decreases the liquid limit of marine clays and consequently the remoulded shear strength (Mitchell and Soga, 2005). There is a clear trend of increasing resistivity with decreasing s_{ur}. This is consistent with the fact that s_{ur} will decrease with increasing intensity of leaching. Although most of the data on quick clay discussed in this thesis are within the resistivity range of quick clays (i.e. 10-100 $\Omega \cdot m$) defined by Solberg et al. (2012), other sites with relatively high silt content exhibit significantly higher resistivity values up to 150 $\Omega \cdot m$. A reasonably good linear relationship between the sensitivity and resistivity is also found. The larger scatter of the data with increasing S_t is due to the decreasing accuracy of the fall cone measurements. Scatter could also be due to ERT inversion ambiguity.

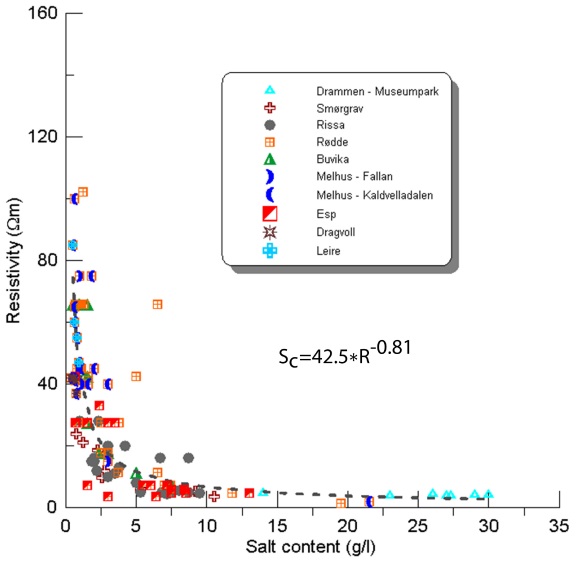

Figure 4.1: Resistivity versus salt content of pore fluid diagram at ten different Norwegian quick-clay sites (adapted from Long et al. (2012)). The corresponding regression correlation equation, which has a regression coefficient of determination of $R^2 = 0.76$ is also given.

4.2 *S*-wave velocity

In addition to knowledge of remoulded shear strength and sensitivity, it is important that intact undrained shear strength is obtained for stability assessment. Since S-wave velocity is directly related to the small-strain shear modulus G_{max} (estimated as $G_{max} = \rho \cdot V_s^2$), it is reasonable to use this parameter for correlation. A well-established practice is to estimate s_u from CPTU data. (Long and Donohue, 2010) developed relationships between V_s and corrected CPT cone resistance (q_t) specifically for Norwegian marine clays. Since these correlations call for geotechnical empirical parameters, we chose to correlate V_s directly to

the net CPT tip resistance $q_t - \sigma_{v0}$ (Paper III). Good results were obtained at Hvittingfoss using the S-wave velocity field from the seismic reflection. It is then possible to derive the shear strength from V_s, using the correlation with the net tip resistance (Paper III).

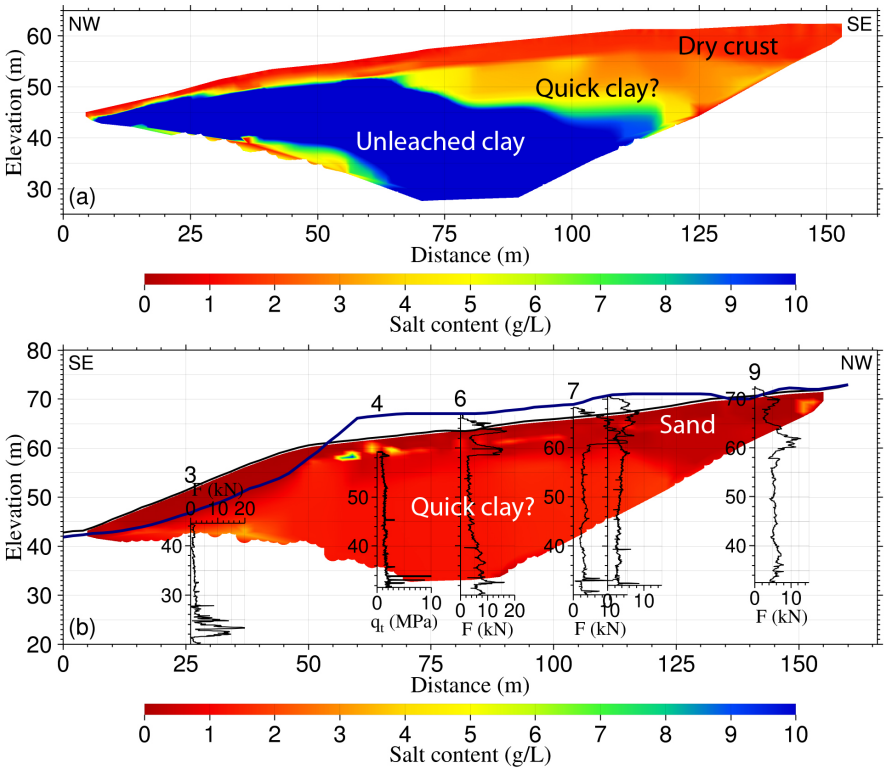

Figure 4.2: Salt content derived from resistivity model at, a) Vålen, and b) Hvittingfoss using the regression correlation presented in Fig. 4.1. According to Torrance (1983) salt content upper limit for quick clay, both leached (potentially quick) and unleached clay can be found, whereas at Hvittingfoss, only leached clay is registered.

Chapter 5

Data integration and joint inversion

The common approach in the earlier experiments has been to invert the seismic and electrical data sets using suitable algorithms to produce two-dimensional V_p, V_s and resistivity models. A coherent and integrated interpretation of the results is, however, not straightforward because each geophysical method senses different soil properties. One way to deal with different data sets is to perform cluster analyses in order to define regions of specific geophysical parameters. We also tried the more advanced fuzzy-logic based data integration to ease and orientate the interpretation process.

On a different, but more integrated level, joint inversion of the different data sets has also been applied. The joint inversion exploits different sensitivities of the methods to model parameters and therefore mitigates solution non-uniqueness and the effects of intrinsic limitations of the different techniques. Moreover, it produces an internally consistent multi-parametric final model that can be profitably interpreted to provide a better understanding of subsurface properties.

In this chapter, an overview is given over the main results acquired in this Ph.D. thesis on cluster analysis, fuzzy-logic integration and joint-inversion. This work is ongoing, and only the joint-inversion approach is presented in a paper (Paper IV).

5.1 Cluster analysis

Cluster analysis, or clustering, is the task of grouping a set of objects in such a way that objects in the same group (cluster) are more similar to each other than to those in other groups. It is a main task of exploratory data mining, and a common technique for statistical data analysis, used in many fields, including machine learning, pattern recognition, and image analysis. The cluster analysis is utilised to create a unified numerical interpretation of the surveyed section. Using clustering algorithms to aid interpretation has been shown to be a step towards a more automated and less ambiguous interpretation by, e.g, (Tronicke et al., 2004; Paasche and Tronicke, 2007; Linder et al., 2010).

Cluster analysis itself is not one specific algorithm, but the general task to be solved. It can be achieved by various algorithms that differ significantly in their notion of what constitutes a cluster and how to efficiently find them. Popular notions of clusters include groups with small distances among the cluster members, dense areas of the data space,

intervals or particular statistical distributions, etc. Clustering can therefore be formulated as a multi-objective optimization problem. The appropriate clustering algorithm and parameter settings (including values such as the distance function to use, a density threshold or the number of expected clusters) depend on the individual data set and intended use of the results. Cluster analysis as such is not an automatic task, but an iterative process of knowledge discovery or interactive multi-objective optimization that involves trial and failure.

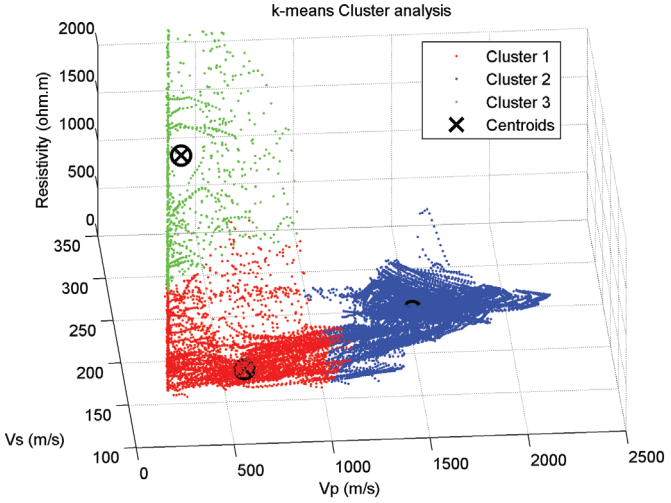

(a) Point cloud.

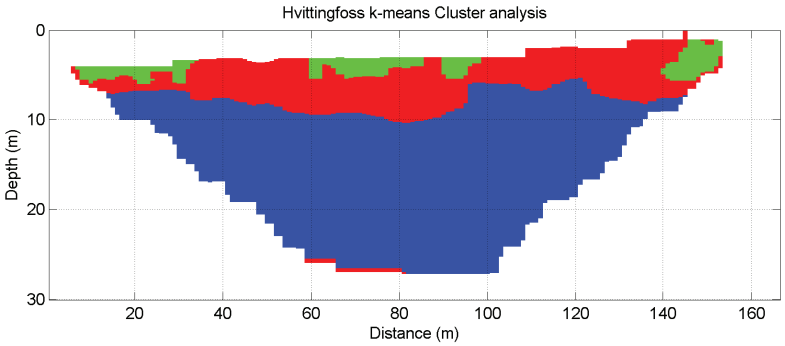

(b) Clustering results.

Figure 5.1: Cluster analysis at Hvittingfoss using V_p, V_s, and resistivity models. Three clusters were used for the k-means clustering. Red, green and blue colours correspond to the same clusters in a) and b).

There are several cluster algorithms that could be applied to geophysical data (Paasche et al., 2006). We have chosen to apply the k-means algorithm (e.g., Joydeep and Alexander 2009) as it shows promising results. k-means algorithm minimizes the sum of distances (square Euclidian distance in our case) from each object to its cluster centroid (the point

to which the sum of distances from all objects in the cluster is minimized), over all clusters. The algorithm moves object between cluster until the sum cannot be decreased further. The result is a set of clusters that are as compact and well-separated as possible. k-means clustering was conducted at the Hvittingfoss test site using 3 clusters ($k = 3$) and all of the 3 models available, i.e., V_p, V_s, and resistivity (Figs. 5.1). Compared to the joint interpretation of the 3 models, interpretation of the result of the cluster analysis is easier. The blue layer can be interpreted as the marine deposit and the red layer can be interpreted as the sand cover with some very dry patches in light green. Even if this interpretation is simplistic, it can help in defining the geological model and finding potential anomalies.

5.2 Fuzzy logic

An innovative approach has been developed by Grandjean et al. (2006) and Grandjean (2012) to combine the geophysical parameters imaged on tomograms and convert them into different geological or geomechanical cross-sections using fuzzy logic. Knowing that seismic data provide information on variations in fissure density and the presence of sheared materials, and that electrical resistivity data provide information on variations in water content, the final cross-sections are computed by combining different transformation functions able to model the conversion from geophysical parameters to ground properties. The computations are realized in a framework of the fuzzy-set mathematical theory that maintains a certain level of objectivity and is able to manage uncertainties. The advantage of the data fusion approach is that it exploits the reliable information contained in the different tomograms and lets the fusion operators enhance the appropriate geophysical anomalies with respect to the stated hypotheses. The basics of this approach are explained in Grandjean et al. (2006), Grandjean (2012) and references therein.

We applied this method to Hvittingfoss test site, defining the transformation functions for V_p, V_s, and resistivity tomograms as described in Figure 5.2. We defined the possibility for soil water saturation using V_p, considering the soil strata to be unsaturated if V_p is lower than 1250 m/s, possibly saturated if the V_p is greater than 1250 m/s and lower than 1500 m/s, and saturated if V_p is greater than 1500 m/s. Similarly we defined the possibility for the soil to be soft clay using V_s, and the possibility for leached clay using the resistivity (Figure 5.2). The medium is respectively considered to be soft clay and not soft clay if V_s is greater than 125 m/s and lower than 250 m/s, and lower than 100 m/s and greater than 300 m/s. The subsurface is respectively considered to be leached clay and not leached clay if the resistivity is greater than 20 $\Omega \cdot m$ and lower than 80 $\Omega \cdot m$, and lower than 10 $\Omega \cdot m$ and greater than 100 $\Omega \cdot m$. Linear uncertainty was assumed between these values.

Result of the fuzzy logic fusion using V_p model from SRT, V_s model from velocity analysis of S-wave seismic reflection data, resistivity model from ERT, their respective likelihood distribution and the belonging functions defined above is presented in figure 5.2. The uppermost domain in the resulting section presents medium possibility values. This layer corresponds to the coarse-grained material deposit and therefore cannot be

considered as highly sensitive clay and could have been removed prior to data fusion. Below, a layer with low possibility values for highly sensitive clay can be found, indicating that the clay in this layer cannot be interpreted as quick clay. Deeper high possibility values for highly sensitive clay is observed, suggesting that quick clay could possibly be found within this layer. This is in agreement with the geotechnical measurements in the vicinity. These preliminary results are promising and more attention should be given to the definition of the transformation function as to focus the data integration on quick clay alone and potentially including results from laboratory measurements. This work is ongoing and has yet to be published.

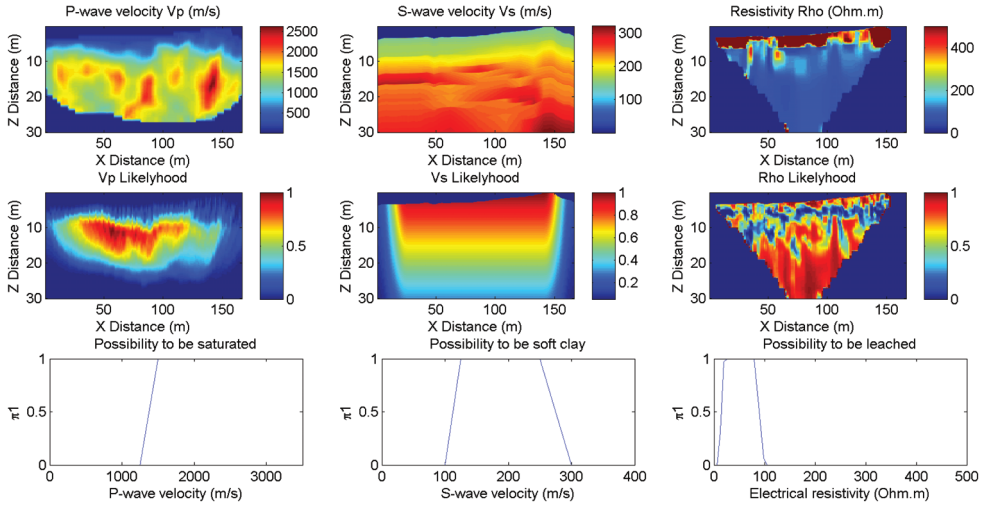

(a) V_p, V_s, and resistivity models with their corresponding likelyhood diagrams and possibility functions.

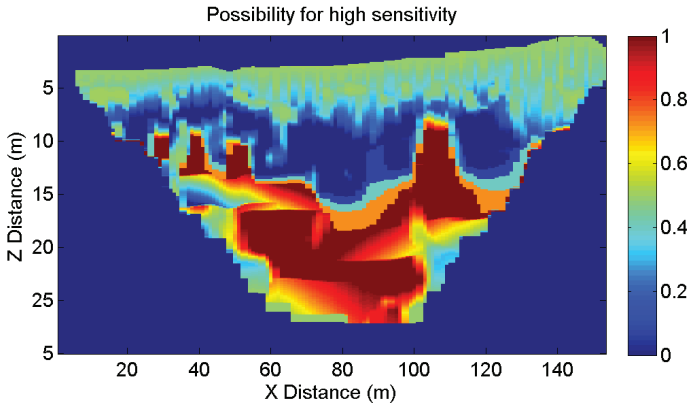

(b) Resulting data integration for high sensitivity.

Figure 5.2: Preliminary results from fuzzy logic data integration using Hvittingfoss V_p model from SRT, V_s model from velocity analysis of S-wave seismic reflection data, and resistivity model from ERT.

5.3 Joint-inversion

A novel inversion algorithm has been implemented to jointly invert apparent resistivity curves from vertical electric soundings, surface-wave dispersion curves, and P-wave traveltimes (Paper IV). The algorithm works for laterally varying layered sites. Surface-wave dispersion curves and P-wave traveltimes can be extracted from the same seismic dataset and apparent resistivity curves can be obtained from continuous vertical electric sounding acquisition. The inversion scheme is based on a series of local 1D layered models whose unknown parameters are thickness, V_s, V_p, and Resistivity of each layer. 1D models are linked to surface-wave dispersion curves and apparent resistivity curves through classical 1D forward modelling, while a 2D model is created by interpolating the 1D models and is linked to refracted P-wave hodograms. A priori information can be included in the inversion and a spatial regularization is introduced as a set of constraints between model parameters of adjacent models and layers. Both a-priori information and regularization are weighted by covariance matrices.

At the Hvittingfoss test site, first-arrival traveltimes were picked at every shot location and surface-wave dispersion curves extracted at 8 locations for each profile. 2D resistivity measurements were carried out on the same profiles using Gradient and Dipole-Dipole arrays with 2-m electrode spacing. The apparent resistivity curves were extracted at the same locations as for the dispersion curves. The data were subsequently jointly inverted and the resulting model compared to individual inversions. Although models from both individual and joint inversions are consistent, the estimation error is smaller for joint inversion, and particularly for first-arrival traveltimes.

5.4 Discussion

Data integration is a whole world in itself and within this Ph.D. project, we merely scratched its surface. The main reason for us to integrate several parameters is because no single one provides the adequate information to characterize quick clay. Therefore, one needs to integrate several parameters providing different information as to better constrain the quick-clay characterization. As such, cluster analysis provides an efficient way to ease the interpretation by extracting data subset of similar patterns in an automated way. The fact there is no needs for a-priori information on the target is very convenient.

Fuzzy-logic integration is based on a-priori knowledge on the target and therefore, orientates the data integration towards an objective, e.g., quick clay characterization. The possibility to account for data uncertainty in the integration process ease the interpretation very much.

In absolute terms, joint inversion should be the methods of choice since its combine the different dataset in the inversion, allowing for the different parameter sensitivity to be complemented. The resulting model parameter should then comply with all the dataset at the same time, providing for the most consisting output model. The results from joint inversion could then also be used as input for cluster analysis or fuzzy logic integration.

Chapter 6

Geophysics for stability assessment

6.1 Safety factor definition

In a simple earth model, the forces acting on a point along the potential failure plane are the shear and normal strength, the pore water pressure, and gravity. Then, slope stability is typically evaluated in terms of a safety factor, which as it applies to the infinite slope model, is the ratio between resisting and driving forces.

The resisting force of earth materials, whether consolidated bedrock or under-consolidated sediments, is the shear strength of the materials. Shear strength is a combination of forces, including the slope normal component of gravity or normal stress, pore pressure within the material, which counteracts the normal stress, cohesion of the material, and the angle of internal friction. The driving force is shear stress, the slope parallel component of gravity.

The role of water is especially critical in slope stability. Water plays a dual role. In increasing the unit weight of material, it increases both the resisting (normal stress) and driving (shear stress) forces. It also creates pore pressure, which opposes the normal stress and therefore reduces the resisting force or shear strength of the material.

It follows that if shear strength is greater than shear stress, then the safety factor is greater than 1 and the slope may be considered stable; if shear strength is less than shear stress, the safety factor is lower than 1 and the slope may be considered unstable. For a safety factor equal to 1, the slope would be considered in a balanced state, but inherently unstable. In cases where the safety factor is lower or equal to 1, the potential for failure is high and mitigation would be warranted.

6.2 Stability assessment

Slope stability analysis has traditionally been performed using the safety factor approach. As it has been used for a long time, there exists a lot of experience based data about the implication of its values. For example, if the safety factor is below certain thresholds in soft clay, this often implies that there is the potential for larger horizontal movements in the soil, as discussed by e.g. Leroueil et al. (1990). Although the required factor of safety might be case sensitive, it is still often selected rather subjectively based on previous

experience or to follow codes and guidelines, while the uncertainties related to loads, material properties, calculation models, and construction are usually not considered.

When conducting a site investigation for slope stability, it is important to look for both the parameters that will increase the driving forces and reduce the resisting ones. Note that human activities affect both of these. A non exhaustive list of parameters affecting the safety factor is given below.

Increasing driving forces:

- Steepening the slope → increases the weight contribution
- Adding weight to (loading) the slope, especially the upper parts
- Increasing the height of a slope (either by human or natural downcutting) → increase the moment for rotational failures
- Seismic vibration

Reducing resisting forces:

- Adding water to the slope causes increased pore pressure → reduces frictional strength
- Steepening the slope → reduces normal stress, and thus reduces internal friction
- Bedding, jointing, or foliation parallel to slope or dipping out of slope → these discontinuities are low-strength zones along which the rock can fail and slide out of the slope
- Intrinsically weak materials (e.g., deeply weathered, sheared, unconsolidated, or clay-rich materials)
- Undercutting the slope → reduces support
- Removing vegetation, especially trees → loss of root strength, also increased water in soil due to reduced evaporation losses
- Seismic vibration

In this respect, geophysical measurements favourably complement geotechnical measurements by providing a support for consistent interpolation between localized soundings. The ground-water table, directly related to porewater pressure measured in boreholes with piezometers, can also be retrieved from GPR or P-wave seismic measurements (Papers II and III). The stratigraphy of the subsurface, even though not as detailed as from geotechnical soundings, can be retrieved from geophysical measurements with a good resolution. The topography of the bedrock, the bedding orientation, or the permeable layers favouring the leaching, can be mapped over large distances and as such provide a better 2D (3D) geological model for stability analysis.

As mentioned previously (Chapters 3 and 4), geophysical parameters can be used directly for subsurface characterization (e.g., resistivity, V_p, V_s), and also for establishing

relationships with geotechnical parameters (Paper III). The small-strain shear modulus or shear strength can be derived from V_s and gives direct input for stability analysis. V_p and V_s also provide information on the extent (2D, 3D) of the weak materials and fill in the gaps between the geotechnical soundings (which are also used for depth calibration). Resistivity can be correlated to salt content, providing a good proxy for the degree of leaching (Papers I, II and III).

Geotechnical and geophysical data integration allows for the construction of a detailed, robust, and consistent geological model that can be used for a more reliable stability analysis. This geological model can also be used as input for landslide modelling, providing the required stratigraphic information and some of the relevant parameters. Parameters such as the internal angle of friction, the effective cohesion can be known from laboratory measurements, while others like the initial stresses have to be derived empirically.

Chapter 7

Monitoring – Dragvoll test site

Within the three years of this Ph.D., we unfortunately did not have the opportunity to conduct any geophysical based site monitoring. Nonetheless, Tonje Eide Helle started her Ph.D. on the monitoring of geotechnical properties of sensitive clay when subjected to salt injection and subsequent diffusion. This project aims to find a way to prevent quick-clay landslides by re-stabilising the highly sensitive clay through the injection of salt in the quick-clay layer. Laboratory scale simulation were conducted and a full scale experiment is undergoing at Dragvoll site, about 2 km South-East of Trondheim. We refer to T.E. Helle's Ph.D. for further details on the project itself.

The geology of the site is known from previous geotechnical investigations, and this site was elected for testing the methods because of its simple geology and the good lateral homogeneity of the deposits. The site has very soft marine clay sediments, found in fairly homogeneous deposits. Below a superficial layer of peat, lie quick clays, filling a bowl-shaped basin formed by the eroded bedrock. In the south-eastern part of the site, the bedrock is almost outcropping, and it dips to 30 m underneath the surface in the north-western part. Six injection wells were drilled end of 2012 on 10 m separated grid.

Prior to drilling and salt injection, geophysical measurements have been performed to characterise the non-perturbed physical properties of the quick-clays. These measurements should then be repeated on a yearly basis to monitor changes of these properties with the diffusion of salt in the quick clays. GPR, ERT and seismic measurements were carried out in October 2012. The seismic measurements were conducted in collaboration with Sisyphe, Université Pierre et Marie Curie. Because of the good correlation of resistivity and salt content pore water, ERT combined with RCPTU measurements is the method of choice. And because the salinity and the composition of ions in the pore water will affect the bonds between the minerals, seismic methods have been proposed here to focus more particularly on the quick-clays mechanical properties through the combined study of pressure (P-) and shear (S-) wave velocities.

Preliminary results are shown in Figure 7.1. As expected, GPR depth penetration is very limited, nevertheless the superficial peat deposit can be clearly imaged and a dipping reflection can be identified and still need to be interpreted. The resistivity profiles exhibit a very homogeneous layer of leached clay (20 – $50\ \Omega \cdot m$) below the peat. V_p and V_s were obtained from P-wave and S-wave refraction as well as surface wave analysis. The resulting velocity models reveal a very low V_s in the peat (50 m/s), and a linearly increasing

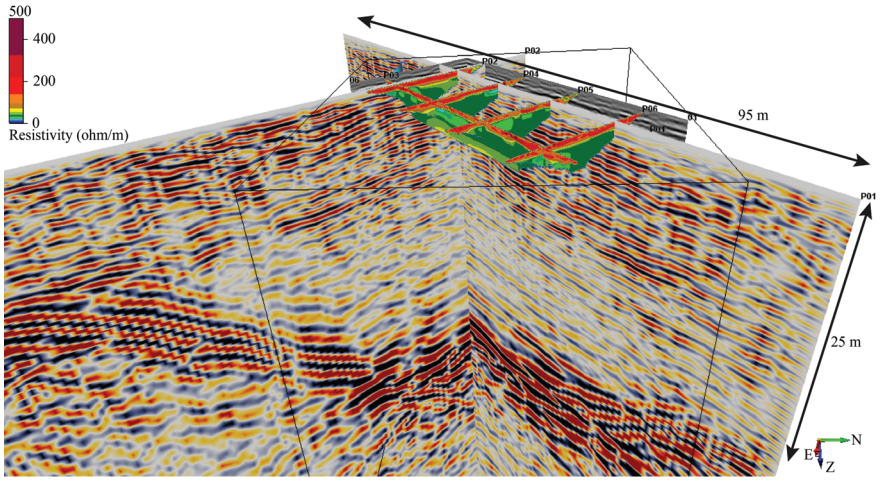

(a) Dragvoll results overview

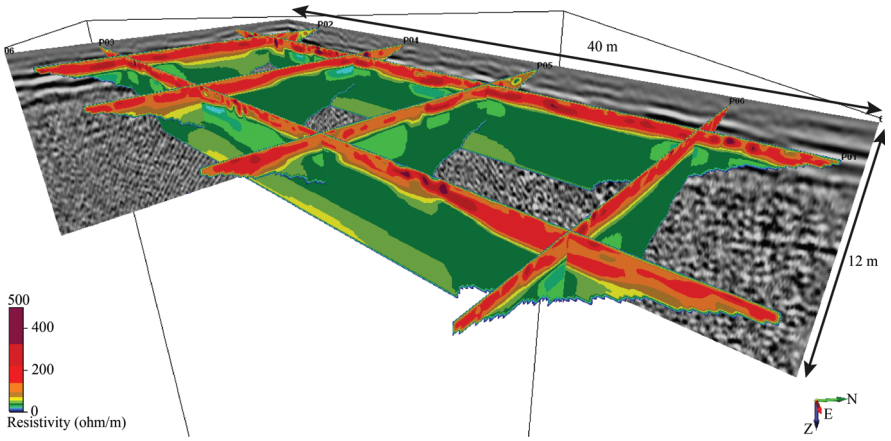

(b) Close up on the resistivity profiles

Figure 7.1: Dragvoll preliminary results from ERT, GPR and S-wave seismic reflection prior to salt injection.

low V_s in the clay layer (120 – 220 m/s). Tomography methods gave quick and reliable lateral information about seismic velocities, but with a limited depth of investigation in such low velocity gradient environments. Surface-wave methods allowed us to extend our knowledge of quick-clay structure in depth. The combined use of refraction seismic and surface-wave dispersion inversion appears to be adapted in the scope of the salt injection and the detection of its effect on quick clay mechanical properties.
New resistivity measurements were carried out in June 2013 and are still being processed.

Chapter 8

Main scientific contribution

The overall goal of this PhD was to evaluate the use of geophysics for quick clay landslide-prone area investigation and define the best use of geophysics for this purpose.
Paper I reviews the quick clay physical properties and evaluate the potential of geophysical measurements for quick clay characterization. This paper also presents preliminary results from a two different sites.
Paper II and **III** present case studies with the geophysical measurements carried out at Hvittingfoss and some site-specific geophysical – geotechnical correlations of interest for quick clay characterization and stability assessment.
Paper IV presents the joint inversion methods developed in collaboration with Flora Garofalo at Politecnico di Torino (Italy). The method is subsequently applied to Hvittingfoss geophysical dataset.

8.1 Paper I

In this paper, we review the physical properties of quick clays in order to find a suitable, integrated and multi-disciplinary approach to improve the possibilities to accurately identify the occurrence of quick clay and map its extent both vertically and laterally. The review of the physical properties of quick clays allows for a better understanding of their occurrence and potential location.

Regarding the interpretation, geophysical data are used in the interpolation between the drill points which also serve as ground-truth, thus providing more realistic stability calculations. Since the profiles cover a relatively large area, the geophysical data will facilitate a more comprehensive understanding of the area and its development both in terms of geology and geotechnical engineering.

The integrated approach is applied in practice to two Norwegian quick-clay sites. The first site, Hvittingfoss, was remediated against potential landslides in 2008 whereas the second one, Rissa, was the scene of a major quick-clay landslide in 1978, but where quick clays are still present over a large areas.

The collected data and site characterizations illustrate the high diversity as well as the complexity and clearly emphasize the need for higher resolution, careful imaging and calibration of the data in order to accomplish the assessment of a quick-clay hazard.

8.2 Paper II and III

These two papers focus on one particular Norwegian site, Hvittingfoss. In addition to the dense geotechnical data set, a set of geophysical methods including Electrical Resistivity Tomography, P-wave seismic refraction tomography, S-wave seismic reflection profiling, and Ground Penetrating Radar, were jointly analyzed and complemented with laboratory data and in situ geotechnical measurements (i.e. CPTU, SCPTU and RCPTU) in order to establish a suitable, integrated and multi-disciplinary approach to map the extent of the quick-clay zone.

Processing, integration and interpretation of the geophysical and geotechnical measurements allowed a precise imaging, both spatially and vertically, of the deposits and of the underlying bedrock. The resulting geological model serves to better understand the local drainage system responsible for the salt leaching from the clay, and, once populated with the quantitative parameters derived from the geophysical measurements, it directly helps to locate the area where highly sensitive clay may be found (i.e. resistivity and GPR attenuation as proxy for salt concentration and degree of leaching, V_s for stiffness and V_p/V_s for saturation).

Correlation of geophysical and geotechnical parameters allows to populate the geological model with parameters relevant for stability analysis (V_s correlation with net tip resistance and subsequently, shear strength). The high-resolution geological model resulting from the integration of several geophysical methods and geotechnical data is then ready for more realistic stability calculation.

This case study also illustrates the advantages of using geophysical measurements in an early phase of site investigation. Providing useful input for the placement of wells, it would potentially limits their number.

8.3 Paper IV

Since we are dealing with geophysical data integration, it is also important to consider joint inversion in order to exploit the different sensitivities of the methods to model parameters and therefore mitigate solution non-uniqueness and the effects of intrinsic limitations of the different techniques.

This paper presents an algorithm in which dispersion curves of surface waves, P-wave refraction seismic, and apparent resistivity are jointly inverted to obtain a final layered model of both V_p and V_s, and resistivity is presented.

The thickness of the layers is jointly solved using the three types of data and the Poisson's ratio is introduced as a physical link between V_p and V_s in order to better constrain the inversion. A collection of 1D layered models are obtained by a deterministic joint-inversion algorithm based on the laterally-constrained inversion scheme. With this approach the final model is better solved than the ones resulting from the inversion of each kind of data.

The algorithm is tested both on a synthetic and a field case. They both provide good agreement with the true and the existing geological models. We proved that the joint inversion of surface-wave dispersion curves, P-wave traveltimes, and apparent resistivity

could provide better results than the individual one, especially by reducing the non-uniqueness of the solution that leads to interpretation ambiguities. The geometry was better solved thanks to the contribution of the three different kinds of data, leading also to an improvement in solving all the other geophysical parameters. The improved results come at a cost of more time-consuming data analysis.

Chapter 9

Concluding remarks

9.1 Conclusions

Potential of Geophysics Study of the quick-clay formation processes and physical parameters allowed to evaluate where geophysics could be used for quick-clay characterization. The major physical parameter affecting the sensitivity of a marine clay found below the marine limit and presenting a flocculated structure with high void ratio, is its pore water ion concentration. Leaching of the salt by fresh groundwater flow reduced the ion concentration and increase the electrical double layer which in terms induces weak bonding of the clay particles. As such, geophysics, providing stratigraphic, resistivity, V_p, and V_s models could potentially help locating the preferential leaching paths, the region of low salt concentration and the region of weak particle bonding.

Adapted geophysical survey strategy Thanks to the study of the physical properties of quick clays, we evaluated the potential of geophysics for their characterization and we could propose an adapted geophysical survey strategy for quick-clay landslide-prone area investigation. Geophysical measurements can be used for pilot study in order to test the geophysical measurements feasability and help determining geotechnical drilling locations. Then in combination with geotechnical soundings, geophysical measurements help to build a consistent, detailed, extended 2D/3D geological model in order to, 1) fill the gap between/from the geotechnical soundings, in terms of stratigraphy and quantitative information, 2) gain a better understanding of groundwater flow and potential leaching zones, and 3) derive quantitative information as proxy for clay sensitivity. One has to keep in mind that this requires careful acquisition, processing and inversion of the different geophysical data.

Geotechnical/geophysical correlation In order to link geophysical parameters to the adapted geotechnical ones, empirical correlations are necessary. Within this Ph.D. project few site specific geophysical/geotechnical parameter correlations were derived, i.e., resistivity and salt concentration and, V_s and net tip resistance or s_u. One of the limitation for derivation of meaningful correlation is the lack of laboratory geophysical measurements. Indeed, even though we dispose of RCPTU and SCPTU, we lack the laboratory mea-

surements that would allow direct correlation of geophysical and geotechnical parameters (i.e., without going through CPTU – laboratory measurements correlations first).

Data integration Interpretation of several model parameters for one purpose is not straightforward and since quick-clay characterization asks for it, one needs to have a convenient way to do the interpretation. Data integration through cluster analysis or fuzzy logic has been performed, giving promising results. It eased significantly the subsequent interpretation of the geophysical data. Fuzzy logic data integration is objective driven, whereas cluster analysis does not require a-priori information. These two methods should therefore used in combination.

Data integration was also attempted from the inversion point of view using joint inversion. The joint inversion exploits different sensitivities of the methods to model parameters and therefore mitigates solution non-uniqueness and the effects of intrinsic limitations of the different techniques. Moreover, it produces an internally consistent multi-parametric final model that can be profitably interpreted to provide a better understanding of subsurface properties.

Integration of geophysical data with geotechnical ones has also to be considered. Geotechnical data provides the ground proofing necessary for the construction of a consistent geological model at depth, and can also be used as a priori information for geophysical data inversion.

Geophysics for stability calculations One of the aim of this project was to enhance the safety analysis by providing more consistent input model for slope stability computation. Slope stability analysis is inherently a 3D issue. To this respect, geophysical measurements contribute to, 1) provide a detailed 2D/3D stratigraphic model (layer geometry is a very important factor for stability calculations), 2) give the bedding orientation, 3) derive s_u from correlation with v_s in 2D (s_u is one of the parameters entering stability calculation), and 4) provide groundwater table.

Geophysical monitoring Within the frame of this Ph.D. thesis, implementation of an efficient method for geophysical monitoring of a quick-clay landslide-prone area sadly never came to light. However, thanks to Tonje Eide Helle's Ph.D. project, geophysical monitoring of a quick-clay site was initiated. Geophysical measurements should be used to monitor the salt diffusion from the injection wells in the quick-clay layers.

9.2 Outlook

This research work has highlighted the usefulness of geophysical measurements when combined with geotechnical soundings for quick-clay landslide prone area investigations in terms of stratigraphy and quantitative information. Further research on the quick-clay characterisation should incorporate geophysical measurements more systematically for, (1) pilot studies for positioning wells, and (2) to fill in the gap between the geotechnical soundings. More experience on the use of geophysics for quick-clay site investigation would

help convincing the geotechnicians on its usefulness. However, geophysics full power might be difficult to apply in consultancy project as it might be too time consuming and therefore too expensive, especially when it comes to seismic reflection.

In this research study, it has been possible to derive site specific correlation between geophysical and geotechnical parameters. Nonetheless, geophysical laboratory measurements would be required to derived more consistent empirical correlations, or maybe directly correlate quick-clay physical properties to geophysical parameters. Moreover, to further constrain correlations by increasing the database, systematic use of RCPTU and SCPTU would be recommended.

Results from this study indicate that the V_s model obtained from geophysical investigation provide insightful information on the subsurface. Therefore for future site investigation, we would recommend to derived V_s whenever possible (e.g., using MASW if S-wave seismic reflection is too expensive). Moreover, the impact of the weak clay particle bonding at low ion concentration on the S-wave propagation (V_s and attenuation) should be further investigated (e.g. through modelling).

This research work also demonstrate the usefulness of data integration compare to simple interpretation of the different models. Data integration for quick-clay landslide-prone area characterization should be further investigated and applied whenever possible. The joint inversion algorithm could also be significantly improved by, e.g., implementing a 2D forward model for resistivity and a physical link between resistivity and seismic (possibly through the use of empirical correlation) and enhance the Jacobian matrix computation efficiency.

Finally, methods and results obtained here have greatly improved the understanding of geophysical measurements usefulness, and these results should be included during quick-clay landslide prone area investigation in similar settings elsewhere. It was shown here that a good understanding of the geological settings at a given site can only be achieved through multidisciplinary studies. Future studies should therefore present a close collaboration between geologists, geophysicists, geotechnical engineers and hydrogeologists.

Bibliography

Appelo, C. and Postma, D. (2005). *Geochemistry, Groundwater and Pollution, Second Edition*. Taylor & Francis.

Bentley, S. and Smalley, I. (1978). Inter-particle cementation in canadian post-glacial clays and the problem of high sensitivity ($s_t > 50$). *Sedimentology*, 25:297–302.

Bjerrum, L. (1954). Geotechnical properties of norwegian marine clays. *Géotechnique*, 4:49–69.

Bjerrum, L. and Rosenqvist, I. (1956). Some experiments with artificially sedimented clays. *Géotechnique*, (10):124–126.

Brand, E. and Brenner, R., editors (1981). *Soft clay engineering*. Elsevier.

Cabrera, J. and Smalley, I. (1973). Quick clays as products of glacial action: a new approach to their nature, geology, distribution and geotechnical properties. *Engineering Geology*, 7:115–133.

Chambers, J., Meldrum, P., Gunn, D., Wilkinson, P., Kuras, O., Weller, A., and Ogilvy, R. (2009). Hydrogeophysical monitoring of landslide processes using automated time-lapse electrical resistivity tomography (alert). *Near Surface Conference, Extended abstract*.

Conlon, R. (1966). Landslide in toulnustouc river, quebec. *Canadian Geotechnical Journal*, (3):113–144.

Crawford, C. (1963). Cohesion in an undisturbed sensitive clay. *Géotechnique*, 13:132–144.

Dalziel, E. and Nicholson, A. (2001). Risk and impact of natural hazards on a road network. *Journal of transportation engineering*, pages 159–166.

Donohue, S., Long, M., O'Connor, P., Helle, T., Pfaffhuber, A., and Rømoen, M. (2010). Multi-method geophysical mapping of quick clay. *Near Surface Geophysics*, (10):207–219.

Easterling, D., Evans, J., Groisman, P., Karl, T., Kunkel, K., and Ambenje, P. (2000). Observed variability and trends in extreme climate events: A brief review. *Bulletin of the American Meteorological Society*, 81(3):417–425.

Furseth, A. (2006). *Skredulykker i Norge*. Tun Forlag Book.

Gallardo, L., Fontes, S., Meju, M., M.P., B., and de Lugao, P. (2012). Robust geophysical integration through structure-coupled joint inversion and multispectral fusion of seismic reflection, magnetotelluric, magnetic, and gravity images: Example from santos basin, offshore brazil. *Geophysics*, 77(5):237–251.

Ghose, R. (2004). Model-based integration of seismic and cpt data to derive soil parameters. In *(Ed.) Proc. 10th European Meeting of Environmental and Engineering Geophysics, Utrecht, The Netherlands, EAGE Publications , Houten, The Netherlands*, number B109, page 4p., Houten, The Netherlands.

Ghose, R. (2006). Change in horizontal stress in soil from changing shear wave velocity - a laboratory investigation. *Expanded Abstracts, EAGE 68th Conference and Exhibition, Vienna*, page 4p.

Ghose, R. (2010). Possibilities for multidisciplinary, integrated approaches in near-surface geophysics. *Expanded Abstracts, 72nd EAGE Conference and Exhibition, Barcelona*, page 4p.

Ghose, R. and Slob, E. (2006). Quantitative integration of seismic and gpr reflections to derive unique estimates for water saturation and porosity in subsoil. *Geophysical Research Letters*.

Ghünter, T. and Rücker, C. (2010). Advanced inversion strategies using a new geophysical inversion and modelling library. *SAGEEP*.

Grandjean, G. (2012). A multi-method geophysical approach based on fuzzy logic for an integrated interpretation of landslides: application to the french alps. *Near Surface Geophysics*, 10:601–611.

Grandjean, G., Malet, J.-P., Bitri, A., and Méric, O. (2006). Geophysical data fusion by fuzzy logic for imaging the mechanical behaviour of mudslides. *Bulletin de la Société Géologique de France*, 177(2):127–136.

Gregersen, O. (1981). The quick clay landslide in rissa, norway. *NGI Publication*, (135):1–6.

Gylland, A. (2012). *Material and slope failure in sensitive clays*. PhD thesis, NTNU, Trondheim, Norway.

Hack, R. (2000). Geophysics for slope stability. *Surveys in Geophysics*, 21:423–448.

Hansbo, S. (1975). *Jordmateriallära*. Almqvist & Wiksell.

Hansen, L., L'Heureux, J.-S., Sauvin, G., Polom, U., Lecomte, I., Vanneste, M., Longva, O., and Krawczyk, C. (2013). Effect of mass-wasting on the stratigraphic architecture of a fjord-valley fill: Correlation of onshore, shear-wave seismics and marine seismic data at trondheim, norway. *Sedimentary Geology*, (289):1–18.

Hunter, J. A., Burns, R. A., Good, R. L., Oullan, S. E., Pugin, A., and Crow, H. (2010). Near-surface geophysical techniques for geohazards investigations: some canadian examples. *The Leading Edge*, 29(8):964–975.

Jongmans, D. and Garambois, S. (2007). Geophysical investigation of landslides: A review. *Bulletin Société Géologique de France*, 178(2):101–112.

Joydeep, G. and Alexander, L. (2009). The k-means algorithm. *In: X. Wu and V. Kumar eds. The Top Ten Algorithms in Data Mining.*

Karlsrud, K., G., A., and O., G. (1985). Can we predict landslide hazards in soft sensitive clays? summary of norwegian pratice and experiences. Technical Report 158, Norwegien Geotechnical Institute, Oslo.

Kenney, T. (1975). Weathering and changes in strength as related to landslides. In et al., E. Y., editor, *Mass Wasting, Proc. 4th Guelph Symp. Geomorphology*, pages 69–78, Guelph, Ont.

Kenney, T. (1976). *Laurits Bjerrum Mem.*, chapter Formation and geotechnical characteristics of glacial-lake varved soils, pages 15–39. Norwegian geotechnical Institute, Oslo.

Krawczyk, C., Polom, U., Malehmir, A., and Bastani, M. (2013). Quick-clay landslides in sweden - insights from shear-wave reflection seismics and geotechnical integration. *Near Surface Geophysics Expanded Abstract*, page 4 p.

Kulhawy, F. and Mayne, P. (1990). Manual on estimating soil properties for foundation design. Technical report, Electric Power Research Institute, Palo Alto, CA.

Lecomte, I., Bano, M., Hamran, S., Dalsegg, E., and Nielsen, K. (2008a). Mapping quick-clay sites for geohazard assessment: the finneidfjord case study, norway. *Extented Abstracts, EAGE Near Surface Annual Meeting, Krakow*, page 4p.

Lecomte, I., Bano, M., Hamran, S.-E., Dalsegg, E., Nielsen, K.-M., Holst Nielse, M., Douillet, G., Fréry, E., Guy, A., and Volesky, S. (2008b). Submarine slides at finneidfjord (norway): geophysical investigations. In *Proceedings 21st SAGEEP.*

Lecomte, I., Bazin, S., Grandjean, G., Michoud, C., Derron, M., Abellan, A., and Jaboyedoff, M. (2010). *Ground-Based Geophysical Investigations.* In the Deliverable 4.1 of the European project SAFELAND: Review of Techniques for Landslide Detection, Fast Characterization, Rapid Mapping and Long-Term Monitoring.

Leroueil, S., Magnan, J., and Tavenas, F. (1990). *Embankments on soft clays.* Ellis Horwood, Chichester.

L'Heureux, J. (2010). *A multidisciplinary study of shoreline landslides: From geological development to geohazard assessment in the bay of Trondheim, Mid-Norway.* PhD thesis, NTNU.

L'Heureux, J., Eilertsen, R., Glimstad, S., Issler, D., Solberg, I.-L., and C.B., H. (2012). The 1978 quick clay landslide at rissa, mid-norway: Subaqueous morphology and tsunami simulations. In et al., Y. Y., editor, *Submarine Mass Movements and Their Consequences, Advances in Natural and Technological Hazards Research*, page 31. Springer Science+Business Media B.V.

L'Heureux, J., Long, M., Vanneste, M., Sauvin, G., Hansen, L., Polom, U., Lecomte, I., Dehls, J., , and Janbu, N. (2013). On the prediction of settlement from high-resolution shear-wave reflection seismic data: the trondheim harbour case study, mid-norway. *Engineering Geology*, (167):72–83.

Linder, S., Paasche, H., Tronicke, J., Niederleithinger, E., and Vienken, T. (2010). Zonal cooperative inversion of crosshole p-wave, s-wave, and georadar traveltime data sets. *Journal of Applied Geophysics*, 72:254–262.

Locat, P., Demers, D., Robitaille, D., Fournier, T., Noël, F., Leroueil, S., Locat, A., and Lefebvre, G. (2012). The saint-jude landslide of may 10, 2012, québec, canada. In Eberhardt, E., Froese, C., Turner, A., and Leroueil, S., editors, *Landslides and engineered slopes – protecting society through improved understanding*, pages 635–640. CRC Press, London, UK.

Long, M. and Donohue, S. (2007). In situ shear wave velocity from multichannel analysis of surface waves (masw) tests at eight norwegian research sites. *Canadian Geotechnical Journal*, 44:533–544.

Long, M. and Donohue, S. (2010). Characterization of norwegian marine clays with combined shear wave velocity and piezocone penetration test (cptu) data. *Canadian Geotechnical Journal*, 47:709–718.

Long, M., Donohue, S., L'Heureux, J., Solberg, I., Rønning, J., Limacher, R., O'Connor, P., Sauvin, G., Rømoen, M., and Lecomte, I. (2012). Relationship between electrical resistivity and basic geotechnical parameters for marine clays. *Canadian Geotechnical Journal*, 49:1158–1168.

Longva, O., Janbu, N., Blikra, L., and Boe, R. (2003). The 1996 finneidfjord slide: seafloor failure and slide dynamics. In Locat, J. and Mienert, J., editors, *Submarine mass movements and their consequences*, pages 531–538, Kluwer, Dordrecht.

Maurer, H., Spillmann, T., Heincke, B., Hauck, C., Loew, S., Spingman, M., and Green, A. (2010). Geophysical characterization of slope instabilities. *First Break*, 28:53–61.

Mc Cann, D. and Forster, A. (1990). Reconnaissance geophysical methods in landslide investigations. *Engineering Geology*, 29:59–78.

Mitchell, J. (1976). *Fundamentals of soil behavior*. John Wiley & Sons, Inc.

Mitchell, J. and Soga, K. (2005). *Fundamentals of soil behavior*. John Wiley & Sons, Inc.

Moholdt, R. (2008). Fossnes på hvittingfoss, vurdering av skredfare og sikringstiltak. in norwegian. Technical Report 20071564-2 30, NGI.

Moon, C. (1974). Quick clays as products of glacial action: a short comment. *Engineering Geology*, 7:359–361.

Moon, C. (1979). Concerning the relation between energy and cementation in quick-clay disturbance. *Engineering Geology*, 14:197–207.

Mota, R. and Monteiro Santos, F. (2010). 2d sections of porosity and water saturation from integrated resistivity and seismic surveys. *Near Surface Geophysics*, 8:575–584.

NGF (1975). Retningslinjer for presentasjon av geotekniske undersøkelser (in norwegian). Technical report, Norsk Geoteknisk Forening.

Niesner, E. (2010). Subsurface resistivity changes and triggering influences detected by continuous geoelectric monitoring. *The Leading Edge*, 9:952–955.

Nordal, S., Alén, C., Emdal, A., Jendeby, L., Lyche, E., and Madshus, C. (2009). Skredet i kattmarkvegen i namsos 13 mars 2009 – rapport fra undersøkelsesgruppe satt ned av samferdselsdepartementet. Technical report, SVV, Trondheim.

Paasche, H. and Tronicke, J. (2007). Cooperative inversion of 2d geophysical data sets: A zonal approach based on fuzzy c-means cluster analysis. *Geophysics*, 72:A35–A39.

Paasche, H., Tronicke, J., Holliger, K., Green, A., and Maurer, H. (2006). Integration of diverse physical-property models: Subsurface zonation and petrophysical parameter estimation based on fuzzy c-means cluster analyses. *Geophysics*, 71:H33–H44.

Penner, E. (1965). A study of sensitivity in leda clay. *Canadian Journal of Earth Sciences*, 2:425–441.

Pfaffhuber, A. A., Bastani, M., Cornée, S., Rømoen, M., Donohue, S., Helle, T. E., Long, M., O'Connor, P., and L., P. (2010). Multi-method high resolution geophysical and geotechnical quick clay mapping. *Near Surface - 16th European Meeting of Environmental and Engineering Geophysics Zurich*, page 4.

Polom, U., Bagge, M., Wadas, S., Winsemann, J., Brandes, C., Binot, F., and Krawczyk, C. (2013). Surveying near-surface depocentres by means of shear wave seismics. *First Break*, 31:67–79.

Polom, U., Hansen, L., Sauvin, G., L'Heureux, J., Lecomte, I., Krawczyk, C., Vanneste, M., and Longva, O. (2012). *High-resolution, SH-wave reflection seismics for characterization of onshore soil conditions in the Trondheim harbor, central Norway*, pages 297–312. 15. Advances in Near-Surface Seismology and Ground-Penetrating Radar, Geophysical Development Series.

Pusch, R. (1966). Quick-clay microstructure. *Engineering Geology*, 1(6):433–443.

Pusch, R. (1973). Physico-chemical processes which affect soil structure and vice versa. In *Proc. Int. Symp. Soil Structure*, pages 27–35.

Quigley, R. (1980). Geology, mineralogy and geochemistry of canadian soft soils: A geotechnical perspective. *Canadian Geotechnical Journal*, 17:261–285.

Rankka, K., Anderson-Sköld, Y., Hultén, C., Larsson, R., Leroux, V., and Dahlin, T. (2004). Quick clay in sweden. Technical Report 65, SGI.

Rosenqvist, I. (1946). Om leiers kvikkagtighet (about quickness of clays). Technical Report 3, Statens Vegvesen.

Rosenqvist, I. (1953). Considerations on the sensitivity of norwegian quick-clays. *Géotechnique*, (3):165–200.

Rosenqvist, I. (1955). Investigations in the clay-electrolyte-water system. *Norwegian Geotechnical Institute Publication*, (9).

Rosenqvist, I. (1978). A general theory for the sensitivity of clays. In *Proc. Interdisciplinary Conf. Mechanisms of Deformation and Fracture*, number 1, pages 258–262, Luleå.

Rubin, Y. and Hubbard, S. (2005). *Hydrogeophysics*. Springer edition.

Skempton, A. (1953). The colloidal activity of clay. In *Proceedings of the Seventh International Conference on Soil Mechanics and Foundation Engineering*, volume 1, pages 57–61.

Smalley, I. (1971). Nature of quick clays. *Nature*, 231:310.

Socco, L., Jongmans, D., Boiero, D., Stocco, S., Maraschini, M., Tokeshi, K., and Hantz, D. (2010). Geophysical investigation of the sandalp rock avalanche deposits. *Journal of Applied Geophysisc*, (70):277–291.

Söderblom, R. (1966). Chemical aspect of quick clay formation. *Engineering Geology*, 1:415–431.

Söderblom, R. (1969). Salt in swedish clays and its importance for quick clay formation. Technical Report 22, SGI.

Söderblom, R. (1974). Organic matter in swedish clays and its importance for quick clay formation. Technical Report 55, SGI.

Solberg, I. (2007). *Geological, geomorphological and geophysical investigations of areas prone to clay slides: examples from Buvika, Mid Norway.* PhD thesis, NTNU, Trondheim, Norway.

Solberg, I., Hansen, L., Rønning, J., Haugen, E., Dalsegg, E., and Tønnesen, J. (2012). Combined geophysical and geotechnical approach to ground investigations and hazard zonation of a quick clay area, mid norway. *Bulletin of Engineering Geology and the Environment*, 71:119–133.

Solberg, I., Rønning, J., Dalsegg, E., Hansen, L., Rokoengen, K., and Sandven, R. (2008). Resistivity measurements as a tool for outlining quick-clay extent and valley-fill stratigraphy: a feasability study from buvika, central norway. *Canadian Geotechnical Journal*, 45:210–225.

Talme, O. (1968). Clay sensitivity and chemical stabilisation. Technical Report 56, Byggforskingsrådet, Stoxkholm.

Torrance, J. (1974). A laboratory investigation of the effect of leaching on the compressibility and shear strength of norwegian marine clays. *Géotechnique*, 24(2):155–173.

Torrance, J. (1978). Post-depositional changes in the pore-water chemistry of the sensitive marine clays of the ottawa area, eastern canada. *Engineering Geology*, 14:135–147.

Torrance, J. (1983). Towards a general model of quick clay development. *Sedimentology*, (30):547–555.

Torrance, J. (2013). *Landslides in sensitive clays: From geosciences to risk management*, chapter 2: Chemistry, sensitivity and quick-clay landslide amelioration. Springer.

Tronicke, J., Holliger, K., Barrash, W., and Knoll, M. (2004). Multivariate analysis of crosshole georadar velocity and attenuation tomograms for aquifer zonation. *Water Resources Research*, 40.

van Dalen, K., Ghose, R., Drijkoningen, G., and Smeulders, D. (2010). In-situ permeability from integrated poroelastic reflection coefficients. *Geophysical Research Letters*.

Varnes, D. (1984). Landslide hazard zonation: a review of principles and practice. *IAEG Commission on Landslides and other Mass-Movements, UNESCO Press*, page 63 p.

Paper I

Towards geophysical and geotechnical integration for quick-clay mapping in Norway

G. Sauvin, I. Lecomte, S. Bazin, J.-S. L'Heureux, M. Vanneste, I.-L. Solberg, and E. Dalsegg

Special Issue, Near Surface Geophysics, 2013, 11, 613-623
doi:10.3997/1873-0604.2012064

Near Surface Geophysics, 2013, **11**, xxx-xxx doi:10.3997/1873-0604.2012064

Towards geophysical and geotechnical integration for quick-clay mapping in Norway

Guillaume Sauvin[1,2,3], Isabelle Lecomte[1,2,3], Sara Bazin[4], Jean-Sébastien L'Heureux[1,4 formerly 5], Maarten Vanneste[4], Inger-Lise Solberg[5] and Einar Dalsegg[5]

[1] *International Centre for Geohazards (ICG), P.O. Box 3930, N-0806 Oslo, Norway, Guillaume.Sauvin@norsar.no*
[2] *University of Oslo (UiO), P.O. Box 1072, Blindern 0316 Oslo, Norway*
[3] *NORSAR, P.O. Box 53, N-2027 Kjeller, Norway, Isabelle.Lecomte@norsar.no*
[4] *Norwegian Geotechnical Institute (NGI), P. O. Box 3930, Ullevål Stadion, 0806 Oslo, Sara.Bazin@ngi.no, Jean-Sebastien.LHeureux@ngi.no and Maarten.Vanneste@ngi.no*
[5] *Geological Survey of Norway (NGU), Leiv Eirikssons vei 39, N-7491 Trondheim, Norway, Inger-Lise.Solberg@ngu.no and Einar.Dalsegg@ngu.no*

Received April 2012, revision accepted November 2012

ABSTRACT

Quick clay is a known hazard in formerly-glaciated coastal areas in e.g., Norway, Sweden and Canada. In this paper, we review the physical properties of quick clays in order to find a suitable, integrated and multi-disciplinary approach to improve our possibilities to accurately identify the occurrence of quick clay and map its extent both vertically and laterally. As no single geophysical method yields optimal information, one should combine a variety of geophysical methods with geotechnical data (*in situ* measurements using Cone Penetration Testing (CPTU), Seismic CPTU (SCPTU) and Resistivity CPTU (RCPTU); laboratory tests) for an in-depth quick-clay assessment at a given site. In this respect, geophysical data are used to fill the gaps between geotechnical boreholes providing ground-truth. Such an integrated and multi-disciplinary approach brings us closer to 2D or pseudo-3D site characterization for quick clays and as such, an improved assessment of the potential hazard they pose. The integrated approach is applied in practice on two Norwegian quick-clay sites. The first site, Hvittingfoss, was remediated against potential landslides in 2008 whereas the second one, Rissa, was the scene of a major quick-clay landslide in 1978, quick clays being still present over a large area. The collected data and preliminary site characterizations illustrate the high diversity as well as the complexity and clearly emphasize the need for higher resolution, careful imaging and calibration of the data in order to accomplish the assessment of a quick-clay hazard.

INTRODUCTION

Quick-clay landslides are a common hazard in formerly glaciated margins like Scandinavia and Canada. Only small perturbations in stress conditions, such as human activity, erosion or excess rainwater saturation, can trigger a failure. For example, the recent quick-clay landslide in Lyngen, near Tromsø (Fig. 1a) was triggered by human activity (construction work) whereas the instability at Byneset (Fig. 1b), west of Trondheim, was due to river erosion. Quick-clay landslides can occur at very low slope angles and are often retrogressive, i.e., they start at a river or sea/fjord and progress upwards.

Quick-clay material originates from highly porous clay deposited in a marine environment during and/or following the last glacial period. Due to isostatic rebound following deglaciation and as a result of lowering the relative sea level, the former marine clay deposits lie today above the sea level and have been exposed to fresh-water environments since. Salt, which originally contributes to the bonding between clay particles, may therefore have been leached from these materials by groundwater and percolating surface water. If sufficient leaching of salt has occurred, a highly sensitive (sensitivity S_t is the ratio of undrained shear strength in its undisturbed condition s_u and undrained remoulded shear strength s_{ur}) or 'quick' material may result (Mitchell 1976; Brand and Brenner 1981).

The final extent of a landslide in clay is governed by several factors including topography, stratigraphy and clay sensitivity (e.g., Mitchell and Markell 1974; Tavenas *et al.* 1983; L'Heureux 2012a). Information about the shape, extent and thickness of the sensitive clay deposits is thus required for hazard mapping (Gregersen 2008). Quick-clay hazard zones in Norway have tra-

FIGURE 1
Pictures of recent quick-clay slides in a) Lyngen, close to Tromsø (Andrea Taurisano, NVE) and b) Byneset, south of Trondheim (Ned Alley, Kriseinfo).

ditionally been investigated solely by means of geotechnical borehole tests, i.e., rotary pressure soundings, cone penetrating tests with pore pressure measurements (CPTU) and laboratory tests on undisturbed samples. The only reliable method for the detection of quick clay used so far in Norway and Sweden is to perform laboratory tests. Mapping of quick-clay formations in this way requires extensive sampling and is therefore not practically applicable but limited to ground-truthing the soil at a few points in the area under investigation. More recently, geophysical methods have been used for quick-clay mapping. These methods include Electrical Resistivity Tomography (ERT) (e.g., Ranka *et al.* 2004; Dahlin *et al.* 2005; Solberg *et al*. 2008) and Resistivity CPTU (RCPTU) (e.g., Rømoen *et al.* 2010; Sauvin *et al.* 2011; Solberg *et al*. 2012b) for calibration and refraction seismic for bedrock mapping and in a few cases Multi-channel Analysis of Surface waves (MASW) (Sauvin *et al.* 2011; Donohue *et al.* 2012).

As no single geophysical method yields the optimal information, it is paramount to combine a suite of geophysical methods (ERT, MASW, seismic refraction tomography (SRT), Ground Penetrating Radar (GPR)) as well as geotechnical data (*in situ* measurements using CPTU, Seismic CPTU (SCPTU) and RCPTU; laboratory tests) for a proper quick-clay assessment of a given site. In this respect, geophysical data are used to fill the gaps between isolated geotechnical boreholes providing the ground-truth. As such, quick-clay mapping gradually moves towards 2D or pseudo-3D site characterization.

In this paper, we first review the formation processes of quick clays and their consequences for their physical properties. We subsequently apply an integrated and multi-disciplinary approach and present results from two particular quick-clay sites in Norway, Hvittingfoss and Rissa.

DEVELOPMENT AND NATURE OF QUICK CLAY

The current Norwegian definition defines clay as 'quick' when (1) its sensitivity is above 30 and (2) its remoulded shear strength is less than 0.5 kPa (NGF 1975; Torrance 1983). In this sense, factors contributing to an increase between s_u and s_{ur} and factors contributing to a lowering of s_{ur} play a role in quick-clay development (for a summary see Fig. 2). Mechanisms that tend to increase the undrained shear strength s_u include flocculation, a process in which the single unstable particles in suspension in saline water tend to lump together, forming flocs or flakes (Rosenqvist 1977; Quigley 1980) and cementation (Crawford 1963; Conlon 1966). On the other side, leaching (Rosenqvist 1953, 1955; Bjerrum 1954) and dispersing agents (Söderblom 1966) lower the undrained remoulded shear strength s_{ur}.

Irrespective of the depositional environment (fresh- or saltwater), a precondition for the formation of quick clay is that the sediment is dominated by non-swelling minerals with low activity, i.e., the ratio of the plasticity index and clay size fraction (Smalley 1971; Cabrera and Smalley 1973; Bentley and Smalley 1978; Moon 1979). Another prerequisite for the development of quick clay is that the sediment must have a flocculated structure with large and dense aggregates separated by large voids (high-void ratio) (Rosenqvist 1977; Quigley 1980). This is usually the case in fine-grained post-glacial sediments that have accumulated in marine or brackish water. A similar structure can also develop under lacustrine conditions (Quigley and Ogunbadejo 1972). This flocculated, high-void ratio structure is mandatory for the development of quick clays because when subjected to changes, the remoulded shear strength can decrease while the undisturbed shear strength and water content remain constant (Fig. 2). Even though an open flocculated fabric is necessary, it is not a sufficient condition for quick-clay development. The fabric of quick clay and that of adjacent zones of much less sensitive clays may indeed be the same.

In theory, geophysical methods can be adopted to distinguish flocculated structures from more dispersed ones. The high-void ratio implies indeed lower density, which in turn might give lower seismic velocities. Yet, the density difference between flocculated and dispersed structures might not be large enough to have a noticeable seismic velocity change in practice. In addition, the higher water content due to larger pores will affect the dielectric constant and resistivity depending on the water composition, hinting that resistivity methods may well provide the better proxy.

Dealing only with marine clays in our study (left-hand side of Fig. 2), leaching of the salt by groundwater is the next essential step in the development of quick clay. In our context, salt refers to chemical compounds consisting in cations and anions. Leaching causes in principle little change in the flocculated

structure itself (only a small decrease in s_u) but the inter-particle repulsion forces may increase (large relative decrease of s_{ur} compared to s_u) and therefore increases the sensitivity (Bjerrum 1954). Although leaching of salt is necessary, it may not be sufficient for the development of quick clay (Penner 1965; Talme 1968; Söderblom 1969). The underlying reason is that the ion composition and the relative amounts of monovalent and divalent cations in the pore water have a controlling influence on the inter-particle forces and thus affect the formation of quick clay (Söderblom 1974). Therefore, depending on the upstream flow path, the dominating ions of the leaching water will vary and so will the sensitivity. A good knowledge of the groundwater flow system is necessary to locate the leaching of marine clays and map the potentially quick-clay areas. The presence of permeable layers, such as sand and silt layers, which are connected to surface water or other water conducting layers, greatly enhances the possibility of leaching. The topography of the bedrock can also affect leaching: if there is a local high in the surface of the bedrock underlying the soil, the outflow of groundwater may be concentrated towards this point (Fig. 2). A concentration of the outflow of water results in more extensive leaching and thus a greater possibility of quick-clay formation at this point.

Using geophysical measurements, a variety of physical properties within the subsurface structure can be mapped in detail and thus, the potential flow paths can be located. Moreover, the amount of leaching (salt concentration in pore water) could possibly be imaged using a dielectric constant geophysical parameter (Solberg *et al.* 2010a,b; Solberg *et al.* 2012a,b) and the weak bonding of clay particles could potentially lead to an S-wave velocity decrease in leached clays (Donohue *et al.* 2009).

TEST-SITE INVESTIGATIONS

In this section, the discussed factors leading to the formation of quick clays and their physical properties are illustrated through geophysical and geotechnical investigations of two quick-clay sites in Norway. The first site is situated in Hvittingfoss (Fig. 3), about 80 km south-west of Oslo and was mitigated against a potential quick-clay landslide in 2008 (Moholdt 2008). The second site is located in Rissa (Fig. 4), about 40 km north-east of Trondheim and is well-known for the 1978 quick-clay landslide that was captured on video (Gregersen 1981; L'Heureux *et al.* 2012b). Table 2 gives the typical geophysical parameter ranges for both sites.

Data and methods

In order to better map the sediment deposits and supplement earlier geotechnical investigations, a number of ERT, seismic refraction, GPR, as well as RCPTU and SCPTU data were acquired in Hvittingfoss and Rissa (Figs 3 and 4). The acquisition parameters for the geophysical data are summarized in Table 1 and data processing is detailed in the following paragraphs.

ERT measurements

Two-dimensional (2D) resistivity measurements were carried out using a Terrameter LS (ABEM) based on the Lund-system developed by Dahlin (1993). Gradient arrays were used at either site, with additional dipole-dipole arrays in Hvittingfoss (Solberg *et al.* 2010b, 2012a). Data acquisition was planned according to modelling results. Data quality is generally good with only a very few measurements removed prior to inversion.

The apparent resistivity data were inverted with RES2DINV software (Loke 2010) using L1-norm inversion optimization.

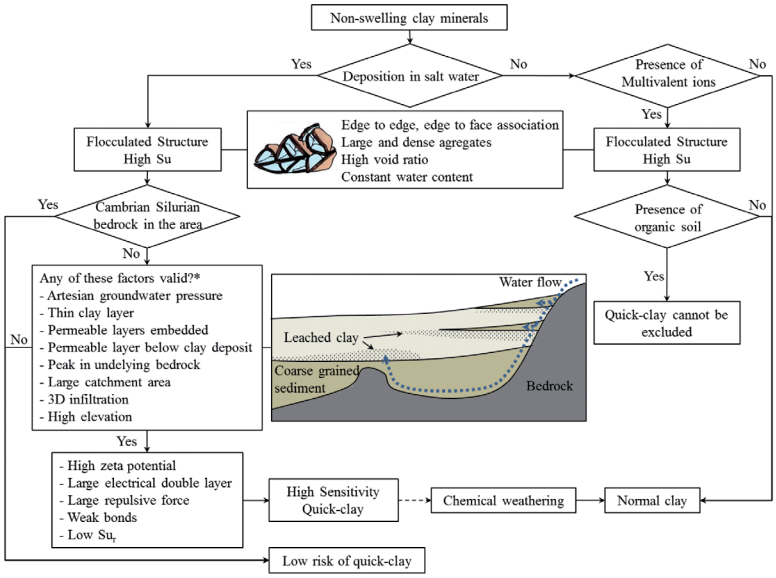

FIGURE 2
Schematic diagram of a quick-clay formation (adapted from Rankka *et al.* 2004). A schematic drawing of a flocculated clay particle along with the corresponding properties, as well as a schematic drawing of the preferential groundwater flows that leach the clay are included.
*The more factors, the higher the probability of a quick-clay formation.

Generally, inversions converged to RMS errors of less than 5% after 7 iterations. A vertical-to-horizontal flatness filter ratio of 0.5 was used for the inversion of the Rissa data to emphasis the horizontal subsurface structures. The 2D ERT profiles were then combined to generate pseudo-3D displays.

Seismic measurements

Two types of seismic measurements were carried out: MASW and SRT. Seismic data were recorded using a Geode (Geometrics) seismograph with a 5 kg sledgehammer as a seismic source and twenty four 4.5 Hz vertical geophones for both surface-wave and refracted-wave investigations. The overall seismic data quality is very good and little preprocessing was needed for both MASW and SRT.

For each of the configurations, dispersion curves were picked interactively using SurfSeis software (phase-velocity/frequency domain; Park *et al.* 1999). For most parts of the profiles, the fundamental Rayleigh mode is dominant. The 1D shear-wave velocity models are derived from the inversion of the dispersion curves using both an NGI inversion code, based on a modified Levenberg-Marquardt method for global minimization and SurfSeis. The 1D shear-wave velocity profiles were subsequently merged in a pseudo-2D profile. The initial soil model was defined based on the minimum and maximum phase velocities measured in the dispersion curves. All inversions performed with the NGI code converged rapidly, usually within 2 iterations and with low uncertainty, the variation coefficient (standard deviation normalized by the mean) being less than 2% above 10 m depth. Then, the uncertainty increases rapidly below 10 m.

Picking of first-arrival traveltimes for SRT was performed semi-automatically on raw data using seismic data processing software (VISTA) and, following fine tuning of the initial model, inversion of the traveltimes was performed using ReflexW (Sandmeier 2010). The inversion algorithm in the latter is based on an iterative adaptation (simultaneous iterative reconstruction technique).

GPR measurements

A Ramac (Malå) non-shielded 50 MHz rough-terrain antenna (RTA) was used for profiling, while standard Ramac 50 MHz

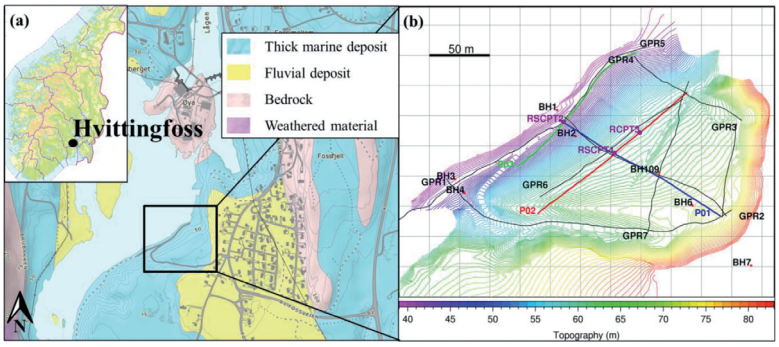

FIGURE 3
Hvittingfoss site: geological (a) and topographical (b) maps. On the latter, black lines are GPR profiles, green is ERT profile 3, red and blue are ERT and seismic refraction profiles 1 and 2. RCPTU, SCPTU and boreholes locations are also given.

TABLE 1
Geophysical data acquired at Hvittingfoss and Rissa. The 'Profile' row gives the number and length of the profiles. dGx and dSx respectively stand for geophone and source spacing.

		Hvittingfoss		**Rissa**	
ERT	Array type	Roll-along Gradient	Roll-along Dipole-Dipole	Roll-along Gradient (NGU reports 2010.045 and 2012.018)	
	Spacing	2 m	2 m	5 m	
	Profile	3 – 160 m	3 – 160 m	17- 400 to 1200 m	
Seismic	Method	P-wave Refraction, roll-along		MASW, roll-along	
	Source	Sledge hammer 5 kg		Sledge hammer 5 kg	
	T, dt	2 s, 0.25 ms		2 s, 0.25 ms	
	dGx	4 m		1 m	
	dSx	4 m		5 and 9 m	
	Profile	2 – 160 m		1 – 272 m	
GPR	Antenna	RTA 50 MHz	CMP 50 MHz	RTA 50 MHz	CMP 50 MHz
	Profile	7 – 80 to 450 m	1	17 along ERT	8

TABLE 2
Typical resistivity, P-wave and S-wave velocities value range for different geological units at both study sites.

	Geological unit	Resistivity (Ωm)	*Vp* (m/s)	*Vs* (m/s)
Hvittingfoss	Coarse grained material	> 150	250-750	
	Clay	25 – 100	> 1200	
Rissa	Coarse grained material	> 150		
	Leached clay	10 – 100		80 – 150
	Non leached clay	1 – 10		100 – 250
	Bedrock	> 1000		

non-shielded antennas were used for Common Mid Point (CMP) measurements. Several sites were carefully chosen for CMP acquisition in order to obtain representative velocity estimates. The GPR data quality is generally good but as the investigated sites are mainly composed of clays, depth penetration is limited because of the inherent high conductivity. GPR data preprocessing mainly consists in applying a dewow filter, subtracting DC shift and applying gain. A velocity model is then built using a diffraction hyperbola and/or CMP in order to perform time migration and depth conversion. GPR was then used to map sand and gravel deposits on top of the clay whenever present.

Geotechnical investigations

Ground conditions in the study areas were previously investigated by different consulting companies. The methods used include 54 mm piston samplers (with laboratory testing), rotary pressure sounding, CPTU, total sounding, rotary sounding and vane shear tests. For further descriptions of the geotechnical methods and interpretation see e.g., Gregersen and Løken (1983) and Lunne *et al.* (1997). To better link the geophysical and geotechnical properties, a few 1D resistivity and shear-wave velocity measurements were retrieved using RCPTU (both sites) and SCPTU (Hvittingfoss only). General stratigraphic information retrieved from GPR measurements and previous geotechnical investigations were used in Hvittingfoss to plan (via modelling) both ERT and seismic refraction investigations.

INVESTIGATION RESULTS

Hvittingfoss

Results

Investigations in Hvittingfoss carried out prior to mitigation showed that a moraine deposit is covered by a 10–40 m thick marine deposit (clay and silts) and that the latter is partly covered by sandy alluvial sediments (Moholdt 2008). Here, the marine deposit is termed 'clay' and the overlying alluvial sediment is termed 'sand' for the sake of simplicity. Note, however, that both formations are quite variable in composition. The depth-to-bedrock was not retrieved from previous investigations that mostly stopped at the moraine material. The sensitivity measured from the fall cone test on samples taken in borehole 2 (Fig. 3) ranges from 120–200, qualifying the soils as quick clay. As a result, the site was mitigated by moving parts of the soil from the upper part downwards to the lower slope to stabilize the latter, particularly considering the risk of erosion due to the river.

The GPR profiles indicate that the shallow sand layer is on average 15 m thick and thins towards the north-west (Fig. 5). Distinct reflectors with noticeable amplitude variations within the sand deposit suggest heterogeneity. Highly-attenuated zones along the profiles correspond to sediments with higher clay/silt content. Amplitude variations observed within the clay body are probably due to variations in grain size, confirmed by the geotechnical boreholes (Moholdt 2008). The boundary between the embankment fill added onto the slope and the original ground is also visible (Fig. 6a).

The 2D ERT profile 3 was acquired along the river and has a poor signal-to-noise ratio. Therefore, only the two higher-quality profiles are presented (Fig. 5b) and their corresponding GPR profiles will be later jointly discussed (Figs 6 and 7). The two 2D resistivity profiles show that low-resistivity values (ca. 15–100 Ωm) dominate at larger depth and that high-resistivity values (ca. >300 Ωm) are present at shallower depths. The latter values correspond to the coarse-grained cover and dry crust. The thickness of this high-resistivity layer varies from 2 m in the middle of the profiles to 15 m towards the eastern end of profile 1. Because of field restriction (profile lengths limited by the river and topography), the ERT penetration depth is too low to reach the underlying moraine deposit (as interpreted from geotechnical soundings). Resistivity values from RCPTU measurements are consistent with the ones from ERT (Fig. 5), thereby confirming the ERT inversion results (Rømoen *et al.* 2010; Sauvin *et al.* 2011; Solberg *et al.* 2011).

The two corresponding P-wave seismic refraction profiles (Figs 5a, 6c and 7c) show a thin top layer of low velocity (ca. 250–750 m/s) overlying a layer of higher velocity (ca. 1250–1750 m/s) at a depth of 3–20 m. North-west of the profiles (towards the river), in the deepest part, the velocity increases to 2250 m/s. Towards the river, the penetration depth along profile 1 is better than for ERT data and the strong increase of P-wave velocity could correspond to the moraine deposit (Fig. 6c). Moreover, the reflection stack section extracted from the seismic refraction data presents both a reflector that could be interpreted as the top of the moraine and as the top of the clay layer (Fig. 6d). From GPR and

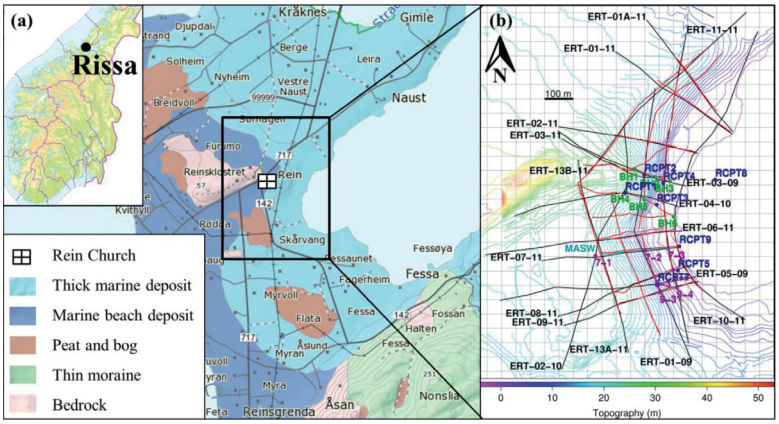

FIGURE 4
Rissa site; geological (a) and topographical (b) maps. On the latter, black lines are ERT profiles and red ones are GPR profiles (GPR line number corresponds to ERT line number). RCPTU, CMP and boreholes locations are also given.

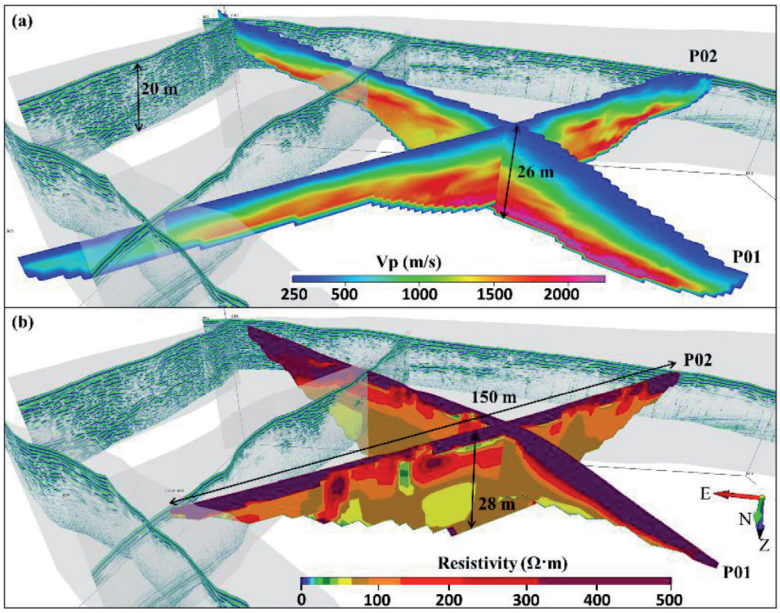

FIGURE 5
Hvittingfoss pseudo-3D view of GPR with the P-wave velocity derived from SRT (a) and resistivity from ERT (b). Vertical exaggeration of factor 2.

seismic reflection sections, which together give the depth to the top of the clay and moraine deposits, the thickness of the clay layer ranges from 10 m towards the river to 30 m at borehole 109.

Interpretation

Geophysical investigations show that the clay layer overlays a moraine deposit and the inherent permeability of the latter increases the probability of leaching. Because leached and non-leached clay have the same structure (flocculated), the P-wave velocity derived from seismic refraction tomography does not provide direct information to discriminate them. However, the lower P-wave velocities within the clay layer correlate with higher resistivity and GPR amplitude variations (Figs 6 and 7), suggesting grain-size variation. The GPR penetration in some part of the 'clay' layer indicates indeed the presence of 'sandy' material. Such permeable layers embedded in the clay may enhance the leaching of the surrounding clay. Unfortunately, the lack of resolution of the ERT data does not allow detailed correlation between resistivity variations and GPR images.

According to both the geological map (Fig. 3) and geotechnical soundings (Moholdt 2008), resistivity values ranging from 15–100 Ωm at this site mainly represent leached clay sediments

and high-resistivity values correspond to coarse sediments. This is in agreement with previous works (Solberg *et al.* 2010, 2011; Long *et al.* 2012). Resistivity values below 15 Ωm are not observed, suggesting that most of the clay has been leached, at least in the vicinity of the two ERT profiles. Therefore, this particular site does not allow for a proper geophysical comparison between leached and non-leached clay. However, the heterogeneity of both the clay and sand layers should be further studied with higher-resolution geophysical imaging, to better constrain their structure and composition, as well as their interface.

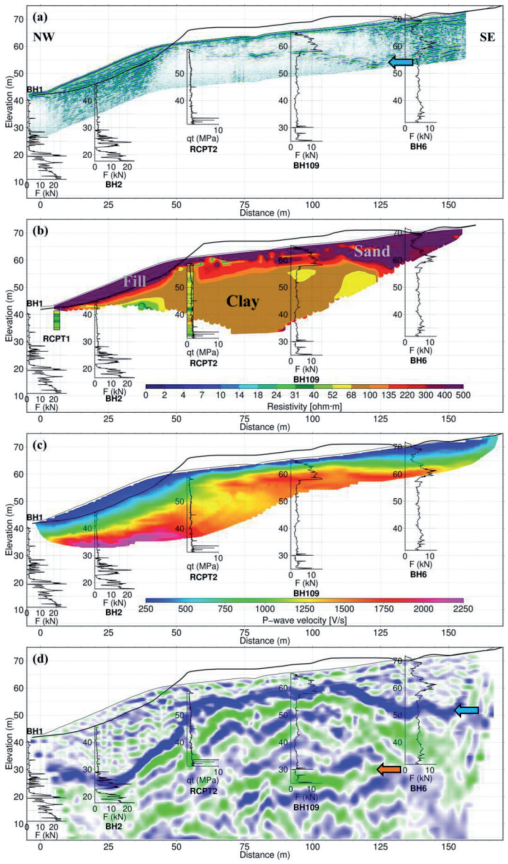

FIGURE 6

Hvittingfoss profile P01, a) GPR; b) resistivity from ERT with resistivity from RCPTU 1 and 2 superimposed, yellow colour corresponds to the resistivity range of quick clay; c) *Vp* from seismic refraction tomography and; d) seismic depth converted stack section (from refraction acquisition). Rotary pressure sounding from boreholes 1, 2, 109 and 6, as well as corrected tip resistance (q_t) from RCPTU 2, are superimposed on each section. Blue and orange arrows indicate sand-clay and clay-moraine interfaces, respectively. Topography prior site remediation is also given.

Rissa

Results

The study site at Rissa is relatively flat with a little hill to the south reaching an elevation of 50 m. To the north-east, the site borders a brackish inlet (Lake Botn). The sediments in the study area are defined as thick marine deposits covered at some location by coarser beach deposits (Reite 1987). Bedrock outcrops occur in the vicinity of the Rein church (Fig. 4). Geotechnical data in the middle of the study area reveal a general picture of a top layer of sand/gravel overlying clay. Some drillings penetrated through the clay and stopped on rock or coarse material. At these locations, medium or highly sensitive clays are found at several places, including thin layers of quick clay. Towards the south-east, medium or highly sensitive clay is more abundant, together with pockets of coarse material (at or below the clay) but the evidence of quick clay had not yet been demonstrated.

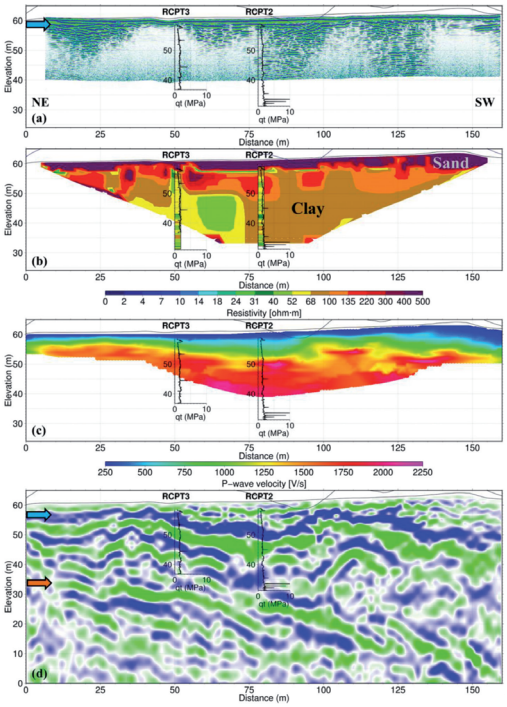

FIGURE 7

Hvittingfoss profile P02, a) GPR; b) resistivity from ERT with resistivity from RCPTU superimposed, yellow colour corresponds to the resistivity range of quick clay; c) *Vp* from seismic refraction tomography and; d) seismic depth converted stack section (from refraction acquisition). Corrected tip resistance (q_t) from RCPTU 2 and 3 are superimposed on each section. Blue and orange arrows indicate sand-clay and clay-moraine interfaces, respectively. Topography prior site remediation is also given.

As for Hvittingfoss, the GPR investigation at Rissa helps mapping sand/gravel deposits on top of the clay and even embedded within the clay. The penetration depth varies from 20 m in bedrock (near the Rein church) to less than 2 m in clay deposits (close to the lake). Interpreted sand layers from GPR data are in agreement with the results from geotechnical soundings and therefore allow for lateral extrapolation (Figs 8 and 9).

Close to the Rein church, a layer characterized by high-resistivity values (up to several thousand Ωm) corresponds to sand and/or gravel overlying the bedrock, which is confirmed by corresponding GPR profiles (Fig. 8a). Otherwise, resistivity pockets below 10 Ωm are probably non-leached marine clay, whereas the layers around 10–200 Ωm could potentially be leached clay (Fig. 8b). The ERT sections also indicate an undulating bedrock surface underneath the clay. By comparing the resistivity values from ERT and interpretations from drilling, most of the quick-clay deposits have resistivity values within 10–100 Ωm. No quick clay can be found for resistivity values below 10 Ωm, whereas some quick-clay areas exhibit relatively higher resistivity values (up to 200 Ωm) than usually attributed to quick clay (Solberg *et al.* 2010a,b). The resistivity range of quick clay as detected by RCPTU measurements at a few locations is in the range of 13–80 Ωm (Aasland 2010; Solberg *et al.* 2010b). Resistivity values from ERT are in good agreement with the ones from RCPTU (Fig. 9a).

The shear-wave velocity profile derived from inversion of Rayleigh wave dispersion curves exhibits velocity values varying between 80 m/s at the surface and 440 m/s in the deeper part (Fig. 10). The top soil has low velocities (< 125 m/s) in the first 5 m of the profile. Below, between 6–15 m depth, velocity values range between 150–250 m/s and correspond mainly to the interpreted leached clay deposit from ERT measurements and CPTU

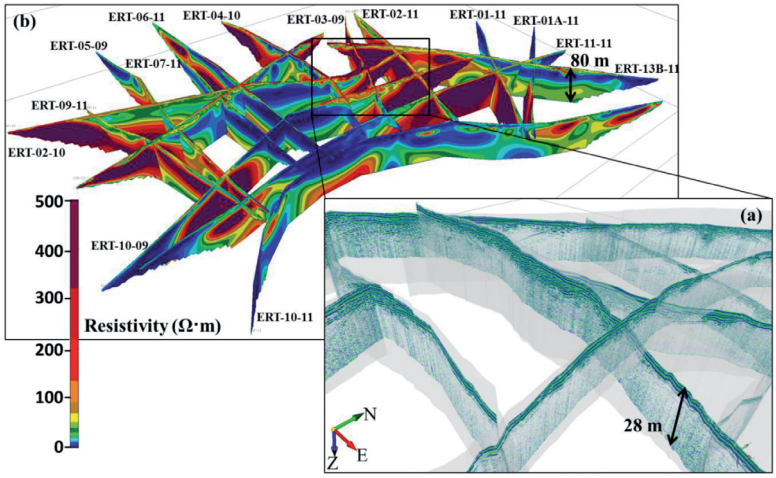

FIGURE 8
a) Rissa pseudo-3D view of resistivity profiles from ERT and b) a close up with GPR profiles. Vertical exaggeration of factor 2.5.

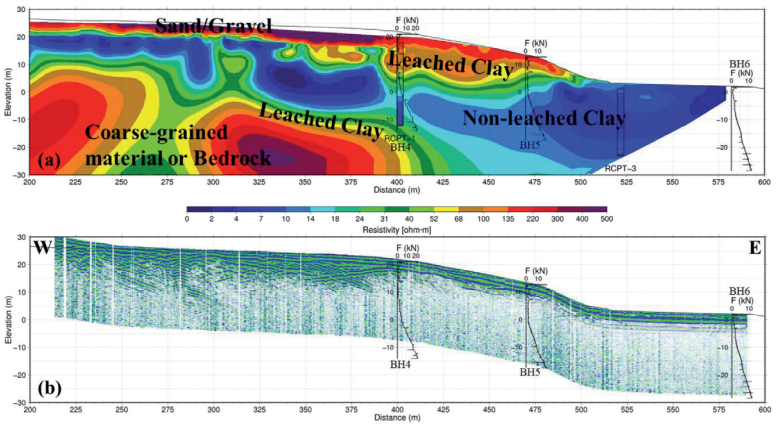

FIGURE 9
Part of the Rissa profile ERT-04-10, a) ERT with resistivity from RCPTU 1 and 3 superimposed, b) nearby GPR. Rotary pressure sounding from boreholes 4–6 are superimposed on each section.

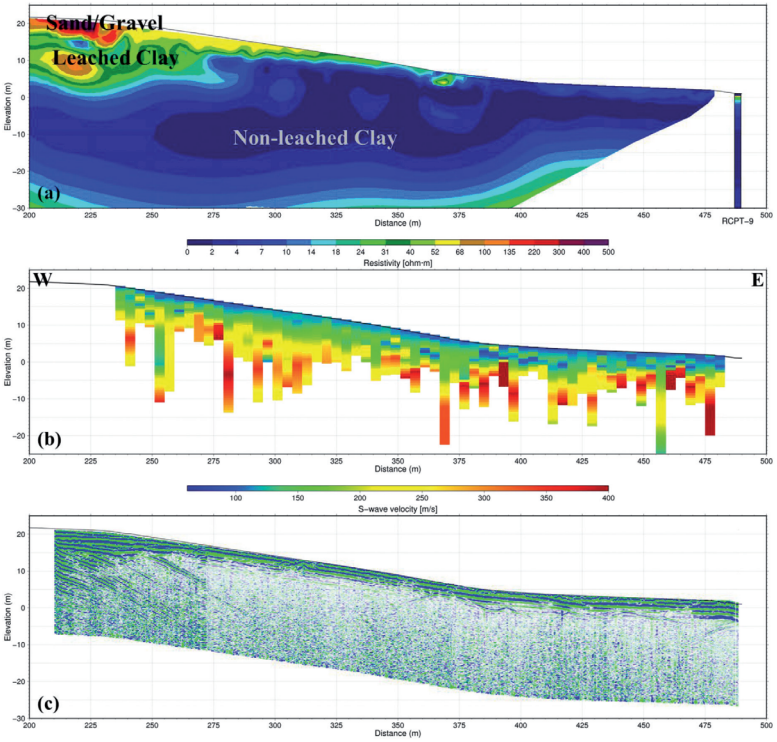

FIGURE 10
Part of the Rissa profile ERT-07-11, a) ERT with resistivity from RCPTU 9 superimposed, b) S-wave velocity from MASW and c) corresponding GPR.

soundings. The highest velocity values (>400 m/s) in the deepest part of the profile have also the highest uncertainty.

Interpretation

The dense grid of resistivity profiles (Fig. 8b) gives a good overall image of the distribution of the leached clay deposits. Most of the leached clay is found close to the surface and in the upper part of the slope i.e., west of the lake. This leached clay is generally lying on top of non-leached clay or bedrock and, less frequently, between non-leached clay and coarse-grain material or bedrock. Coarse-grain material inferred from GPR (Fig. 8a) and ERT (Fig. 8b) occurs at the surface in different locations. The clay adjacent to these coarse-grain pockets is typically leached. The general topography of the bedrock retrieved from ERT measurements (with large uncertainty on depth) gives the large catchment area that influences the groundwater flow. Moreover, knowing the depth-to-bedrock and the location of coarse-grain deposits, the thickness of the clay layers can be evaluated. Most of the non-leached clay is present where the clay deposit is the thickest. This is consistent with the fact that, due to its low permeability, the thicker the clay layer is, the longer it takes to leach the salt from it. Some drillings show thin layers of sand embedded in the clay, which cannot be retrieved from resistivity profiles due to lack of resolution. These permeable layers greatly influence the leaching of the clay and, in some places, can also be tracked on GPR profiles at shallow depths.

Two profiles were selected for a more detailed interpretation and data integration i.e., profile 4 south of the Rein church and profile 7 where the seismic data were recorded. Profile 4 runs from a rocky outcrop down to the lake (Fig. 4). ERT data and geotechnical soundings (Fig. 9a) along this profile were thoroughly studied in Solberg *et al.* (2010a). The nearby GPR profile (Fig. 9b) acquired in 2011 gives better insight into the distribution of the coarser-grain material deposit. The interface between this coarse unit and the clays can be retrieved and study of amplitude variations within the clay layer provides additional information on the degree of leaching. ERT and the geotechnical sounding in profile 7 were interpreted in Solberg *et al.* (2012a). The ERT data (Fig. 10a) show 5–15 m of leached clay immediately below the surface. Underneath and near the surface towards the east of the profile, one finds over 20 m of non-leached clay, which is confirmed by geotechnical boreholes. Below the clay, geotechnical sounding shows that coarser materials are present on top of the bedrock.

The ERT results were complemented with shear-wave velocities from MASW (Fig. 10b) and GPR measurements (Fig. 10c).

The GPR data along this profile help delineating the coarse-grain deposit at the surface in the western part; however, the low-resistive, non-leached clay attenuates the signals. Only subtle lateral variation can be noticed in the pseudo-2D shear-wave velocity plotted along this profile. Near the surface, a slight velocity decrease (~20 m/s) can be observed, in the western part of the profile, where leached clay was interpreted from ERT data. This velocity reduction is only marginally higher than the uncertainty and thus it needs to be confirmed by direct measurements (e.g., SCPTU, laboratory measurements).

CONCLUSIONS

Even if only laboratory measurements could tell whether or not a clay reaches the necessary value of sensitivity to be quick, the review of the physical properties of quick clays allows for a better understanding of their occurrence and potential location. The necessary conditions that a clay deposit must fulfil in order to be quick could be mapped using an integrated geophysical and geotechnical approach. Structural information retrieved from geophysical measurements may help locating preferential leaching paths, depending on bedrock topography, presence of underlying and/or embedded coarse-grained sediments and thickness of the clay layers. Resistivity variations and GPR attenuation within clay layers could also reflect the variation of salt concentration in the pore water and/or the variation in grain size. Combined to geotechnical soundings, it can also directly help to track layers of high sensitivity.

When geophysical measurements are used in an early phase of site investigations, they may provide useful input to the placement of wells. This would potentially limit the number of wells and information from drilling operations can be more valuable. Regarding the interpretation, geophysical data are used in the interpolation between the drill points, thus providing more realistic stability calculations. Since the profiles cover a relatively large area, it will facilitate a more comprehensive understanding of the area and its development both in terms of geology and geotechnical engineering.

The weak bonding of clay particles that could potentially lead to a decrease of S-wave velocity and attenuation in leached clays needs to be further investigated. Similarly, the potential distinction between flocculated and dispersed structures using seismic velocities has to be studied in detail. In this light, laboratory measurements and/or seismic velocity calibration would be needed. It would also be interesting to dispose of an S-wave seismic data set to validate its use for quick-clay characterization.

ACKNOWLEDGEMENTS

The authors acknowledge Nele Christine Meyer (ICG/UiO), Nadège Langlet (NORSAR/EOST), Sylvain Tissot (ICG/EOST), Christian Maskrey (ICG), Håkon Akerholt (NGI), Tor Overskeid (NGI) and Karine Petrus (NORSAR/EOST) for their help on the field and the University of Oslo for some of the equipment. The authors are grateful to Torleif Dahlin, Ranajit Ghose and Mike Long for several interesting and useful discussions in this ongoing project. Joonsang Park and Inge Viken are acknowledged for the development of the NGI inversion code of surface waves. The authors also thank Gedco and Sandmeier for providing academic licences. G. Sauvin thanks the funding partners of his PhD: the Norwegian Public Roads Administration, the Norwegian National Rail Administration, the Norwegian Water Resources and Energy Directorate and the International Centre for Geohazards. This is ICG contribution no. 395.

REFERENCES

Aasland R. 2010. *Kartlegging av kvikkleire med 2D resitivitet og RCPT I Rissa*. Master Thesis at the Department of Civil and Transport Engineering, NTNU.

Bentley S.P. and Smalley I.J. 1978. Inter-particle cementation in Canadian post-glacial clays and the problem of high sensitivity (St > 50). *Sedimentology* **25**, 297–302.

Bjerrum L. 1954. Geotechnical properties of Norwegian marine clays. *Géotechnique* **4**, 49–69.

Brand E.W. and Brenner R.P. 1981. *Soft Clay Engineering*. Elsevier.

Cabrera J.G and Smalley I.J. 1973. Quick clays as products of glacial action: A new approach to their nature, geology, distribution and geotechnical properties. *Engineering Geology* **7**, 115–133.

Conlon R.J. 1966. Landslide in Toulnustouc river, Quebec. *Canadian Geotechnical Journal* **3,** 113–144.

Crawford C.B. 1963. Cohesion in an undisturbed sensitive clay. *Géotechnique* **13**, 132–144.

Dahlin T. 1993. *On the automation of 2D resistivity surveying for engineering and environmental applications*. Doctoral Thesis, Lund University, Sweden

Dahlin T., Larsson R., Leroux V., Larsson R. and Rankka K. 2005. Resistivity imaging for mapping of quick clays for landslide risk assessment. I. *Proceedings of 11th Annual Meeting EAGE – Environmental and Engineering Geophysics*, Palermo, Italy, 4–7 September, 2005. A046.

Donohue S., Long M., O'Connor P., Helle T.E., Pfaffhuber A.A. and Rømoen M. 2012. Multi-method geophysical mapping of quick clay. *Near Surface Geophysics* **10**, 207–219.

Gregersen O. 1981. The quick clay landslide in Rissa, Norway. *NGI Publication* **135**, 1–6.

Gregersen O. 2008. Program for økt sikkerhet mot leirskred – Metode for kartlegging og klassifisering avfaresoner, kvikkleire. Norwegian Geotechnical Institute Report 20001008-2 (3rd revision). 24p. (In Norwegian.)

Gregersen O. and Løken T. 1983. Mapping of quick clay landslide hazard in Norway. Criteria and experiences. *SGI Technical Report* **17**, 61–174.

L'Heureux J.S. 2012a. A study of the retrogressive behaviour and mobility of Norwegian quick clay landslides. *Proceedings of the 11th International and 2nd North American Symposium on Landslides*, Banff, Canada.

L'Heureux J.S., Eilertsen R.S., Glimstad S., Issler D., Solberg I.-L. and Harbitz C.B. 2012b. The 1978 quick clay landslide at Rissa, mid-Norway: Subaqueous morphology and tsunami simulations. In: *Submarine Mass Movements and Their Consequences, Advances in Natural and Technological Hazards Research* (eds Y. Yamada *et al.*), p. 31. Springer Science+Business Media B.V. DOI 10.1007/978-94-007-2162-3_45.

Loke M.H. 2010. Res2DInv ver 3.59.102. Geoelectrical Imaging 2D and 3D. Instruction Manual. Geotomo Software, www.geoelectrical.com.

Long M., Donohue S., L'Heureux J.S., Solberg I.L., Rønning J.S., Limacher R. *et al*. 2012. Relationship between electrical resistivity and basic geotechnical parameters for marine clays. *Canadian Geotechnical Journal.*

Lunne T., Robertson P.K. and Powel J.J.M. 1997. Cone Penetration Testing in Geotechnical Practice. *Chapman and Hall, London.*

Mitchell J.K. 1976. *Fundamentals of Soil Behavior*. John Wiley and Sons, Inc.

Mitchell R.J. and Markell A.R. 1974. Flowslides in sensitive soils. *Canadian Geotechnical Journal* **11**(11), 31.

Moholdt R. 2008. Fossnes på Hvittingfoss, Vurdering av skredfare og sikringstiltak. NGI Report, 20071564-2 30.

Moon C.F. 1979. Concerning the relation between energy and cementation in quick clay disturbance. *Engineering Geology* **14**, 197–207.

NGF (Norsk Geoteknisk Forening). 1975. *Retningslinjer for presentasjon av geotekniske undersøkelser.* (In Norwegian.)

Park C.B., Miller D.M. and Xia J. 1999. Multichannel analysis of surface waves. *Geophysics* **64**(3), 800–808.

Penner E. 1965. A study of sensitivity in Leda clay. *Canadian Journal of Earth Sciences* **2**, 425–441.

Quigley R.M. 1980. Geology, mineralogy and geochemistry of Canadian soft soils: A geotechnical perspective. *Canadian Geotechnical Journal* **17**, 261–285.

Quigley R.M. and Ogunbadejo T.A. 1972. Clay layer fabric and oedometer consolidation of a soft varved clay. *Revue canadienne de Géotechnique* **9**, 165–175.

Rankka K., Anderson-Sköld Y., Hultén C., Larsson R., Leroux V. and Dahlin T. 2004. Quick clay in Sweden. *SGI Technical Report* **65**.

Reite A.J. 1987. Rissa. Kvartærgeologisk kart 1522 II - M 1:50 000. Beskrivelse. *NGU Skrifter* **82**.

Rømoen M., Pfaffhuber A.A., Karlsrud K. and Helle H.E. 2010. Resistivity on marine sediments retrieved from RCPTU soundings: A Norwegian case study. CPT'10: 2nd International Symposium on Cone Penetration Testing, Huntington Beach, California, USA.

Rosenqvist I.T. 1953. Considerations on the sensitivity of Norwegian quick clays. *Géotechnique* **3**, 165–200.

Rosenqvist I.T. 1955. Investigations in the clay-electrolyte-water system. *Norwegian Geotechnical Institute Publication* **9**.

Rosenqvist I.T. 1977. A general theory for quick clay properties. *Proceedings of the Third European Clay Conference,* Oslo, 215–228.

Sandmeier K.J. 2010. ReflexW, 5.5 ed, Karlsruhe. Processing of seismic, acoustic or electromagnetic reflection, refraction and transmission data.

Sauvin G., Bazin S., Vanneste M., Lecomte I. and Pfaffhuber A.A. 2011. Towards Joint Inversion/Interpretation for Landslide-prone Areas in Norway – Integrating Geophysics and Geotechnique. Expanded Abstracts. Near Surface – 17th European Meeting of Environmental and Engineering Geophysics.

Smalley I.J. 1971. Nature of quick clays. *Nature* **231**.

Söderblom R. 1966. Chemical aspect of quick clay formation. *Engineering Geology* **1**, 415–431.

Söderblom R. 1969. Salt in Swedish clays and its importance for quick clay formation. *SGI Technical Report* **22**.

Söderblom R. 1974. Organic matter in Swedish clays and its importance for quick clay formation. *SGI Technical Report* **55**.

Solberg I.L. 2007. *Geological, geomorphological and geophysical investigations of areas prone to clay slides: Examples from Buvika, Mid Norway*. PhD thesis, Department of Geology and Mineral Resources Engineering, Norwegian University of Science and Technology, p. 213.

Solberg I.L., Aasland R., Dalsegg E., Hansen L., L'Heureux J.S. and Rønning J.S. 2010a. Kvikkleireproblematikk i Rissa – Bruk av resistivitetsmålinger. Fjellsprengningsdagen, Bergmekanikk- og Geoteknikkdagen, Oslo 25–26.11.2010, 37.

Solberg I.L., Dalsegg E. and Hansen L. 2010b. Geofysiske målinger for løsmassekartlegging i Rissa, Sør-Trøndelag. *NGU Report* 2010.045

Solberg IL, Dalsegg E. and L'Heureux J.S. 2012a. Resistivitetsmålinger for løsmassekartlegging ved Rein kirke i Rissa, Sør-Trøndelag. Data og tolkninger. *NGU Report* 2012.018.

Solberg I.L., Hansen L., Rønning J.S., Haugen E., Dalsegg E. and Tønnesen J.F. 2012b. Combined geophysical and geotechnical approach to ground investigations and hazard zonation of a quick clay area, Mid Norway. *Bulletin of Engineering Geology and the Environment* **71**, 119–133.

Talme O. 1968. Clay sensitivity and chemical stabilisation. Byggforskingsrådet Technical Report 56, Stockholm.

Tavenas F., Flon P., Leroueil S. and Lebuis J. 1983. Remolding energy and risk of retrogression in sensitive clays. Symposium on slopes on soft clays, Linkoping. *Swedish Geotechnical Institute Report* **17**, 205–262.

Torrance J.K. 1974. A laboratory investigation of the effect of leaching on the compressibility and shear strength of Norwegian marine clays. *Géotechnique* **24**, 155–173.

Torrance J.K. 1978. Post-depositional changes in the pore-water chemistry of the sensitive marine clays of the Ottawa area, eastern Canada. *Engineering Geology* **14**, 135–147.

Torrance J.K. 1983. Towards a general model of quick clay development. *Sedimentology* **30**, 547–555.

Paper II

Geophysical Data Integration for Quick-Clay Mapping: The Hvittingfoss Case Study, Norway

G. Sauvin, I. Lecomte, S. Bazin, J.-S. L'Heureux, M. Vanneste

In *Landslides in Sensitive Clays: From Geosciences to Risk Management*, (eds. J.-S. L'Heureux et al.), Advances in Natural and Technological Hazards Research 36, Springer Science+Business Media Dordrecht 2013, pp. 236-246
doi:10.1007/978-94-007-7079-9_ 18

Paper III

On the integrated use of geophysics for quick-clay mapping: The Hvittingfoss case study, Norway

G. Sauvin, I. Lecomte, S. Bazin, L. Hansen, M. Vanneste, and J.-S. L'Heureux

Journal of Applied Geophysics, Revised

On the integrated use of geophysics for quick-clay mapping: The Hvittingfoss case study, Norway.

Guillaume Sauvin[1,2,3,*], Isabelle Lecomte[1,2,3], Sara Bazin[4], Louise Hansen[5], Maarten Vanneste[4], and Jean-Sébastien L'Heureux[4].

1) Oslo University, Box 1072 Blindern, 0316 Oslo, Norway

2) International Centre for Geohazards (ICG), P.O. Box 3930, N-0806 Oslo, Norway

3) NORSAR, P.O. Box 53, N-2027 Kjeller, Norway, Guillaume.Sauvin@norsar.no, Isabelle.Lecomte@norsar.no

4) Norwegian Geotechnical Institute (NGI), Sara.Bazin@ngi.no, Jean-Sebastien.LHeureux@ngi.no, Maarten.Vanneste@ngi.no

5) Geological Survey of Norway (NGU), Leiv Eirikssons vei 39, N-7491 Trondheim, Norway, Louise.Hansen@ngu.no

(*) Corresponding author, (+47) 96871869

Running head: Geophysics for quick-clay mapping.

ABSTRACT

Quick-clay landslides are a known hazard in formerly glaciated coastal areas; hence, large efforts are devoted to map the distribution of quick clays. In this paper, we focus on one particular Norwegian site (Hvittingfoss, 80 km south-west of Oslo), which was remediated against potential landsliding in 2008. A set of geophysical methods including Electrical Resistivity Tomography, P-wave seismic refraction tomography, S-wave seismic reflection profiling, and Ground Penetrating Radar, were jointly analysed and complemented with laboratory data and *in situ* geotechnical measurements (i.e., seismic and resistivity cone penetration testing with pore pressure measurement) in order to improve our geological understanding of the site and to establish a suitable, integrated and multi-disciplinary approach to better map the special extent of the quick-clay zone. The integration of the different geophysical methods and geotechnical measurements allowed a more precise imaging and characterization, both spatially and vertically, of the sedimentary sequences and of the underlying bedrock. The resulting geological model is then populated with the quantitative parameters derived from the geophysical measurements. Considering the inherent complexity of quick-clay mapping, the collected data illustrate the benefit of an integrated approach, and emphasise the need for high resolution, proper imaging, calibration and ultimately joint inversion of the different data.

KEYWORDS

Geophysical data integration; quick clay; georadar; resistivity; S-wave seismic reflection; seismic refraction; CPTU; landslide

HIGHLIGHTS

- Obtain high-resolution internal stratigraphy of the deposits.
- Establish correlations between geophysical and geotechnical parameters.
- Populate the geological-model with geotechnical parameters.
- Adopt a detailed geological-model for quick clay landslide assessment.

1. INTRODUCTION

A good understanding of soil conditions is a prerequisite for the safe development of urban zones. Some of the most densely populated regions of Norway lie within landslide-prone areas related to quick clays. According to Norwegian standards, quick clays have an undrained remoulded shear strength below 0.5 kPa (NGF, 1975). These sediments, originally deposited in a marine environment, emerged following glacio-isostatic rebound and fall of the relative sea level during the Holocene. Long-term leaching of salt due to groundwater flow and percolating surface water affects clay-particle bonding and makes the soil highly susceptible to liquefaction when disturbed (Mitchell, 1976; Brand and Brenner, 1981). Landslides involving quick clays often occur on low-angle slopes and they can be triggered by small perturbations in stress conditions caused by, e.g., human activity or erosion, e.g,, Saint-Jean-Vianney in 1971 (Tavenas et al., 1971, Potvin et al., 2001), Rissa in 1978 (Gregersen, 1981, L'Heureux et al., 2012), Finneidfjord in 1996 (Longva et al., 2003), Kattmarka in 2009 (Nordal et al., 2009), and St-Jude in 2010 (Locat et al., 2012). Several factors determine the final extent of a landslide in clay. These include, topography, stratigraphy and the clay sensitivity (i.e., ratio of undrained shear strength in its undisturbed condition s_u and undrained remoulded shear strength s_{ur}, see Table 1 for a list of acronyms) as well as the spatial distribution of the highly sensitive clay deposit or "quick clay" (e.g., Mitchell and Markell, 1974, Tavenas et al., 1983, L'Heureux, 2012). As such, one requires a variety of physical and geotechnical data for a proper landslide hazard mapping in the framework of planning and protection in such areas (Gregersen, 2008).

As of yet, the standard way of investigating quick-clay sites is largely based on the interpolation of results from 1D geotechnical soundings, such as Rotary Pressure Soundings (RPS) or Cone Penetration Testing with pore pressure measurements (CPTU). Often, with laboratory measurements, necessary for site-specific slope stability assessment, complement these *in situ* measurements. The soil properties necessary for determining the safety factor (i.e., density, internal angle of friction, effective cohesion, groundwater table height, undrained shear strength) are then assigned to each layer.

Whereas this traditional approach has been applied in several case studies and engineering projects, it suffers from spatial under-sampling of the soil properties, which may have important implications for the project. Indeed, important stratigraphic features are not necessarily properly mapped using solely 1D boreholes. Geophysical techniques, such as P-wave seismic refraction and electric methods, are sometimes used to interpolate/extrapolate between/from geotechnical boreholes, in which the latter serve as the necessary points for ground-truth, validation and calibration (Calvert and Hyde, 2002, Rankka et al., 2004, Dahlin et al., 2005, Solberg et al., 2008, 2012, Lundström et al., 2009, Donohue et al., 2012, Löfroth et al. 2012, Adamczyk et al. 2013). The geophysical methods yield different and complementary properties of the sub-surface. P-wave seismic refraction, for example, allows determining the P-wave velocities as well as depth to bedrock, whereas resistivity (as a pore-water ion-concentration indicator) is a proxy to differentiate leached from unleached clays (Rankka et al., 2004, Dahlin et al., 2005, Lundström et al., 2009, Donohue et al., 2012, Solberg et al. 2012, Sauvin et al. 2013). However, geophysical methods do not directly provide static or geotechnical soil parameters, notwithstanding the fact that the geophysical methods add complementary information, like 2D stratigraphy which is essential in safety assessment, and for which seismic reflection profiling is ideally suited. With respect to elastic properties, shear wave velocity relates to the stiffness soil, and is therefore an important geophysical parameters, particularly when vibration are of concerns. Shear wave velocities can be determined from either multi-channel analysis of surface wave (Donohue et al., 2012, Sauvin et al., 2013) or shear wave seismic reflection profiling and detailed velocity analysis and modelling (Pugin et al., 2009, 2013, Hunter et al., 2010, Crow et al., 2011; Polom et al., 2011, 2013, Malehmir et al., 2013a).

From our experience, there is no single geophysical method that yields the optimal information to accurately map the distribution of the quick-clay deposits. As a consequence, one should combine a variety of geophysical techniques (e.g., Electrical Resistivity Tomography - ERT; Multi-channel Analysis of Surface Wave; seismic refraction tomography; P- and S-wave seismic reflection; Ground Penetrating Radar - GPR); as well as geotechnical data (in-situ measurements using CPTU, seismic-CPTU and

106 resistivity-CPTU, laboratory tests) to build a consistent geo-model that can be populated
107 with multiple geophysical and geotechnical parameters. As such, quick-clay mapping
108 gradually moves towards 2D or pseudo-3D site characterization, thus improving the
109 stability assessment of the area. The present study illustrates the benefits of such multi-
110 disciplinary investigation, 1) to derive a consistent high-resolution geological model, as
111 also supported by previous studies (Malehmir et al., 2013b, Dahlin et al., 2013, Donohue et
112 al., 2012, Sauvin et al., 2013), and 2) for a more accurate correlation with relevant
113 geotechnical parameters.

114 Hvittingfoss, 80 km South-West of Oslo, Southern Norway (Figure 1), is located
115 within a quick-clay area which has been mapped during the nationwide quick-clay mapping
116 program, i.e., based on topography and geotechnical soundings. Because of river erosion at
117 the foot of the site, the steep slope and the inhabited area nearby, there was a concern about
118 the soil conditions and stability. Hence, in 2008, following geotechnical investigations, the
119 site was mitigated to prevent potential quick-clay landslide failure (Norwegian
120 Geotechnical Institute, 2008). Geotechnical investigations included geotechnical drillings,
121 mainly RPS, few CPTUs, and laboratory testing on samples extracted from one borehole.
122 The factor of safety was then determined using soil parameters simply linearly interpolated
123 between the boreholes for the interpreted soil units (Figure 1).

124 Because of the large amount of geotechnical data, this site was selected as a field
125 laboratory to evaluate the potential of geophysical quick-clay investigations. Geophysical
126 techniques used include ERT, GPR, P-wave seismic refraction tomography, and S-wave
127 seismic reflection data. In order to link the geophysical results to the geotechnical
128 parameters of interest, we also acquired additional resistivity-CPTU and seismic-CPTU
129 data.

130 The goals of the geophysical investigations are to obtain high-resolution information
131 on the internal stratigraphy of the deposits, to map the depth to bedrock, and to populate the
132 resulting geological model with geotechnical parameters (e.g., determine elastic properties
133 such as S-wave velocity of the sediment as a key proxy for their stiffness). Our objective is

to test the benefits of such a multi-disciplinary and multi-method investigation to enhance the geological model that could then be used for stability assessment in quick-clay prone areas.

2. SETTING

Bedrock around Hvittingfoss is dominated by syenite, quartz-syenite, romb porphyry, monzonite, and quartz-monzonite (Dahl, 1997). It crops out locally, to the waterfall just north of the investigated site and on Fossness plateau north-east of the site (Figure 1). Geotechnical soundings in Hvittingfoss area show an up to 30-m thick valley-filled by sand and gravel "alluvium" lying on top of glacio-marine clays which in turns cover the bedrock (boreholes 9 and 11; Figure 1; Norwegian Geotechnical Institute, 2008).

The top alluvial deposit is a sand and gravel unit, which is thickest on the Fossness plateau (Norwegian Geotechnical Institute, 2008) and thins both northwards and southwards across the investigated area. It overlays thick glacio-marine sediments, composed of silty clay with some thin layers of sand and gravel. These were deposited as the glacier ice was retreating in the Lågen valley (Dahl, 1997). Following deglaciation, the area was subject to glacio-isostatic rebound, causing a drop of relative sea level, thus locally exposing glacio-marine sediments above the present sea level and thereby to fresh groundwater leaching.

Laboratory measurements on samples from borehole 3 (Figure 1) indicate that the clay fraction in the glacio-marine deposits ranges from 18 to 30%, and the plasticity index is lower than 10-15% down to 12 m depth. Layers of silt, sand, and gravel lie underneath (Norwegian Geotechnical Institute, 2008). Part of the glacio-marine deposit was interpreted as quick clay as the penetration resistance of the RPS is nearly constant with depth, indicating that the soil is extremely soft (Rygg, 1988). The sensitivity of the clay measured from the fall cone test on samples exceeds 200 in borehole 3 and 500 in borehole 10 located further south. This values are well above the lower-bound value of 30 used in Norway, and thus the soils are classified as quick clays (Figure 1).

Due to the active erosion effect of the river to the west, stability has been gradually decreasing, endangering the housing area to the east. For that reason, the site was mitigated in 2008 by moving parts of the soil from the upper part of the slope downwards to the lower part, and erosion from the river was prevented by adding boulders at the bottom of the slope.

3. METHODS

In this section, we describe the applied geophysical methods (ERT, GPR, P- and S-seismics, as well as resistivity-CPTU and seismic-CPTU), including data acquisition details and processing steps. We also present the existing geotechnical data used in our study.

3.1 ERT measurements

We used results from previous geotechnical investigations (Norwegian Geotechnical Institute, 2008), to define a preliminary simple earth resistivity model, which we used in forward modelling in order to design a proper data acquisition. We subsequently collected 2D resistivity measurements using a Terrameter LS (ABEM) with both gradient and dipole-dipole array configurations. Acquisition was performed in roll-along mode with 64 electrodes with 2 m spacing, resulting in two 160-m long profiles (Figure 1). Full waveform data indicate that signal-to-noise ratio is high, and virtually no data had to be filtered out prior to inversion. 2D models of the earth subsurface resistivity were inverted from apparent resistivity using RES2DINV software (Loke, 2010) which uses the smoothness-constrained Gauss-Newton least-square inversion technique (Sasaki, 1992). Inversions converged to RMS errors of less than 5% after 7 iterations. Since both the gradient and dipole-dipole array configuration give similar resistivity model, and because of its lower sensitivity to noise (Dahlin and Zhou, 2006), we only present the results from inversion of gradient array configuration here. The 2D ERT profiles were then combined to generate pseudo-3D displays.

There is a rapid and sharp resistivity change across the boundary between the fluvial (sand, above) and the fjord (clay, below) deposits. In order to better constrain the resistivity

188 inversion within the clay deposits, the stratigraphic information from GPR and S-wave
189 seismic reflection were used as inversion constraints for ERT, i.e., the subsurface in the
190 inversion model can be divided into zones, one above and one below the interpreted
191 interface between the coarse grained material cover and the underlying clay deposit. Within
192 each unit, the resistivity values are constrained to vary smoothly, but an abrupt transition
193 across the zone boundary is allowed by removing all constraints between the resistivity
194 values below and above the zone boundary (Smith et al. 1999). Similar constrained
195 inversion presented by Bazin et al. (2013) for quick-clay mapping gave promising results.

196 **3.2 Seismic measurements**

197 Both P- and S-wave seismic measurements were conducted. The P-wave seismic
198 acquisition was initially designed for seismic refraction tomography alone. Acquisition was
199 performed using 24 4.5-Hz geophones, a Geode (Geometrics) seismograph and a 5-kg
200 sledgehammer as seismic source. Receivers and source spacing is 4 m, with shots in
201 between receiver stations. The recording length is 2 s with a time sampling of 0.25 ms. The
202 high quality of the seismic data (Figure 2) allowed for an accurate picking of the P-wave.
203 The S-wave seismic acquisition was designed for seismic reflection imaging, using three
204 Geode seismographs with a seismic horizontal vibrator unit developed by Polom (2011) as
205 shear-wave source and 71 horizontal geophones (12 Hz natural frequency). Due to the field
206 conditions along profiles 1 to 3 (high thick grass), geophones were planted, whereas a
207 landstreamer (Malehmir et al., 2013a, Krawczyk, 2013) was used as a test on the gravel
208 path for profile 4 (Figure 3). Source and receiver spacing is 1 m with shots located at
209 receiver stations, and "SH-mode" oriented, i.e., with vibration and recording oriented
210 horizontally and perpendicularly to the profile. The recording length is 11 s and time
211 sampling 1 ms, with a 10-s long 20-160 Hz up-sweep as source signal.

212 Picking of first-arrival travel times for seismic refraction tomography was performed
213 semi-automatically on raw data and the inversion of the travel times was performed. The
214 inversion algorithm adopts an iterative adaptation (Simultaneous Iterative Reconstruction

Technique, Nolet, 1987), and the final result is cross-checked by modelling with an eikonal solver (Vidale, 1988).

The S-wave seismic data processing is summarized in Table 2. A similar processing was applied to S-wave data set acquired in Trondheim harbour and discussed in details in Sauvin (2009) and Polom et al. (2010). We refer to these documents for further information on the different processing steps. The overall seismic data quality is good, but strong surface wave energy hinders some of the useful reflection energy (Figure 4).

3.3 GPR measurements

A Ramac (Malå) non-shielded 50-MHz rough-terrain antenna was used for profiling and standard Ramac 50-MHz non-shielded antennas for Common MidPoint (CMP) measurements. The GPR grid covers 100 m by 70 m with 1 m spacing between in-lines and cross-lines, which gives a total of 172 2D profiles. In order to obtain a representative velocity field, CMP acquisition was performed at every 10th grid point (10-m spacing) in both in-line and cross-line directions (Figure 1).

The fact that the pseudo-3D GPR cube is built up from several 2D near-zero-offset in-lines and cross-lines implies that some editing of each of individual profiles was necessary. First, we applied a static shift to each profile, in order to correctly position the zero time. To validate static shift value, we iteratively generated a cube from these profiles, inspect linear anomalies on time slices and adjust the static shifts. Then, standard dewow filtering (removal of low frequency noise related to the antenna characteristics), DC-shift subtraction and gain corrections (as well as careful background noise removal) were applied to all 2D profiles. Because of the topographic conditions, and since hip-chain was used for distance measurements between the grid point poles, the profile positions were iteratively verified by generating cubes from the 2D lines and shifting the anomalous ones from inspecting time slices. Finally, the resulting cube is depth converted using the velocity model extracted from diffraction hyperbolae and velocity analyses on CMP gathers.

3.4 Geotechnical investigations

Ground conditions in the study areas were previously investigated by different consulting companies (Norwegian Geotechnical Institute, 2008). The methods included 54-mm piston samplers (with laboratory testing), Rotary Pressure Sounding, CPTU, Total Sounding, Rotary Sounding and Vane Shear Tests. For the present study, we collected additional *in situ* data from resistivity-CPTU (3 locations) and seismic-CPTU (1 location) in order to link laboratory measurements with *in situ* measurements. One has to keep in mind that soft layers that are 75 to 100 mm thick can be fully detected by the cone resistance of the CPTU, whereas stiff layers may need to be as thick as 750 mm or more for the cone resistance to reach its full value (Lunne et al., 1997).

4. RESULTS AND INTERPRETATION

In this section, we present the results and interepretation from the integration of geophysical, geotechnical and geological data at the Hvittingfoss test site. We furthermore, assess how geophysical data can contribute to provide a more complete geological model, from a stratigraphic and quantitative point of view.

4.1 Geophysical results

4.1.1 Detailed presentation of results

Figures 5 and 6 show the results of (a) ERT inversion together with (b) GPR profiles, (c) S-wave interval velocity from reflection seismic velocity analysis, (d) the S-wave seismic reflection section, and (e) P-wave velocity from seismic refraction tomography, for profiles 1 and 2, respectively.

The results of resistivity imaging are spatially consistent (Figures 5a and 6a) and mismatch at intersection point could be explained by 3D effects or equivalence phenomena. Similarly, P- and S-wave velocity fields derived from P-wave seismic refraction tomography and S-wave seismic reflection velocity analyses are in good agreements and present generally increasing profiles with depth (Figures 5c, e and 6c, e). Since the GPR depth penetration is limited due to the strong attenuation of the GPR signal in clay (Figures

5b and 6b), the GPR data are mainly used for a detailed stratigraphic analysis of the upper, coarser material. The high-resolution of the S-wave seismic data (theoretical minimal vertical resolution of 0.4 m) allows for establishing a detailed geological interpretation at depth (Figures 5d and 6d) and detailed features can be extracted within some of the identified units.

The anthropogenic fill (above the blue line in Figure 5, and referred as unit D in Figures 7, 8 and 9) has very high resistivity values (ca. > 500 Ω·m), as well as low P- and S-wave velocities (ca. < 250 m/s and < 150 m/s, respectively). The GPR data lack a coherent reflection pattern within the fill but its base (or top of the original topography) coincides with a strong reflection (Figure 5b). Upslope from this manmade fill, there is a reasonably consistent upper layer (referred as unit C) with high resistivity (ca. > 300 Ω·m), ranging in depth from 2 m in the middle of the profiles to about 15 m towards the eastern end of profile 1. P- and S-wave velocities within this layer are continuous and range from 250 to 750 m/s, and 150 to 180 m/s, respectively. GPR reflections are continuous over short distances and the S-wave seismic reflection pattern is horizontally stratified with medium continuity. Underneath this upper soil unit, resistivity decreases rapidly to low values (ca. 20-100 Ω·m) whereas P- and S-wave velocities increase from 1250 to 1750 m/s and 200 to 300 m/s, respectively. Both resistivity and seismic velocities results reveal some lateral variations within this layer (referred as subunits B3 and B4). The GPR signal is highly attenuated, showing only few very-low-amplitude reflectors. The S-wave seismic reflection pattern is horizontally stratified with rather good continuity. Underneath (subunits B1 and B2), only S-wave velocities from seismic reflection data could be retrieved since the penetration depth of the seismic refraction and ERT is not sufficient. S-wave velocity ranges from 250 to 380 m/s down to around 20 m elevation (around 40 m below the surface), and the reflection pattern is generally horizontally stratified with alternating low and high amplitudes. Below (unit A), the S-wave velocities exceed 400 m/s and the top is clearly delineated by a continuous high-amplitude reflection clearly. S-wave velocity values derived from seismic reflection and seismic-CPTU correlate well (Figures 5c and 6c), and, even if generally higher, resistivity values from ERT measurements and

297 resistivity-CPTU are in good agreement as well (Figures 5a and 6a), confirming the models
298 derived from surface measurements.

299 *4.1.2 Joint Interpretation and construction of the geological model*

300 The benefit of a multidisciplinary approach lies in the quantified joint interpretation of
301 different vintage of geophysical and geotechnical data. For Hvittingfoss, we present the
302 interpretaion along the S-wave seismic reflection profile 2 in Figure 7, in a pseudo 3D
303 fence of the S-wave seismic reflection in Figure 8, and the properties of each interpreted
304 unit is summarized in Figure 9.

305 All profiles were interpreted correlating the picked events from one profile to another
306 at the crossing points in the depth domain and correlating each profile to the geotechnical
307 data. Four main stratigraphic units (A to D, from bottom to top) are identified by the
308 internal reflection patterns and reflection amplitudes in the seismic and GPR reflection
309 sections as well as variations in resistivity, P- and S-wave velocities. Unit A is interpreted
310 as bedrock, units B and C as fjord and fluviodeltaic deposits, and unit D as anthropogenic
311 fill. Unit B can be further divided into four subunits (B1-B4), having slightly different
312 reflection patterns. The units make up a typical fjord-fill succession above bedrock which
313 corresponds to the model, proposed by, e.g., Corner, 2006.

314 The anthropogenic fill, Unit D, is known from the pre-existing topography and is
315 characterized by very high resistivity as well as low P- and S-wave velocities. Unit C,
316 interpreted as fluviodeltaic deposit, is characterized by high resistivity values, low P- and
317 S-wave velocities, horizontally-stratified S-wave seismic reflection pattern and continuous
318 to semi-continuous GPR reflections. RPS drilling resistance is typically high (up to 15 kN),
319 but varies with depth. This unit is mainly composed of coarse-grained material (sand and
320 gravel), with some thin clay layers. Distinct GPR reflections with noticeable amplitude
321 variations within the sand deposit suggest spatial heterogeneity. Highly-attenuated zones
322 along the profiles correspond to sediments with higher clay/silt content (Figures 5b and 6b).
323 The fjord deposit (unit B) is further divided in subunits according to changes in S-wave
324 seismic reflection patterns, RPS drilling resistance variations and geotechnical laboratory

test results. Subunit B4 is a fjord-marine sediments deposited in a quiet fjord environment. B4 corresponds to continuous to semi-continuous, sub-horizontal, stratified sequences on the S-wave seismic profile. RPS drilling resistance is constant with depth indicating quick clays. Laboratory measurements confirm the presence of quick clay in the lowest part of this unit, and normal clay above. Resistivity values in this subunit range between 15 and 100 Ω·m, thus close to the resistivity range (10-80 Ω·m) characteristic of leached clay and potentially quick clay (Solberg et al., 2012). The low P-wave velocities within this layer correlate with higher resistivity and GPR amplitude variations, suggesting grain-size variation. Subunit B3 is interpreted as fjord-marine sediments deposited in a glacier-distal fjord environment. The S-wave seismic reflection pattern is generally horizontally stratified with low amplitudes. Laboratory measurements indicate fine-grained sediments (silty-clay) with some thin hard parts (clasts or lenses of thin sand layers) towards the base. The entire subunit has likely an elevated sensitivity, inferred from the nearly constant RPS drilling resistance with depth. Resistivity values in this subunit are similar to subunit B4, i.e. between 20 and 80 Ω·m. No resistivity values below 15 Ω·m are observed, suggesting that most of the imaged fjord deposits have been leached in the vicinity of the two ERT profiles. Subunit B2 is interpreted as glaciomarine sediments deposited in a fjord environment close to a glacier. This subunit is characterized by high amplitude, horizontally stratified S-wave seismic reflection pattern. Results from laboratory measurements indicate fine and coarse layers succession (silty-clay/sand/gravel). The RPS drilling resistance is generally high but varies with depth (borehole 3 in Figure 7). Subunit B1 is interpreted as glaciomarine sediments deposited in an environment relatively close to the glacier. This subunit is interpreted from S-wave seismic reflection alone, since none of the other methods reach such depth. It is characterized by internal irregular reflection pattern with lower amplitudes and frequency content compared to the rest of unit B. Finally, unit A is the bedrock or stiff sub-stratum with internal irregular to poorly stratified reflection patterns, a continuous and very-high amplitude reflection at the top and high S-wave seismic velocity (> 450 m/s).

Since the interfaces are known from GPR and S-wave seismic reflection data, they can be used as sharp geological boundaries to invert for resistivity, in order to retrieve the

resistivity variations within subunits B3 and B4 decoupled from the high resistivity values of unit C (Figure 10). Little changes are observed, but the north-eastern part of the profile has more uniform resistivity values within subunits B4 and B3 when using sharp boundaries as inversion constraints.

4.2 Correlation with geotechnical parameters

In addition to the stratigraphic information extracted from geophysical and geotechnical data, results from geophysical measurements can be used, 1) as direct quantitative information, and 2) for correlation with geotechnical parameters, and 3) inter/extrapolation from geotechnical soundings, in order to, ultimately, populate the geological model with relevant quantitative parameters, which will contribute to improved hazard assessment.

Correlation of the geophysical data with the existing RPS and CPTU is good, and allows for an accurate interpretation of the upper units (Figures 5, 6 and 7). The geological model is therefore confirmed, and, wherever possible, filled with geophysical parameters. Parameters of interest for safety factor computation, e.g., density, internal angle of friction, effective cohesion, groundwater table height, undrained shear strength, and sensitivity, cannot be directly extracted from geophysical measurements (except maybe for the density, using micro-gravimetry, and the water table level), and therefore, one has to use the multi-disciplinary data to establish empirical correlations between geophysical and geotechnical parameters.

Previous studies (Long et al., 2012) report good relationships between resistivity and pore-water salt content have been presented, as well as resistivity and clay content or plasticity. However, no simple connections between s_{ur} or sensitivity and resistivity exist as such relationship depends on particle size distribution, mineralogy, ionic content, role of dispersing agents, etc. According to Torrance (1983), salt concentration has to be below 2 g/l for a clay to be considered “quick”, therefore, resistivity profiles inverted from ERT measurement can possibly be used as a necessary criterion for highly sensitive clay, based on salt content. From various Norwegian quick-clay sites, Long et al. (2012) derived the

following regression correlation between the resistivity R and the salt concentration S_c with a regression coefficient of determination R^2=0.8:

$$R = 49.4 \times {S_c}^{-0.83} \quad (1)$$

As another salt-content indicator, the GPR attenuation could potentially be used. The higher the salt content, the lower the resistivity, and hence, the higher the GPR attenuation.

As directly related to pore-water pressure, the ground-water table level is important when it comes to stability assessment. The water table can generally be retrieved from GPR measurements, but, in our case, because of the clay layer attenuating the electromagnetic signal, the detection of the groundwater table was not viable everywhere. However, combined with P-wave seismic refraction, the water table could be traced along the profiles (Figure 5). The ground-water table depth was also measured using piezometers in boreholes 1, 3 and 5, validating the results from the seismic refraction.

The internal angle of friction and effective cohesion are known from laboratory measurements on samples and are generally fixed for a given type of soil. Similarly, the density is measured and associated to a layer throughout the entire area. No correlations associated to these parameters were derived from geophysical measurements.

Since S-wave velocity (Vs) is directly connected to the small-strain shear modulus G_{max} ($G_{max} = \rho Vs^2$), it seems reasonable to use this parameter for correlation. As a first attempt, we correlate Vs to the net tip resistance q_n ($q_n=q_t-\sigma_{v0}$, corrected tip resistance minus the total vertical stress).

Even if the vertical resolution in the S-wave data and velocity results is too low for detection of very thin, decimetre-size layers evidenced on CPTU data, one can notice similar trends in q_n and Vs when directly compared (Figure 11). Almost every sign change in q_n slope coincides with abrupt variations in S-wave velocity (Figure 11). It is therefore possible to divide the Vs logs in sections (layers) corresponding to main sign changes in q_n derivative with depth (Figure 11). Since the layering derived from q_n slope variations

exhibits similarity with the actual stratigraphic interpretation, we can use the stratigraphy as main boundaries to infer empirical relationships between q_n and Vs (Figure 12). Therefore, using the S-wave seismic reflection patterns, one can estimate the net tip resistance from the S-wave interval velocity field in between continuous reflections, in agreement with the stratigraphic interpretation. Additionally, if more than one CPTU log is available along the same seismic profile, one can define an empirical correlation between q_n en Vs for every layer and at each CPTU location. The coefficients of the empirical correlations can then be interpolated and used to derive a more consistent q_n field from Vs. The coefficients used for the linear empirical correlations are given in Table 2 and the inferred net tip resistance field using the interpolated coefficients is presented in Figure 13.

5. DISCUSSION

The stratigraphic model inferred from geophysical interpretation is used to fill the gap between the 1D geotechnical boreholes and it provides the missing stratigraphic information as a priori information in inversion and joint analysis of the data. The geo-model can then be populated with quantitative parameters.

Interpretation of the geophysical data provides detailed stratigraphic information and a consistent geological model (e.g. Figures 8 and 9). The stratigraphy is of high importance in safety factor computations, and therefore the more detailed it is, the better the hazard assessment can be conducted. In this particular case, the geometry of the main layers interpreted from geophysical measurements is not too different from the one established from geotechnical soundings alone. However, the interpretation from complementary geophysical data could make a distinct difference at other sites, e.g., in the case where the spatial under-sampling of the geotechnical measurements leads to an inaccurate geological model. Additionally, when it comes to stability assessment relative to quick clay, one has to evaluate the remoulded shear strength of the clay. As the sensitivity of marine clays relates to the degree of leaching it has undergone, it is also important to know the preferential groundwater paths, i.e., locate the permeable layers and the highs in bedrock topography

435 (Sauvin et al. 2013, and references therein). The topography of the bedrock and the
436 geometry of the coarse grain layers were retrieved. This provides insights on the sub-
437 surface groundwater migration and the preferential leaching paths for the clay which
438 influence the local drainage (Løken, 1968) and therefore had a significant effect on the
439 formation of quick clay at that site (Malhemir et al. 2013a,b). The stratigraphic model
440 derived from geophysical interpretation is used to fill the gap between the 1D geotechnical
441 soundings and provides the missing stratigraphic information. The model can then be
442 populated with quantitative parameters.

443 As previously mentioned, the sensitivity of marine clays is related to the degree of
444 leaching it has undergone. Leached clay has a lower pore-water ion concentration
445 compared with unleached clay. Resistivity, being a function of pore-fluid conductivity,
446 could potentially give an estimate of the salinity of the clay and therefore be correlated to
447 the degree of leaching. Solberg et al. (2012) estimated that highly-sensitive or quick-clay
448 resistivity values generally exceed 10 Ω·m, and this is in agreement with the resistivity –
449 salt concentration correlation proposed by Long et al. (2012). Nevertheless, resistivity is
450 also a function of many other physical properties such as porosity, water saturation, and
451 grain size distribution, which means that resistivity alone could help mapping high sensitive
452 clay, but also that it is insufficient.

453 Looking at the geophysical parameters variation within each unit/subunit, it appears
454 that the sub-surface is more complex than initially thought using solely the geotechnical
455 boreholes. The geophysical data reveal lateral variations in the physical properties. Looking
456 at resistivity, P- and S-wave velocity variations in subunits B4-B3 along profile 2, and the
457 corresponding GPR profile (Figure 6), it appears that the interpreted quick-clay layer
458 (subunit B4) is not homogeneous and it includes non-quick clay zones with higher
459 resistivity (even on the resistivity profile inverted using sharp boundaries, Figure 10),
460 higher S-wave velocity and better GPR depth penetration. Similarly, geophysical
461 parameters vary along profile 1 (Figure 5), suggesting an inhomogeneous distribution of the
462 quick clays. These results suggest that quick-clay investigations using discrete and spatialy

isolated geotechnical boreholes can benefit significantly from complementary geophysical parameters profiles to interpolate in between, and extrapolate from these point-wise calibration points. This is further emphasized by the good consistency between S-wave velocity and resistivity values from seismic-CPTU and resistivity-CPTU measurements with those from S-wave seismic reflection and ERT.

Correlation of S-wave velocity with net tip resistance within layers defined upon net tip resistance slope variation is good and is used to populate the geological model (Figure 13). For stability assessment, estimation of the undrained shear strength s_u is usually achieved through empirical correlations with CPTU results and laboratory measurements. One of the empirical approaches available for interpretation of s_u from CPT/CPTU results uses the net tip resistance as follows (Karlsrud et al., 1997):

$$s_u = \frac{q_n}{N_{kt}}, \tag{2}$$

where N_{kt}, is a cone factor based on effective cone resistance, and typically obtained from matching CPTU data with results from advanced geotechnical laboratory tests (e.g., triaxial shear strength tests under compression). Using this correlation, one can also correlate the S-wave velocity field to the undrained shear strength.

One critical aspect in our work is to establish empirical relationships between G_{max} and soil index properties, and hence, relating dynamic and static soil properties. Norwegian practice normalises G_{max} with respect to the sum of consolidation stress and attraction to obtain a dimensionless parameter that depends on friction only (e.g. Janbu, 1985). For the case of the small-strain shear modulus, Langø (1991) suggested that the normalized small-strain shear modulus g_{max} can be written as

$$g_{max} = \frac{G_{max}}{\sigma'_m + a} \tag{3}$$

where σ'_m and a are the mean effective consolidation stress and the attraction measured in triaxial tests, respectively. According to Langø (1991), Long and Donohue (2007, 2010), and L'Heureux et al. (2013) a systematic variation in normalised shear modulus may be

obtained by plotting g_{max} as a function of water content (Figure 14). There is a reasonable correlation between g_{max} and the water content. Here, the attraction (a) was assumed to be equal to 3 kPa, which is a typical value for the clays studied by Janbu (1985). The results are consistent with data found in literature (Figure 14) suggesting that the correlation defined previously between Vs and the net tip resistance could be extended to other clay sites.

6. CONCLUSIONS

In addition to the dense geotechnical dataset available at Hvittingfoss test site, a number of geophysical methods were combined in order to improve our geological understanding of the site, which can lead to improved hazard assessment. Following careful planning, acquisition and processing of different types of geophysical data using geotechnical boreholes as ground proofing, we established a more detailed stratigraphy model based on the integration of all geophysical methods and geotechnical measurements available. As such, geophysics is used to fill the gap between the isolated 1D geotechnical boreholes. The resulting geological model also serves to better understand the local drainage system responsible for the salt leaching from the clay, information which cannot be derived unambiguously from geotechnical measurements alone. The geological model is then populated with the quantitative parameters derived from the geophysical measurements, which directly helps to map and identify the area where highly sensitive clay may be found (i.e. resistivity and GPR attenuation as proxy for salt concentration and degree of leaching, Vs for stiffness and Vp/Vs for saturation). S-wave velocity correlation with net tip resistance allows populating the geological model with geotechnical parameters, particularly suited for hazard assessment when vibrations are generated (e.g., blasting). The high-resolution geological model resulting from the integration of several geophysical methods and geotechnical data helps locating the potential quick clay and can subsequently be used as input for more realistic and advanced 2D to 3D stability simulations. Correlation between geophysical parameters and remoulded shear strength is still lacking, and therefore, more lab measurements would be required.

519 ## ACKNOWLEDGEMENTS

520 The authors are grateful to Magnus Rømoen for providing the geotechnical data previously
521 acquired. The authors also thank Gedco and Sandmeier for providing academic licences to
522 ICG (Vista and ReflexW, respectively). The authors acknowledge Nadège Langlet, Sylvain
523 Tissot, Christian Maskrey, Håkon Akerholt, Tor Overskeid, Karine Petrus, Mesay Geletu
524 Gebre, Gunther Druivenga (GEOSYM) and Berit Paulsen for their help in the field.
525 Guillaume Sauvin thanks the sponsors of his PhD thesis: the Norwegian Public Roads
526 Administration, the Norwegian National Railway Administration, the Norwegian Water
527 Resources and Energy Directorate, and the International Centre for Geohazards.

528

REFERENCES

Adamczyk, A., M. Malinowski, and A. Malehmir, 2013, Application of first-arrival tomography to characterize a quick-clay landslide site in southwest Sweden. Acta Geophysica, **61**, 1057-1073.

Bazin S., and A.A. Pfaffhuber, 2013, Mapping of quick clay by electrical resistivity tomography under structural constraint. Journal of Applied Geophysics, **98**, 280-287.

Brand E.W., and R.P. Brenner, 1981, Soft clay engineering, Elsevier.

Calvert H.T., and C.S.B. Hyde, 2002, Assessing landslide hazard in the Ottawa Valley using electrical and electromagnetic methods. In: Proceedings of the Symposium on the Application of Geophysics to Engineering and Environmental Problems (SAGEEP), Las Vegas. Environmental and Engineering Geophysical Society, Wheat Ridge, 10-14 February 2002.

Crow H.L., J.A. Hunter, and D. Motazedian, 2011, Monofrequency in situ damping measurements in Ottawa area soft soils. International Journal of Soil Dynamics and Earthquake Engineering **31**, 1669-1677.

Dahl Å., K. S. Olsen, and R. Sørensen, 1997, Holmestrand 1813 IV, Quaternary geological map – M 1:50000 with description. NGU.

Dahlin T., R. Larsson, V. Leroux, R. Larsson, and K. Rankka, 2005, Resistivity imaging for mapping of quick clays for landslide risk assessment. In: Proceedings of the 11th annual meeting EAGE - environmental and engineering geophysics, Palermo, 4-7 September 2005, A046.

Dahlin T., and B. Zhou, 2006, Multiple-gradient array measurements for multichannel 2D resistivity imaging. Near Surface Geophysics, **4**, 113-123.

Dahlin T., H. Löfroth, D. Schälin, and P. Suer, 2013, Mapping of quick clay using geoelectrical imaging and CPTU-resistivity. Near Surface Geophysics **11**, 659-670.

554 Donohue S., M. Long, P. O'Connor, T. Eide-Helle, A.A. Pffaffhuber and M. Rømoen,
555 2012, Multi-method geophysical mapping of quick clay. Journal of Near Surface
556 Geophysics, EAGE, **10**(3), 207-219.

557 Gregersen O., 1981, The quick clay landslide in Rissa, Norway. Norwegian Geotechnical
558 Institute Publication, vol 135, 1-6.

559 Gregersen O., 2008, Program for økt sikkerhet mot leirskred – Metode for kartlegging og
560 klassifisering avfaresoner, kvikkleire. Norwegian Geotechnical Institute Report
561 20001008-2 (3rd revision). 24p. (In Norwegian).

562 L'Heureux J.S., 2012, A study of the retrogressive behaviour and mobility of Norwegian
563 quick clay landslides. Proceedings of the 11th International and 2nd North American
564 Symposium on Landslides, Banff, Canada.

565 L'Heureux J.S., R.S. Eilertsen, S. Glimstad, D. Issler, I. Solberg, C.B. Harbitz, 2012, The
566 1978 quick clay landslide at Rissa, mid-Norway: subaqueous morphology and tsunami
567 simulations. In: Yamada Y et al. (eds) Sub-marine mass movements and their
568 consequences, vol 31, Advances in natural and technological hazards research.
569 Springer, Dordrecht, 507-516

570 L'Heureux J.S., M. Long, M. Vanneste, G. Sauvin, L. Hansen, U. Polom, I. Lecomte, J.
571 Dehls, and N. Janbu, 2013, On the prediction of settlement from high-resolution shear-
572 wave reflection seismic data: The Trondheim harbour case study, mid Norway.
573 Engineering Geology (2013), doi: 10.1016/j.enggeo.2013.10.006

574 Hunter J.A., H.L. Crow, G. Brooks, D. Motazedian, et al., 2010, Seismic site classification
575 and site period mapping in the Ottawa area using geophysical methods, Geological
576 Survey of Canada, Open File Report 6273.

577 Janbu N., 1985, Soil models in offshore engineering. Géotechnique, **35**, 241-281.

578 Karlsrud K., T. Lunne, K. Brattlien, 1996, Improved CPTU correlations based on block
579 samples, Proc. Nordic Geotechnical Conference, Reykjavik, 1996, Vol. 1, pp. 195–
580 201.

581 Krawczyk C.M., U. Polom and T. Beilecke, 2013, Shear-wave reflection seismic as a
582 valuable tool for near-surface urban applications. The Leading Edge, Special section:
583 Urban geophysics, **32**, 256-263.

584 Langø H., 1991, Cyclic shear modulus of natural intact clays. Ph.D. thesis, Norwegian
585 Institute of Technology (NTH), Trondheim, Norway.

586 Locat P., D. Demers, D. Robitaille, T. Fournier, F. Noël, S. Leroueil, A. Locat, G.
587 Lefebvre, 2012, The Saint-Jude landslide of May 10, 2012, Québec, Canada. In:
588 Eberhardt E., Froese C., Turner A.K., Leroueil S (eds) Landslides and engineered
589 slopes - protecting society through improved understanding, vol 1. CRC Press,
590 London, UK, 635-640.

591 Löfroth H., P. Suer, D. Schalin, T. Dahlin, and V. Leroux, 2012, Mapping of quick clay
592 using sounding methods and resistivity in the Göta River valley. Geotechnical and
593 Geophysical Site Characterisation 4. In: Couthino R.C., Mayne P.W. (eds) Proceedings
594 of the 4th international conference on site characterisation (ISC-4) 2, 1001-1008, CRC
595 Press, Taylor & Francis Group, Balkema.

596 Loke M.H., 2010, Res2DInv ver 3.59.102. Geoelectrical Imaging 2D and 3D. Instruction
597 Manual. Geotomo Sotware, http://www.geotomosoft.com/.Long M., and S. Donohue,
598 2007, In situ shear wave velocity from multichannel analysis of surface waves
599 (MASW) tests at eight Norwegian research sites. Canadian Geotechnical Journal, **44**,
600 533-544.

601 Long M., S. Donohue, 2010, Characterization of Norwegian marine clay with combined
602 shear wave velocity and piezocone cone penetration test (CPTU) data. Canadian
603 geotechnical Journal, **47**, 709-718.

604 Long M., S. Donohue, J.S. L'Heureux, I.L. Solberg, J.S. Rønning, R. Limacher, P.
605 O'Connor, G. Sauvin, M. Rømoen, I. Lecomte, 2012, Relationship between electrical
606 resistivity and basic geotechnical parameters for marine clays. Canadian Geotechnical
607 Journal, **49,** 1158-1168.

608 Longva O., N. Janbu, L.H. Blikra, R. Boe, 2003, The 1996 Finneidfjord slide: seafloor
609 failure and slide dynamics. In: Locat J., Mienert J. (eds) Submarine mass movements
610 and their consequences. Kluwer, Dordrecht, 531-538.

611 Lundström K., R. Larsson, and T. Dahlin, 2009, Mapping of quick clay formations using
612 geotechnical and geophysical methods. Landslides **6**, 1-15.

613 Lunne T., P.K. Robertson, and J.J.M. Powell, 1997, Cone Penetration Testing in
614 Geotechnical Practice. Chapman & Hall, London.

615 Løken T., 1968, Kvikkleiredannelse og kjemisk forvitring i norske leirer. Norwegian
616 Geotech-nical Institute, Oslo. Publication 75, 19-26. (In Norwegian).

617 Malehmir, A., M. Bastani, C. Krawczyk, M. Gurk, I. Nazli, U. Polom, and L. Persson,
618 2013, Geophysical assessment and geotechnical investigation of quick-clay landslides -
619 a Swedish case study. Near Surface Geophysics, **11**, 341-350.

620 Malehmir, A., U.M. Saleem, and M. Bastani, 2013, High-resolution reflection seismic
621 investigations of quick-clay and associated formations at a landslide scar in southwest
622 Sweden. Journal of Applied Geophysics, **92**, 84-102.

623 Mitchell J.K., 1976, Fundamentals of soil behavior. John Wiley and Sons, Inc.

624 Mitchell R.J., and A.R. Markell, 1974, Flowslides in sensitive soils. Canadian Geotechnical
625 Journal, **11**, 11-31.

626 Norwegian Geotechnical Institute, 2008, Fossnes på Hvittingfoss, Vurdering av skredfare
627 og sikringstiltak. Norwegian Geotechnical Institute report, 20071564-2 30.

628 NGF (Norsk Geoteknisk Forening), 1975, Retningslinjer for presentasjon av geotekniske
629 undersøkelser (In Norwegian).

630 Nolet G., 1987, Seismic tomography, D. Reidel Publ. Co., Dordrecht.

631 Nordal S., C. Alén, A. Emdal, L. Jendeby, E. Lyche, and C. Madshus, 2009, Skredet i
632 Kattmarkvegen i Namsos 13. mars 2009 - Rapport fra undersøkelsesgruppe satt ned av
633 Samferdselsdepartementet. Tapir Uttrykk, Trondheim (In Norwegian).

634 Polom U., L. Hansen, G. Sauvin, J.S. L'Heureux, I. Lecomte, C.M. Krawczyk, M.
635 Vanneste, and O. Longva, 2010, High-resolution SH-wave Seismic Reflection for
636 Characterization of On-shore Ground Conditions in the Trondheim Harbor, Central
637 Norway. In: Miller, R.D., Bradford, J.D. and Holliger, K. (Eds.) Advances in Near-
638 Surface Seismology and Ground-Penetrating Radar. SEG, Tulsa, 297-312.

639 Polom U., G. Druivenga, E. Grossmann, S. Grüneberg, and W. Rode, 2011, Transportabler
640 Scherwel-lenvibrator. Patent application DE 103 27 757 A1, Deutsches Patent- und
641 Markenamt (in German).

642 Polom U., M. Bagge, S. Wadas, J. Winsemann, C. Brandes, F. Binot, and C.M. Krawczyk,
643 2013, Surveying near-surface depocentres by means of shear wave seismics. First
644 Break, **31**, 67-79.

645 Potvin J., F. Pellerin, D. Demers, D. Robitaille, P. La Rochelle, and J.Y. Chagnon, 2001,
646 Revue et investigation supplémentaire du site du glissement de Saint-Jean-Vianney.
647 54th Canadian geotechnical conference, Calgary, vol 2, 792-800.

648 Pugin A.J.M., S.E. Pullan, and J.A. Hunter, 2009, Multicomponent high-resolution seismic
649 reflection profiling. Leading Edge **28**(10), 1248-1261.

650 Pugin A.J.M., K. Brewer, T. Cartwright, S.E. Pullan, D. Perret, H. Crow, and J.A. Hunter,
651 2013, Near surface S-wave seismic reflection profiling – new approaches and insights.
652 First Break **31**(2), 49-60.

653 Rankka K., Y. Anderssen-Skold, C. Hulten, R. Larsson, V. Leroux, and T. Dahlin, 2004,
654 Quick clay in Sweden. Report 65. Swedish Geotechnical Institute, Linkoping

655 Rosenqvist I.T., 1953, Considerations on the sensitivity of Norwegian quick-clays.
656 Geotechnique **3**, 195-200.

657 Rygg N., 1988, Rotary pressure sounding: 20 years of experience. Proc. Pen Testing, 1988,
658 ISOPT-1, De Ruiter ed., Balkema, 453-457.

659 Sasaki Y., 1992, Resolution of resistivity tomography inferred from numerical simulation.
660 Geophysical Prospecting, 40, 453-464.

661 Sauvin G., I. Lecomte, S. Bazin, J.S. L'Heureux, and M. Vanneste, 2013, Towards
662 geophysical and geotechnical integration for quick clay mapping in Norway. Journal of
663 Near Surface Geophysics, EAGE, **11**, doi: 10.3997/1873-0604.2012064.

664 Sauvin G., 2009, S-wave seismic for geohazards: A case study from Trondheim Harbor:
665 Diploma engineering thesis, University of Strasbourg, 2009-6-1.

666 Solberg I.L., L. Hansen, J.S. Rønning, E. Dalsegg, L. Hansen, K. Rokoengen, and R.
667 Sandven, 2008, Resistivity measurements as a tool for outlining quick-clay extent and
668 valley-fill stratigraphy: a feasibility study from Buvika, central Norway. Canadian
669 Geotechnical Journal, **45**, 210-225.

670 Solberg I.L., L. Hansen, J.S. Rønning, E. Haugen, E. Dalsegg, J.F. Tønnesen, 2012,
671 Combined geophysical and geotechnical approach to ground investigations and hazard
672 zonation of a quick clay area, Mid Norway. Bull. Eng. Geol. Environ, **71**, 119-133.

673 Smith T., M. Hoversten, E. Gasperikova, and F. Morrison, 1999, Sharp boundary inversion
674 of 2D magnetotelluric data. Geophysical Prospecting, **47**, 469-486.

675 Tavenas F., J.Y. Chagnon, P. La Rochelle, 1971, The Saint-Jean-Vianney landslide:
676 observations and eyewitnesses accounts. Canadian Geotechnical Journal, **8**,463-478.

677 Tavenas F., P. Flon, S. Leroueil and J. Lebuis, 1983, Remolding energy and risk of
678 retrogression in sensitive clays. Symposium on slopes on soft clays, Linkoping,
679 Swedish Geotechnical Institute Report, No. 17: 205-262.

680 Torrance J.K., 1983, Towards a general model of quick clay development. Sedimentology,
681 **30**, 547-555.

682 Vidale J., 1988, Finite-Difference calculation of travel times, Bulletin of
683 Seismological.Society of America, **78**, 2062-2076.

684

TABLES

Table 1: List of acronyms.

Table 2: Processing flowchart and corresponding parameters for S-wave seismic reflection data.

Table 3: Table summarizing the empirical factor for net tip resistance – Vs correlation, q_n = a*Vs+b, for each CPTU along seismic lines and every layers. The last column indicates the correlation parameters for all the CPTU and all the layers together.

FIGURES

Figure 1: Map showing a) quaternary geology of the Hvittingfoss area and b) the topography of the investigation site, with location of geophysical measurements, blue lines for ERT and P-wave seismic, red and blue for S-wave seismic and green rectangle for GPR, as well as location of geotechnical data, red dots for rotary pressure soundings and purple triangles for CPTU tests.

Figure 2: Selected P-wave seismic pre-processed record examples of profile 2. X axis corresponds to shot and channel number (4-m spacing). The dashed blue lines correspond to the theoretical gradient of 333 m/s air wave velocity, which is not much recorded. The first arrival corresponding to the refracted waves are also displayed on these records (red picks). The blue arrows point at surface-wave energy and the green ones point at reflected energy. For the sake of the display, a 350 ms AGC is applied.

Figure 3: Pictures depicting S-wave seismic reflection acquisition using wheelbarrow mounted horizontal seismic vibrator with landstreamer along the gravel path for profile 4.

Figure 4: Selected S-wave seismic pre-processed record examples of profile 2. X axis corresponds to shot and channel number (2-m spacing). Strong surface-wave energy was recorded (blue arrows) and hides some of the important reflections (green arrows). The grey arrows point at refracted wave energy.

Figure 5: Profile 1, a) inverted resistivity from Gradient array, b) GPR profile extract from the depth converted GPR cube superimposed, c) S-wave interval velocity, d) depth converted S-wave seismic reflection, and e) P-wave velocity from seismic refraction tomography. One can notice the strong GPR reflection between the old (blue line) and new (black line) topography. Resistivity values as well as S-wave velocity from borehole 4 are also depicted with the same colour scale as for ERT and S-wave seismic respectively. The water table interpreted from GPR, seismic refraction and piezometer is also displayed in dashed line.

719 **Figure 6**: Profile 2, a) inverted resistivity from Gradient array, b) GPR profile extract from
720 the depth converted GPR cube superimposed, c) S-wave interval velocity, d) depth
721 converted S-wave seismic reflection, and e) P-wave velocity from seismic refraction
722 tomography. Resistivity values from borehole 4 and 5 as well as S-wave velocity from
723 borehole 4 are also depicted with the same colour scale as for ERT and S-wave seismic
724 respectively.

725 **Figure 7**: Profile 2, S-wave seismic reflection profile with borehole 3 (10 m offset), 4 and
726 5. The interpreted stratigraphy is superimposed on the S-wave seismic reflection profile and
727 the corresponding layers are coloured in b). The resistivity values and the corrected tip
728 resistance from boreholes 4 and 5, as well as the drilling resistance from borehole 3 are also
729 depicted.

730 **Figure 8**: (a) Pseudo 3D view of time-to-depth converted S-wave seismic reflection
731 profiles and boreholes 1, 6, and 7. The interpreted top of units are also displayed; black, top
732 unit C (actual topography); yellow, turquoise, green, and blue, top subunit B4, B3, B2, and
733 B1, respectively; red, top unit A.

734 **Figure 9**: Main stratigraphic interpretation of the S-wave seismic reflection and GPR data.
735 Correlation with resistivity and corrected tip resistance values from resistivity-CPTU as
736 well as S-wave interval velocity derived from seismic reflection velocity analysis is also
737 presented. The geotechnical information is also given wherever available.

738 **Figure 10**: Profile 2, resistivity inverted from gradient array, using a) smooth inversion,
739 and b) sharp boundary inversion. The interface in-between unit C and unit B (white line)
740 was used as the decoupled sharp boundary.

741 **Figure 11**: q_n compared with the interval S-wave velocities at a) boreholes 3, b) 7, c) 4, and
742 d) 5. The stratigraphic interpretation (horizontal dashed lines, top unit B4, yellow; top unit
743 B3, blue; top unit B2 green) as well as the sections corresponding to general slope changes
744 in q_n (horizontal black and orange lines) are also displayed.

Figure 12: Cross plot of q_n and Vs for a) boreholes 3, b) 7, c) 4, and d) 5. Blue, red and green colours correspond to the layers defined in Figure 12. The black lines represent the linear fit for each section and their respective correlation coefficients are given in Table 3.

Figure 13: S-wave seismic reflection profile 2 with net tip resistance estimated from S-wave seismic velocity within subunits B4 and B3 superimposed. The green, blue and yellow lines correspond to interpreted tops of units B2, B3, and B4. The orange line is the interpreted interface within unit B3 corresponding to slope change in q_n (orange line in Figure 11). Net tip resistance from boreholes 4 and 5 are also displayed with the same colour scale.

Figure 14: Relationship between water content and normalised small strain shear modulus for Hvittingfoss and previous studies.

757 **Table 1**: List of acronyms.

Acronym	Meaning
AGC	Automatic Gain Control
CPTU	Cone Penetration Testing with pore pressure measurements
CMP	Common MidPoint
ERT	Electrical Resistivity Tomography
G_{max}	Small-strain shear modulus
GPR	Ground Penetrating Radar
RPS	Rotary Pressure Sounding
Vp	P-wave velocity
Vs	S-wave velocity
q_t	Corrected CPTU tip resistance
q_n	Net CPTU tip resistance
s_u	Undrained Shear strength
s_{ur}	Undrained Remoulded Shear strength
ρ	Density

758

759 **Table 2**: Processing flowchart and corresponding parameters for S-wave seismic reflection data.

Processing Step	Parameters
SEG-2	SEG-2 file import
Cross-Correlation	Signal contraction: cross-correlation with pilot sweep
Subtractive Stack	Sum of correlated records with opposite sweep-signal polarities
Geometry Settings	CMP geometry binning
Elevation Statics	Source/receiver elevation-statics corrections for P01 only
Gain	Amplitude preserving analytical spherical-divergence correction of t^2
Deconvolution	Surface-consistent predictive deconvolution with 70-90 ms operator length, prediction lag of 5 ms and prewhitening of 0.1 %
Time Variant BP filter	Time-variant bandpass filter (zero-phase Ormsby filter), from 35-40-155-160 to 20-25-115-120 Hz
FK filtering	Dip filter varying along the profile to further suppress Love-wave energy
Mutes	Top and bottom mutes
Residual Statics / Velocity Analysis	Velocity analysis (every 10 m) performed recursively with residual-statics corrections
NMO	Normal-move out corrections using best fitting velocity field
Stacking	CMP gather stacking
Time-to-depth conversion	Time-to-depth conversion using smoothed velocity field

760

761 **Table 3**: Table summarizing the empirical factor for net tip resistance – Vs correlation, $q_n = a*Vs+b$, for each
762 CPTU along seismic lines and every layers. The last column indicates the correlation parameters for all the
763 CPTU and all the layers together.

	CPTU-02		CPTU-109		RCPTU-02		RCPTU-03		All	
	a	b	a	b	a	b	a	b	a	b
B4-MB3			2	424.6	3.36	336.6	4.94	85.9	3.37	225.06
MB3-B3	0.9	800	-7.7	3162	-9.5	3501	-2.2	1813		
B3-B2	21.3	-4022	35.2	-8837	22.4	-4749	20	-4185		

764

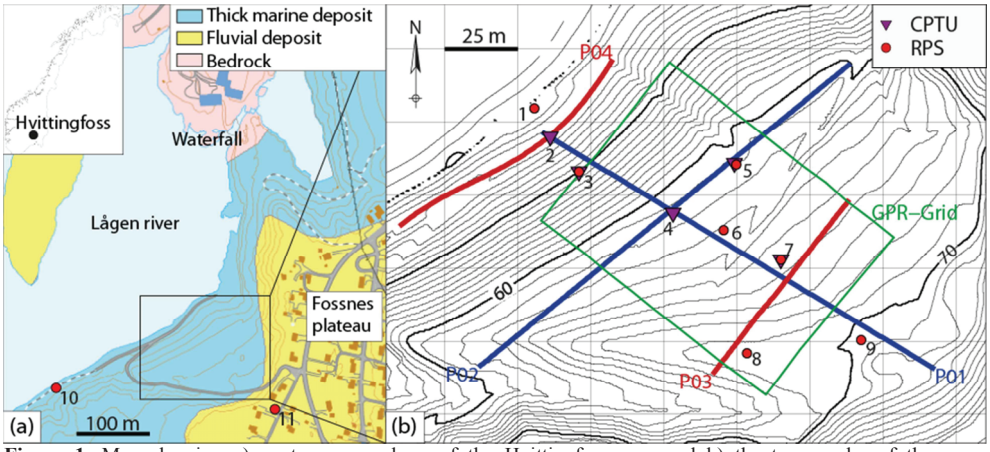

Figure 1: Map showing a) quaternary geology of the Hvittingfoss area and b) the topography of the investigation site, with location of geophysical measurements, blue lines for ERT and P-wave seismic, red and blue for S-wave seismic and green rectangle for GPR, as well as location of geotechnical data, red dots for rotary pressure soundings and purple triangles for CPTU tests.

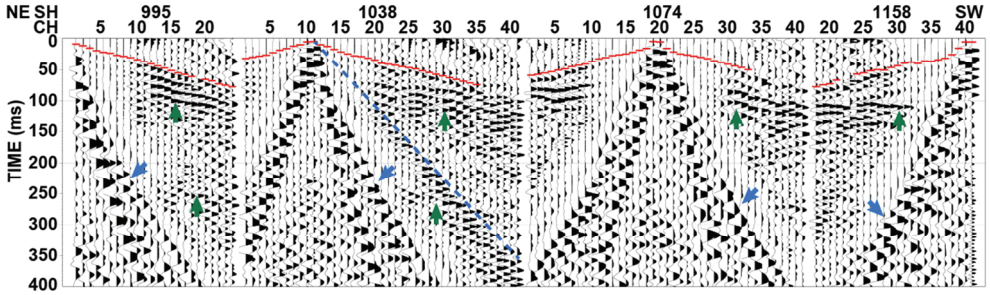

Figure 2: Selected P-wave seismic pre-processed record examples of profile 2. X axis corresponds to shot and channel number (4-m spacing). The dashed blue lines correspond to the theoretical gradient of 333 m/s air wave velocity, which is not much recorded. The first arrival corresponding to the refracted waves are also displayed on these records (red picks). The blue arrows point at surface-wave energy and the green ones point at reflected energy. For the sake of the display, a 350ms AGC is applied.

780
781
782 **Figure 3**: Pictures depicting S-wave seismic reflection acquisition using wheelbarrow mounted horizontal
783 seismic vibrator with landstreamer along the gravel path for profile 4.
784

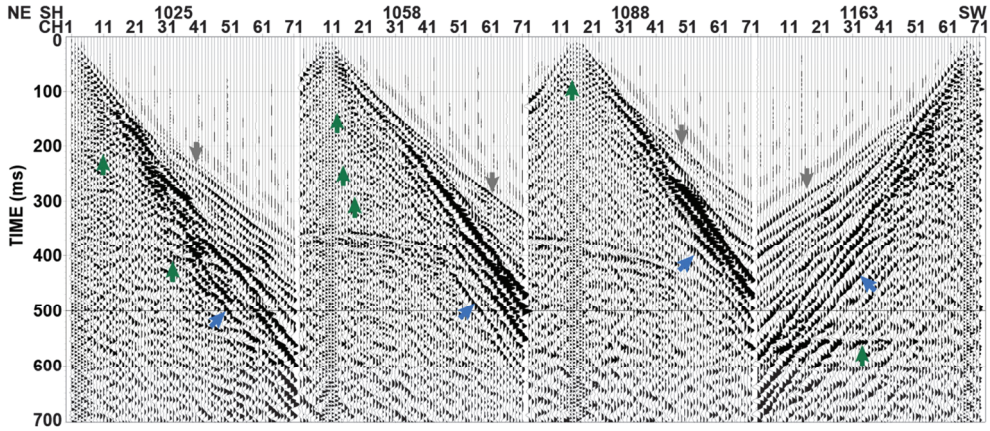

Figure 4: Selected S-wave seismic pre-processed record examples of profile 2. X axis corresponds to shot and channel number (2-m spacing). Strong surface-wave energy was recorded (blue arrows) and hides some of the important reflections (green arrows). The grey arrows point at refracted wave energy.

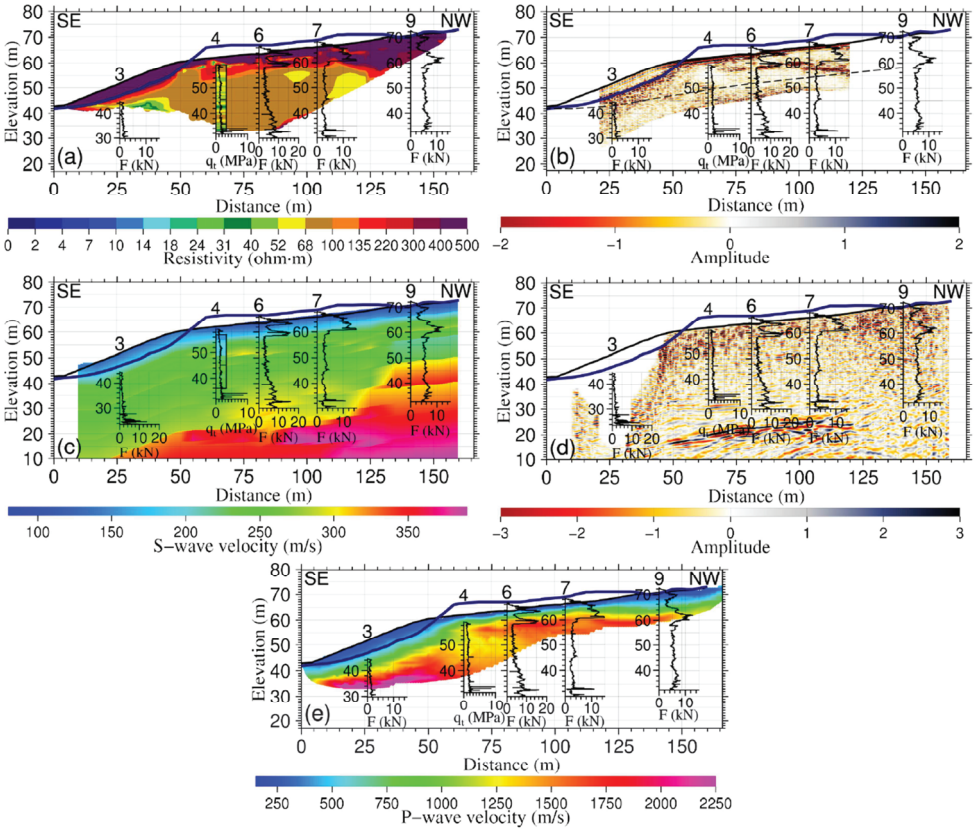

Figure 5: Profile 1, a) inverted resistivity from Gradient array, b) GPR profile extract from the depth converted GPR cube superimposed, c) S-wave interval velocity, d) depth converted S-wave seismic reflection, and e) P-wave velocity from seismic refraction tomography. One can notice the strong GPR reflection between the old (blue line) and new (black line) topography. Resistivity values as well as S-wave velocity from borehole 4 are also depicted with the same colour scale as for ERT and S-wave seismic respectively. The water table interpreted from GPR, seismic refraction and piezometer is also displayed in dashed line.

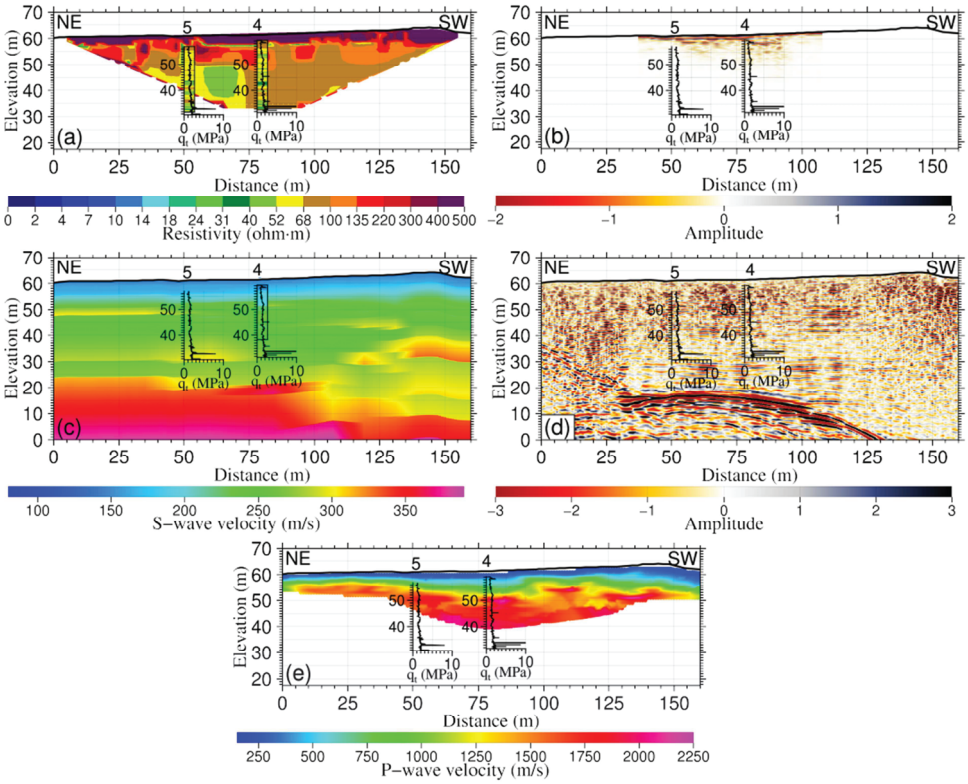

Figure 6: Profile 2, a) inverted resistivity from Gradient array, b) GPR profile extract from the depth converted GPR cube superimposed, c) S-wave interval velocity, d) depth converted S-wave seismic reflection, and e) P-wave velocity from seismic refraction tomography. Resistivity values from borehole 4 and 5 as well as S-wave velocity from borehole 4 are also depicted with the same colour scale as for ERT and S-wave seismic respectively.

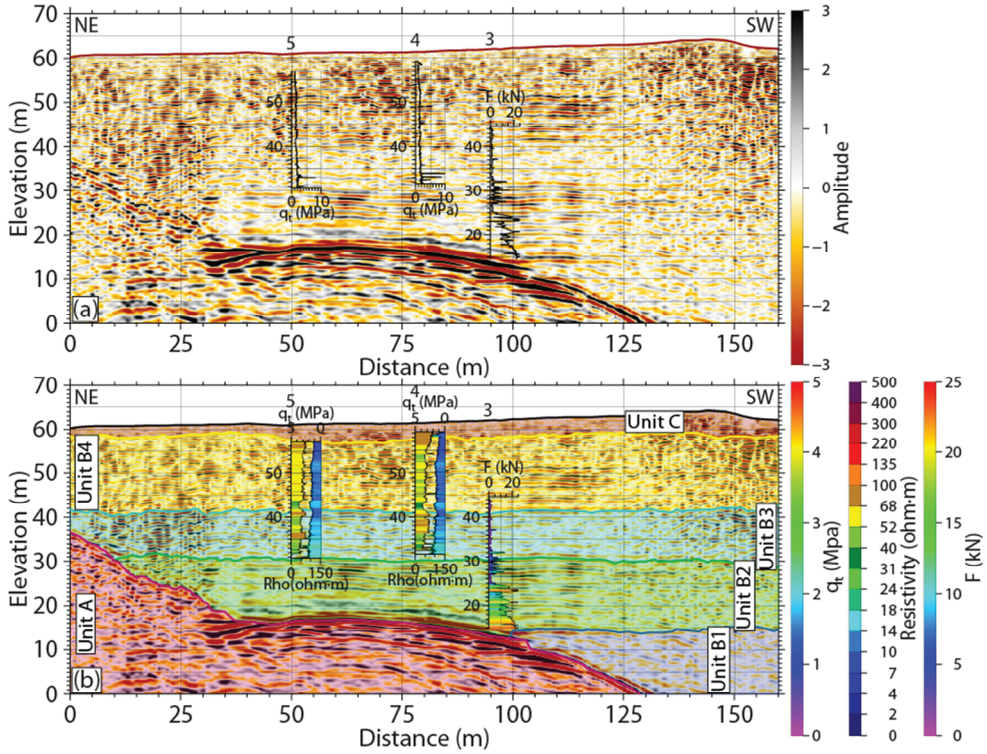

Figure 7: Profile 2, a) S-wave seismic reflection profile with borehole 3 (10 m offset), 4 and 5. The interpreted stratigraphy is superimposed on the S-wave seismic reflection profile and the corresponding layers are coloured in b). The resistivity values and the corrected tip resistance from boreholes 4 and 5, as well as the drilling resistance from borehole 3 are also depicted.

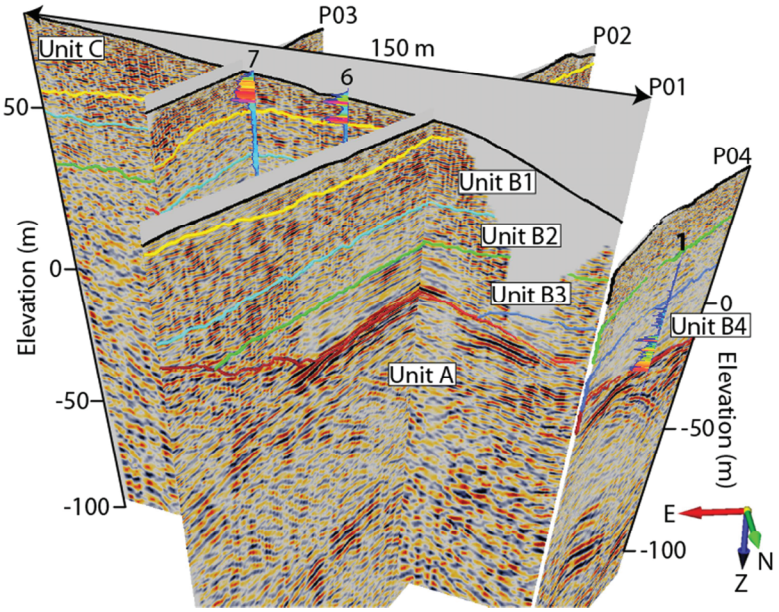

Figure 8: a) Pseudo 3D view of time-to-depth converted S-wave seismic reflection profiles and boreholes 1, 6, and 7. The interpreted top of units are also displayed; black, top unit C (actual topography); yellow, turquoise, green, and blue, top subunit B4, B3, B2, and B1, respectively; red, top unit A.

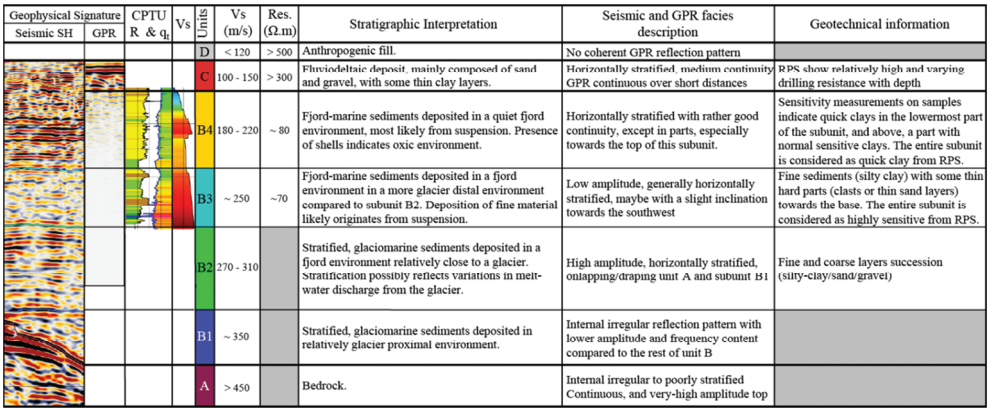

Figure 9: Main stratigraphic interpretation of the S-wave seismic reflection and GPR data. Correlation with resistivity and corrected tip resistance values from RCPTU as well as S-wave interval velocity derived from seismic reflection velocity analysis is also presented. The geotechnical information is also given wherever available.

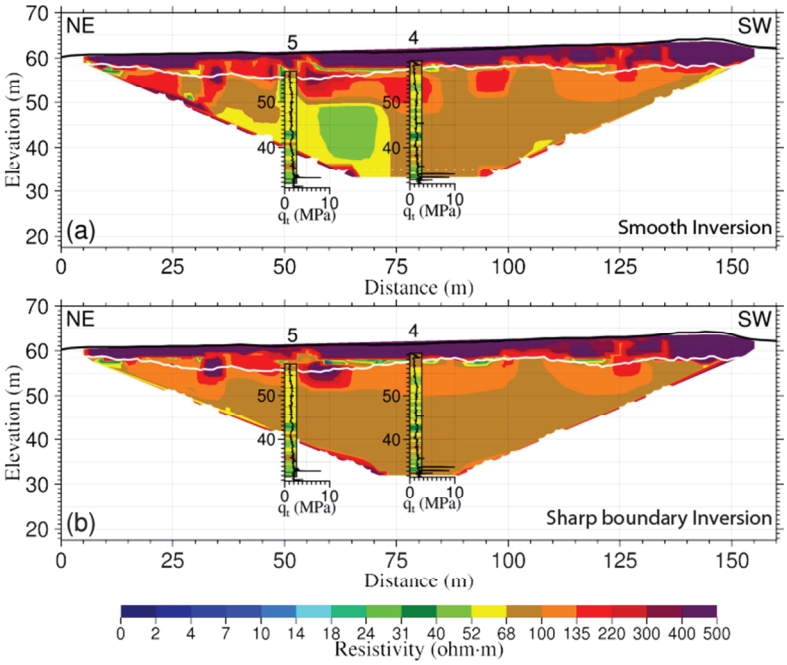

Figure 10: Profile 2, resistivity inverted from gradient array, using a) smooth inversion, and b) sharp boundary inversion. The interface in-between unit C and unit B (white line) was used as the decoupled sharp boundary.

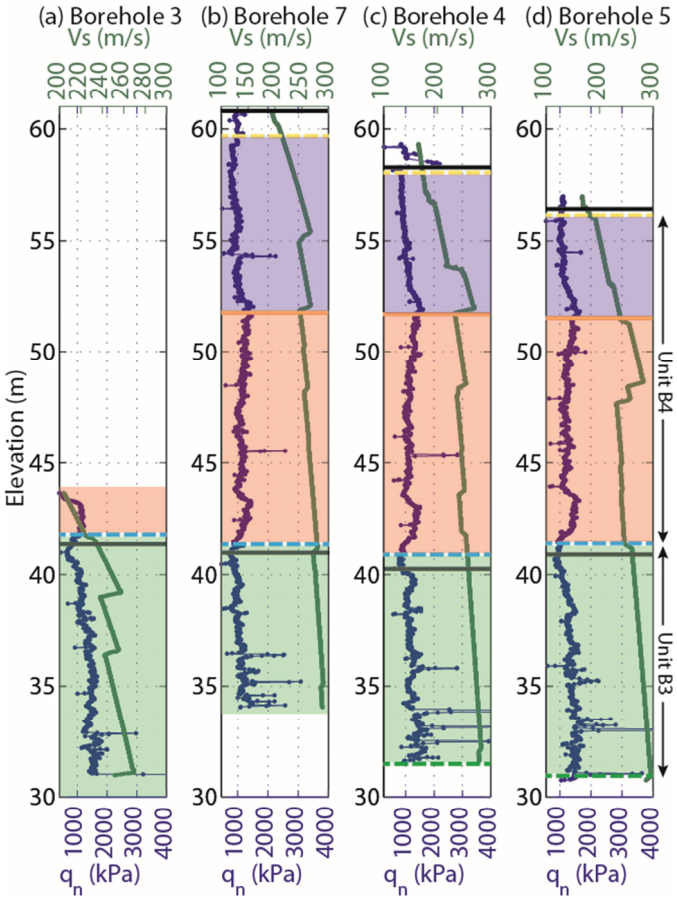

Figure 11: q_n compared with the interval S-wave velocities at a) boreholes 3, b) 7, c) 4, and d) 5. The stratigraphic interpretation (horizontal dashed lines, top unit B4, yellow; top unit B3, blue; top unit B2 green) as well as the sections corresponding to general slope changes in q_n (horizontal black and orange lines) are also displayed.

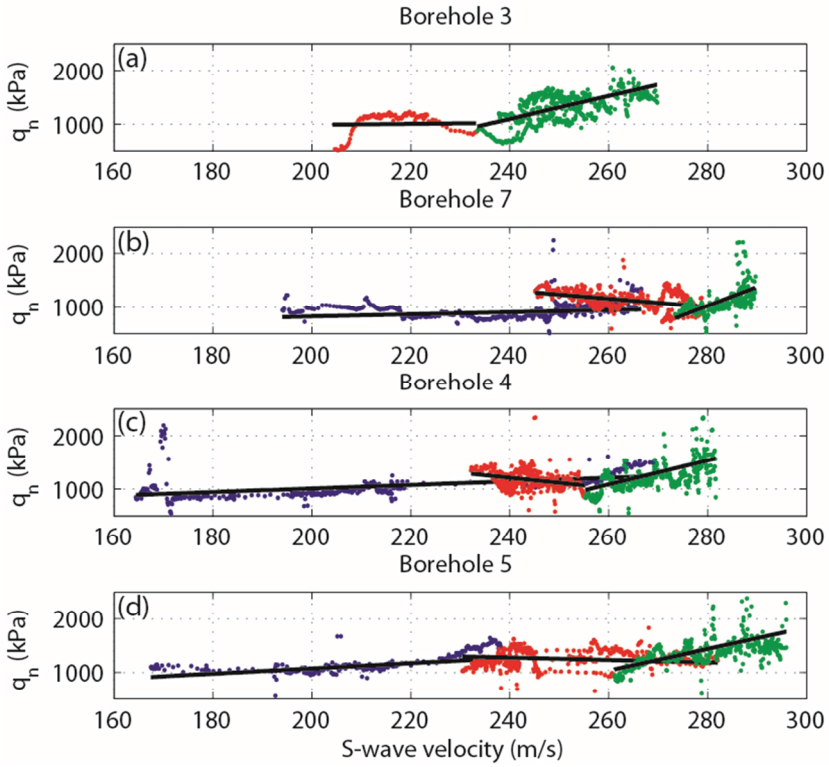

Figure 12: Cross plot of q_n and Vs for a) boreholes 3, b) 7, c) 4, and d) 5. Blue, red and green colours correspond to the layers defined in Figure 12. The black lines represent the linear fit for each section and their respective correlation coefficients are given in Table 3.

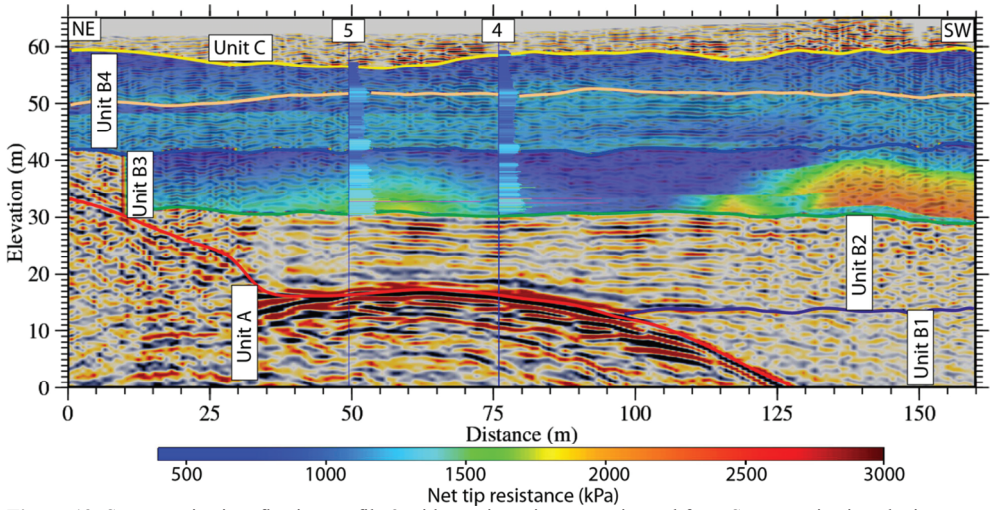

Figure 13: S-wave seismic reflection profile 2 with net tip resistance estimated from S-wave seismic velocity within subunits B4 and B3 superimposed. The green, blue and yellow lines correspond to interpreted tops of units B2, B3, and B4. The orange line is the interpreted interface within unit B3 corresponding to slope change in q_n (orange line in Figure 11). Net tip resistance from boreholes 4 and 5 are also displayed with the same colour scale.

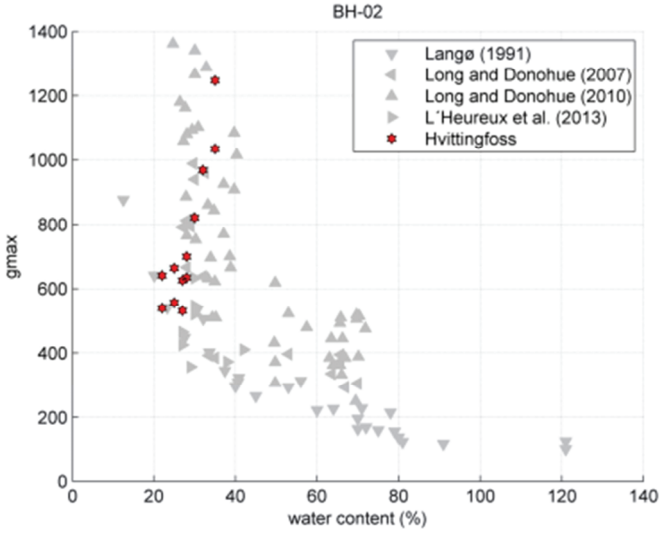

848
849 **Figure 14**: Relationship between water content and normalised small strain shear modulus for Hvittingfoss
850 and previous studies.

851

Paper IV

Joint inversion of surface-wave dispersion, P-wave refraction and apparent resistivity data

F. Garofalo, **G. Sauvin**, L.V. Socco, and I. Lecomte

Geophysics, In prep.

Extended Abstract I

Towards joint inversion/joint interpretation for landslide-prone areas in Norway – Integrating Geophysics and Geotechnique

G. Sauvin, S. Bazin, M. Vanneste, I. Lecomte, and A.A. Pfaffhuber

Near Surface Geoscience, Extended Abstract, 2012

E11

Towards Joint Inversion/Interpretation for Landslide-prone Areas in Norway - Integrating Geophysics and Geotechnique

G. Sauvin* (University of Oslo / ICG / NORSAR), S. Bazin (NGI), M. Vanneste (ICG / NGI), I. Lecomte (ICG / NORSAR) & A.A. Pfaffhuber (NGI)

SUMMARY

Quick clay may be described as highly sensitive marine clay that changes from a relatively stiff condition to a liquid mass when disturbed. Extended quick clay layers account for a lot of geo-hazards in Scandinavia and North-America and hence their occurrence and extent need to be mapped. Geophysical methods have been tested for small scale quick-clay mapping at a research site (Vålen) close to Oslo, Norway. By scrutinizing results from Electric Resistivity Tomography (ERT) and Multi-channel Analysis of Surface Waves (MASW) and integrating them with geotechnical borehole data with the help of a resistivity logging tool (RCPTu), we confirm the value for such integrated studies in for quick-clay hazard zonation. Geophysical investigations allow indeed interpolation in between limited borehole results and thus provide a more cost-efficient and extended result than with boreholes alone.

Introduction

Some of the most inhabited areas of Norway are located in potential quick-clay zones and hence large efforts are being taken to map their occurrence and extent. Quick-clay material originates from highly porous marine-clay in coastal environment deposited during the last glacial period. Due to isostatic rebound following deglaciation, the former marine clays lies currently above sea-level and have been exposed to fresh-water environment. Salt, which originally contributed to the bonding between the clay particles, may therefore have been leached from these materials by ground water and percolating surface water. If sufficient leaching of salt occurred, a highly sensitive or "quick" material may result. Quick-clay hazard zones have traditionally been mapped in Norway using geotechnical field investigations such as rotary pressure soundings, cone penetrating tests with pore pressure measurements (CPTu) and laboratory tests on undisturbed samples. The shape, extent and thickness of quick-clay areas govern the potential retrogressive slide area and detailed data are demanded by modern hazard management schemes. In this study, we focus on the area around the Vålen site, which has a documented history of quick-clay landsliding, the most recent event occurring in 1984. Several escarpments are visible in the area surrounding the site. The main objective was to characterize the quick-clays using multi-disciplinary geophysical techniques. In earlier studies, quick-clay mapping in Sweden and Norway was performed using mainly Electrical Resistivity Tomography (Ranka et al 2004; Dahlin et al. 2005; Solberg 2007) and only few Multichannel Analysis of Surface waves (Long and Donohue 2007). Integration of these geophysical methods together and along with geotechnical methods, such as CPTu, should be investigated further.

The Vålen quick-clay laboratory site

The Vålen site is located near the town of Vestfossen, approximately 65 km south-west of Oslo (Figure 1). As a marine-clay deposit in coastal, post-submarine area, this laboratory site of the Norwegian Geotechnical Institute (NGI) is subject to quick-clay landslides. Figure 1 shows probable quick-clay extent based on the Norwegian quick-clay hazard map derived from point-wise geotechnical investigations, i.e., cone penetration tests with pore pressure measurements (CPTu), CPTu with resistivity (R-CPTu) (Rømoen et al. 2010) and cores. Motivated by positive results obtained in similar area (Pfaffhuber et al. 2010), electrical resistivity tomography (ERT; electrode-based DC) and seismic measurements (Multichannel Analysis of Surface Waves; MASW) were performed summer 2010 to better constrain the whole geological setting. The expected quick-clay layers are targeted to check their geophysical/geotechnical response to the different measurement techniques adopted. The results presented here are now guiding new and more complete acquisitions to be carried out during spring-summer 2011, keeping in mind a multi-method approach for joint inversion and interpretation.

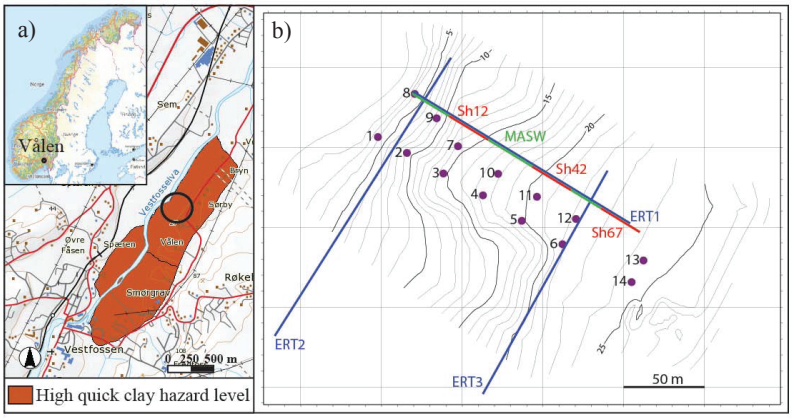

Figure 1 *a) Vålen location map (adapted from www.skreddnet.no) and b) site map with topography (1-m contour intervals), vertical soundings (CPTs; 1-14), standard electrode-based ERT (blue lines) and MASW profiles (green line with 3 shot spread superposed in red).*

Electrical Resistivity Tomography (ERT)

Three ERT profiles were first recorded using a Terrameter LS with four cables of 21 takeouts (64 active electrodes). A roll-along gradient configuration with 2-m (profile 1 and 3) or 4-m (profile 2) electrode spacing was used to acquire the data, leading to a total length of 160 m for profiles 1 and 3, and 200 m for profile 2.
The apparent resistivity and chargeability data were inverted in both data type with the standard Res2Dinv software (Loke, 2004) using L_1-norm inversion optimization. All inversions performed converged to RMS errors of less than 1.5 % within 7 iterations. The 2D ERT profiles were then combined to generate a pseudo 3D display (Figure 2).
A high-resistive 1-to-5-m thick layer can be identified on all profiles and interpreted as a dry crust surface layer. According to Solberg et al. (2008), resistivity values in the 10-80 Ω·m range may indicate quick-clay. This may therefore denote the presence of quick-clay as marked in Figure 2. Resistivity values in profile 1 suggest the presence of two distinct layers of quick-clay, one East that can also be observed on profile 3, and one West which is present on profile 2 and could correspond to a deeper lens of quick-clay. An approximately 10-m thick pocket of unleached marine clay may lie between the two layers of quick clay. These two quick-clay layers were already suggested by the geotechnical boreholes. All boreholes went down to the bedrock which is made of shale and has a resistivity range similar to unleached clay.

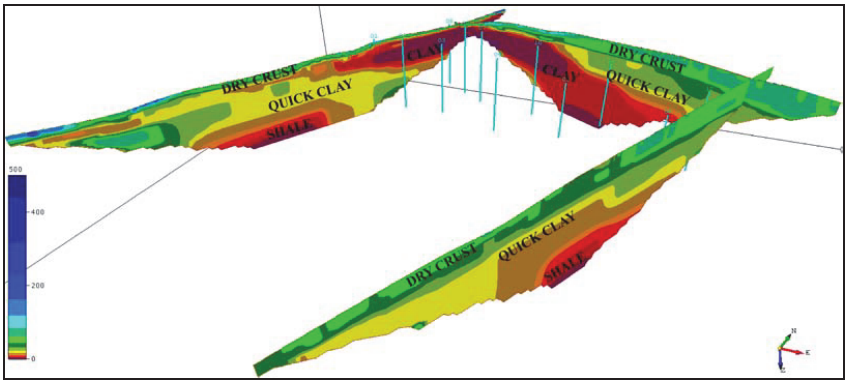

Figure 2 *Pseudo 3D representation of resistivity models with interpretation. Position and depth range of boreholes (down to bedrock) are represented as well. (generated with freeware OpendTect)*

Multichannel Analysis of Surface Waves

Seismic surface-wave data were recorded using a Geometrics Geode seismograph with 24 4.5-Hz vertical geophones and a 5-kg sledgehammer as seismic source. The survey was carried out in roll-along mode. The offset between the source and the nearest geophone was kept at 5 m, with a geophone spacing of 1 m, leading to a geophone spread of 23 m. Data were recorded from 67 shot positions with 2-m shot spacing, thus yielding a 132-m long 2D line (Figure 1). For each configuration, the shots were repeated twice and stacked on-site to improve the signal-to-noise ratio. The sampling interval was 0.25 ms, with a record length of 1 s. For each of the configurations, the dispersion curves were picked interactively using either a commercial software (SurfSeis; phase-velocity/frequency domain; Park et al., 1999) or MATLAB-based routines (frequency/wavenumber domain), and inverted with 2 different methods (Figure 3). For most parts of the profile, the fundamental Rayleigh mode is dominant. However, the data covering the south-eastern part of the line show both fundamental and higher modes.
The 1-D shear-wave velocity models are derived from the inversion of the dispersion curves using both an NGI inversion code, based on a modified Levenberg-Marquardt method for global minimization, and SurfSeis. All inversion performed with the NGI code converged rapidly, usually within 2 iterations, and with low uncertainty, the variation coefficient (standard deviation normalised

by the mean) being less than 2% above 10-m depth. The uncertainty increases considerably below 15 m. The fundamental Rayleigh mode alone was used in the inversion as it is typically solely present (shot 12 in Figure 3). Nevertheless, as noted earlier, multi-modal inversion should also be considered for some shots (shot 67 in Figure 3).

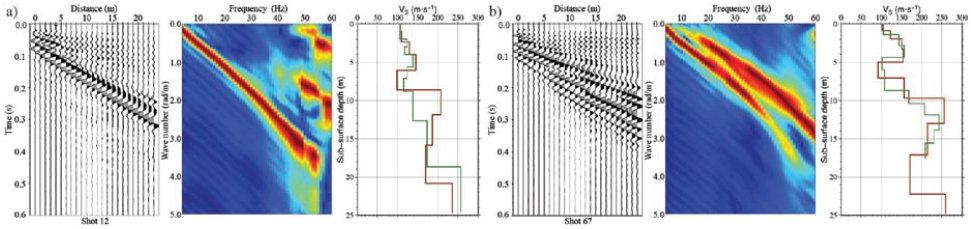

Figure 3 *From left to right, examples of raw (unprocessed), normalized traces, the corresponding dispersion curve in f-k domain and inverted V_s profile for shot indices 12, a) and 67, b) in Figure 1. Inversion results present soil models inverted using SurfSeis (red) and NGI code (green).*

Data integration

Even though the ERT and MASW sections alone give an indication of the likely geology, integration of the models is needed to disambiguate the interpretation. Moreover, R-CPTu and CPTu soundings along with soil laboratory tests and derived soil classifications need to be added for a complete geological/geotechnical interpretation of the resistivity and shear-wave velocity integrated model.

The interpreted quick-clay layers on Figure 4 were derived from CPT measurements 7 to 14. The sensitivity, indicating presence of quick-clay, can be evaluated from the slope of the penetration resistance curve, where the resistance remains constant over a distance or even drops with a negative slope by depth. This is explained by the collapsible nature of the quick-clay, along with an almost negligible component of added rod friction in the quick-clay zone. The soundings are located approximately 15 m South-West of the ERT profile and therefore this non-co-location may explain the slight difference in results, indicating a lateral variability of the soil. Even though not exactly at the same location, the resistivity from R-CPTu measurement shows good correlation with the inverted resistivity from the ERT (Figure 4).

As shown in previous studies in similar areas (Long and Donohue, 2007), shear-wave velocities, as measured using MASW approach for interpreted quick-clay zones from resistivity model, and soundings are slightly less (up to 17 $m \cdot s^{-1}$) compare to those for unleached clay.

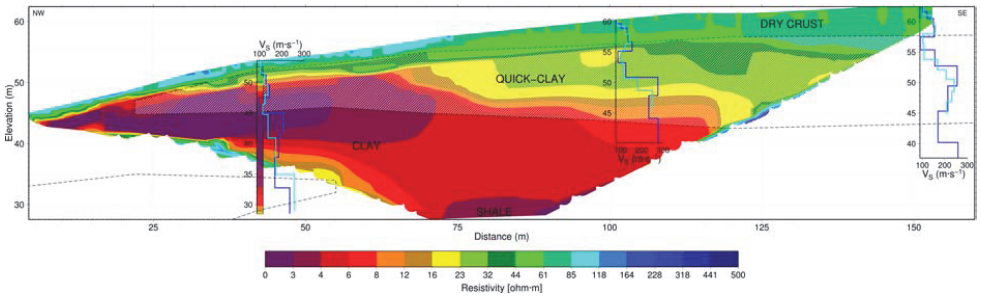

Figure 4 *Profile 1: ERT inverted resistivity (same colour scale as Figure 2) with inverted 1D V_s profiles corresponding to shot positions 12, 42 and 67 (Figure 1). Inverted V_s profiles are located in the middle of the shot-geophones array. Shot position 12 corresponds to borehole 7 which includes R-CPT measurements, represented in the black box with the same colour scale as for the ERT. The shade areas delineated by the dashed lines are the interpreted quick-clay layers from geotechnical measurements 7 to 13. Note that this line of soundings is not exactly at the same location as the ERT profile (Figure 1).*

Conclusions

Based on ground resistivity and shear-wave velocity models derived from ERT and MASW, combined with limited CPTu and via the R-CPT data, we confirmed the value and importance of surface geophysics for quick-clay hazard studies.

- Electrical resistivity is a suitable indicator for quick-clay if calibrated to sparse conventional site investigation soundings and laboratory tests.
- Even though the resolution limit of the MASW approach is reached, shear-wave velocities for quick-clay appear to be slightly less than those measured for non quick-clay and may help to discriminate in case of ambiguities. However shear-wave velocity derived from high-resolution seismic reflection and seismic-CPT would be needed to confirm MASW shear-wave velocities.

When geotechnical data are available at the same site, they are usually used for an a-posteriori comparison of the results rather than introducing them as a-priori information in the inversion process. In general, borehole tests are considered more reliable than surface-based geophysical surveys, even though the uncertainties of the final results are often similar. Therefore, joint-inversion of the various soil parameters with ground-truthing should be tried in order to derive more constrained models.

Acknowledgements

We thank Marianne Lanzky Kolstrup (NGI/UiO) and Amandine Sergeant-Boy (NORSAR/EOST) for their help on the field and the University of Oslo for some of the equipment. G. Sauvin thanks the funding partners of his PhD: the Norwegian Public Roads Administration, the Norwegian National Rail Administration, the Norwegian Water Resources and Energy Directorate and International Centre for Geohazards. This is contribution no. 358 for the International Centre for Geohazards (ICG).

References

Dahlin, T., Larsson, R., Leroux, V., Larsson, R. and Rankka, K. [2005] Resistivity imaging for mapping of quick clays for landslide risk assessment. *I: Proceedings of 11th Annual Meeting EAGE - Environmental and Engineering Geophysics*, Palermo, Italy, 4-7 September, 2005. A046

Loke, M.H. and Barker, R.D. [1996] Rapid least-squares inversion of apparent resistivity pseudosections by a quasi-Newton method. *Geophysical Prospecting*, **44**, 131-152 .

Long, M. and Donohue S. [2007] In situ shear wave velocity from multichannel analysis of surface waves (MASW) tests at eight Norwegian research sites. *Canadian Geotechnical Journal*, **44**, 533-544.

Park, C.B., Miller, D.M. and Xia, J. [1999] Multichannel Analysis of surface waves. *Geophysics*, **64**, no. 3, 800-808.

Pfaffhuber, A. A., Bastani, M., Cornée S., Rømoen M., Donohue S., Helle T. E., Long M., O'Connor P. and Persson L. [2010] Multi-method high resolution geophysical and geotechnical quick clay mapping. *Near Surface - 16th European Meeting of Environmental and Engineering Geophysics* Zurich, Switzerland, 6-8 September 2010. 9161

Ranka, K., Andersson-Sköld, Y., Hultén, C., Larsson, R., Leroux, V. and Dahlin, T. [2004] Quick clay in Sweden. Swedish Geotechnical Institute, Report 65.

Rømoen, M., Pfaffhuber, A. A., Karlsrud, K. and Helle, H.E. [2010] Resistivity on marine sediments retrieved from RCPTu soundings: a Norwegian case study. *CPT'10: 2nd international symposium on Cone Penetration Testing* Huntington Beach, California, USA.

Solberg, I.L. [2007] Geological, geomorphological and geophysical investigations of areas prone to clay slides: Examples from Buvika, Mid Norway. *PhD thesis*. Departement of Geology and Mineral Resources Engineering, Norwegian University of Science and Technology, 213pp.

Extended Abstract II

Quick-clay landslide-prone grounds in Norway and Sweden: a complex problem requiring a combined geophysical and geotechnical approach.

G. Sauvin, I. Lecomte, S. Bazin, J.-S. L'Heureux, and A. Malhemir

EAGE, Workshop: *Integrated Geosciences for Subsurface Instabilities, Offshore and Onshore*, Extended abstract, 2012

Quick-clay landslide-prone grounds in Norway and Sweden: a complex problem requiring a combined geophysical and geotechnical approach.

Guillaume Sauvin (Oslo Univ./ICG/NORSAR), Isabelle Lecomte (ICG/NORSAR/Oslo Univ.), Sara Bazin (NGI), Jean-Sébastien l'Heureux (ICG/NGU) & Alireza Malehmir (Uppsala Univ.).

SUMMARY

Quick-clay sliding occurs in formerly glaciated coastal areas in, e.g., Norway, Sweden and Canada. The soil was originally deposited in shallow marine environments which emerged following isostatic rebound and fall of the relative sea level since the last glacial maximum. Long-term leaching of salt, due to groundwater flow and percolating surface water, affects clay-particles bonding and makes the soil highly susceptible to failure when disturbed. We review the properties of quick-clays in order to define a suitable, integrated and multi-disciplinary approach to improve identification and mapping of quick-clay areas. Though electrical resistivity tomography is actually the geophysical method of choice, it is paramount to combine a range of geophysical and geotechnical approaches for a better assessment of a given quick-clay site. The discussed integrated approach is here presented for 2 Norwegian and 1 Swedish quick-clay sites. The collected data and preliminary site characterization will illustrate the high diversity of quick-clay grounds as well as the complexity related to an integrated approach.

Workshop 04
Integrated Geosciences for Subsurface Instabilities, Offshore and Onshore.
Convenors: Isabelle Lecomte (ICG / NORSAR), Stéphane Garambois (LGIT / University of Grenoble) & Maarten Vanneste (ICG / NGI).
Sunday 3 June, 09:00 – 17:00 hrs

Introduction

Quick-clay sliding occurs in formerly glaciated areas in, e.g., Norway, Sweden and Canada. Quick-clays are characterized by very high sensitivity and low un-drained remoulded shear strength. The soil was originally deposited in marine environments which emerged following isostatic rebound and fall of the relative sea level since the last glacial maximum. Long-term leaching of salt, due to groundwater flow and percolating surface water, affects clay-particles bonding and makes the soil highly susceptible to failure when disturbed (e.g., human activity, erosion). Due to the presence of extensive quick-clays in populated areas, particular hazard management schemes are a necessity.

We review the properties of quick-clays in order to define a suitable, integrated and multi-disciplinary approach to improve identification and mapping of quick-clay areas. Though ERT is actually the geophysical method of choice (due to conductivity being mostly related to salt content; Solberg et al., 2011), it is paramount to combine a range of approaches (e.g., adding refraction tomography, MASW, GPR, etc), as well as geotechnical data (in-situ measurements using CPTu, SCPTu and RCPT; laboratory tests) for a better assessment of a given site. Geophysics is needed to both judiciously locate geotechnical boreholes for ground truth and fill the gaps between them, moving towards 2D, pseudo-3D or 3D site characterization for quick-clays, and possibly to 4D, i.e., monitoring. The discussed integrated approach is here presented for 2 Norwegian and 1 Swedish quick-clay sites. The collected data and preliminary site characterization illustrate the high diversity of quick-clay grounds as well as the complexity related to an integrated approach.

Quick clays

Quick clays are found in areas which were once glaciated during the Pleistocene epoch (165000 to 10000 years ago). These areas are characterized by isostatic uplift which took place after the retreat of ice. The actual Norwegian definition of quick clay is that the sensitivity (s_t, i.e, ratio of undrained shear strength s_u and un-drained remoulded shear strength s_{ur}) must exceed 30 and that the remoulded shear strength must be less than 0.5 kPa. The Swedish definition is slightly different; sensitivity has to be over 50 and remoulded shear strength below 0.4 kPa (Rankka et al., 2004). The development of very high sensitivity is usually the result of processes that have taken place after the deposition of the clay.

For the development of quick clay it is generally agreed that the sediment must have a flocculated structure with a high void ratio. This structure is the normal state in fine-grained post-glacial sediments which have accumulated in marine or brackish water where silt and clay-sized particles settle rapidly together to form flocculated high void ratio sediments. A similar - though not as random - flocculated structure develops under lacustrine conditions if the cation-exchange sites are dominated by divalent rather than monovalent cations. These freshwater sediments alternate silt-rich and clay-rich layers with a high degree of flocculation in the clay-rich layers. Under both salt and freshwater conditions, high concentration of suspended particles entering the water body encourages flocculation. Sediments composed of low-activity minerals and having a flocculated structure have a higher void ratio and hence higher water content than would similar sediments having an oriented structure. They also have a greater degree of resistance to change in water content if environmental conditions change.

The leaching of flocculated marine clays will only induce a minor decrease in void ratio compared with the one that occurs when the structure is completely broken down to allow particle orientation. This flocculated, high void ratio structure is essential for the development of quick-clay because it provides for the maintenance of an essentially constant undisturbed strength and constant water content while other changes which decrease the remoulded strength are occurring. Leaching of the salt by soft water (higher amount of monovalent ions relatively to divalent ions) induce large diffuse double layers which imply larger repulsive forces between the particles. After remoulding, these forces will prevent flocculation of the clay particles. This reduces the remoulded shear strength and increases the sensitivity of the clay. If the sediment can consolidate in response to change, and thereby

decreases its water content and increases its remoulded strength, quick-clay behaviour cannot develop. Models for explaining the development of quick clays must therefore invoke mechanisms which will both increase the ratio between the undisturbed and remoulded strengths, and provide for a remoulded strength less than 0.5 kPa. Proposed mechanisms include leaching, dispersing agents, cementation, and the special characteristics of finely ground primary minerals (Rosenqvist, 1978).

Test site investigations

Two Norwegian sites and a Swedish one will be presented, but the latter site (near Göta river, south-West Sweden) is not detailed in the present abstract and can be found instead in Malehmir (2012; this conference), who especially emphasizes the use of reflection seismic in that case (Figure 1). Among the 2 Norwegian sites, Hvittingfoss is located 80 km south-west of Oslo and Rissa 40 km north-east of Trondheim (Figure 2). Hvittingfoss has been mitigated for quick-clay risk by removing part of the sediments in the upper part of the area and adding it onto the slope. Various geotechnical measurements (cone penetration testing undrained – CPTu; core sampling with laboratory testing, pore-pressure measurements, etc) are available for both sites and provide point-wise indication of sensitive clays. In order to fill in the gap between wells, to gain information on the quick-clay spatial extent, and to better constrain the whole geological setting, electrical resistivity tomography (ERT; electrode-based DC) and seismic measurements (Multichannel Analysis of Surface Waves – MASW - and refraction seismic tomography) were performed summer 2011. The expected quick-clay layers are targeted to check their geophysical/geotechnical responses to the different selected measurement techniques.

a) 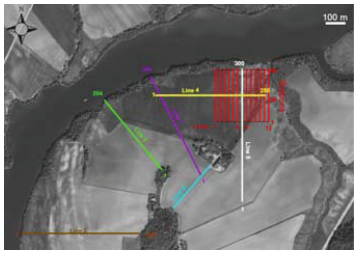

b) 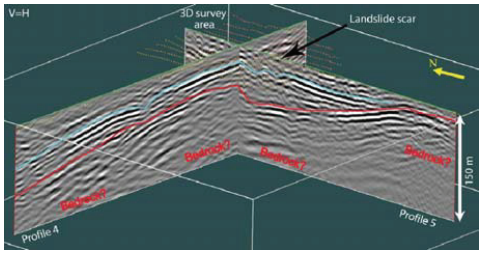

Figure 1 *Swedish site: a) Location near Göta river. b) P- reflection seismic (Malehmir, 2012).*

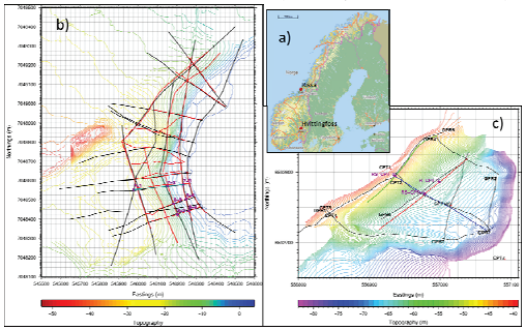

Figure 2 *Norwegian sites: a) Location map. Rissa b) and Hvittingfoss c) site maps with topography and location of vertical soundings, ERT profiles, MASW- and refraction-seismic profiles.*

Methods

2D resistivity measurements were carried out (Terrameter LS; ABEM). Roll-along Gradient configuration with electrode spacing ranging from 2- to 5-m was used. The apparent resistivity data was inverted (Res2Dinv) using L1-norm inversion optimization. Inversions performed converged generally to RMS errors of less than 5 % within 7 iterations. The 2D ERT profiles were then combined to generate pseudo-3D displays (Figures 3 and 4).

Two types of seismic measurements were carried out: MASW to retrieve S-wave velocities and P-wave refraction tomography to retrieve P-wave velocities. Seismic data were recorded with a 5-kg sledge-hammer as seismic source, 24 4.5-Hz vertical geophones, a sampling interval of 0.25 ms, and a record length of 2 s for both surface-wave and refracted-wave investigations. The surface-wave survey was carried out in roll-along mode. The offset between the source and the nearest geophone were 5 and 9 m, with a geophone spacing of 1 m. For each of the configurations, the dispersion curves were picked and inverted to 1-D shear-wave profiles using commercial software (SurfSeis). Refraction seismic was also acquired in roll-along mode. The geophones were set every 4 m along each profile and seismic shots were fired every 4 m. Data processing, picking of first-arrival traveltimes and their inversion were performed using commercial software (VISTA and REFLEXW).

As EM energy is rapidly attenuated in clayey sediments, GPR is usually not considered of much use in quick-clay sites. However, GPR was used in Hvittingfoss and Rissa to map the coarse-grained sediment (sand/gravel) deposits on top of the clay and/or shallow embedded layers. Presence of such permeable layers, within and/or on top of the clay greatly influences the groundwater flow, and therefore the potential leaching of the salt from the clay. A non-shielded 50-MHz rough-terrain antenna (RTA; Malå) was used for profiling, while a standard 50-MHz non-shielded antenna was used for CMPs. Several positions were chosen for CMP acquisition in order to better constrain velocity.

Results and discussion

Resistivity measurements allow first for structural interpretation. Evaluation of bedrock depth and dry-crust thickness, detection of underlying coarse-grained sediment and thickness of clay layers can be interpreted. All these structural information help localising potential zones of leaching. But the main advantage of resistivity in quick-clay studies is its ability to potentially discriminate leached clays from un-leached clays. Indeed, as the salt concentration is lower in leached clays, the resistivity is then higher than in the corresponding un-leached clays. According to Solberg et al. (2011), a first-order classification of resistivity is as follow: un-leached clay deposits: 1–10 Ωm; leached clay deposits, possibly quick: 10–100 Ωm; dry-crust clay deposits and coarse sediments: >100 Ωm.

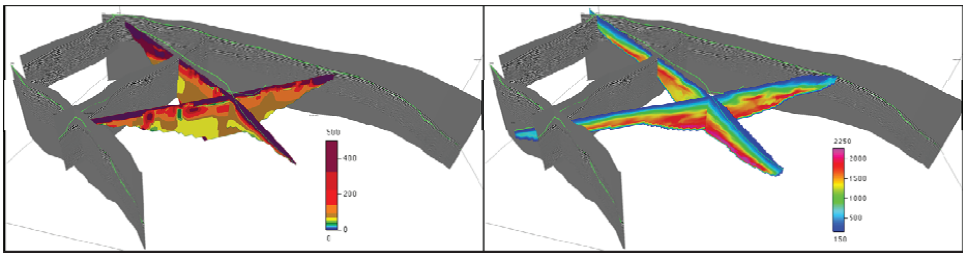

Figure 3 *Hvittingfoss: 3D plots of resistivity (left) and P-wave velocity (right) profiles, together with depth converted GPR profiles. The green horizon corresponds to the topography prior to remediation.*

P-wave and S-wave velocity profiles derived from seismic refraction tomography and MASW, respectively, also provide structural information that may be used to evaluate leaching in the clay layers. As the clay fabric of highly sensitive clay does not differ from normal clay, P-wave velocities cannot help discriminate between normal and quick-clay. Nonetheless, P-wave velocity fluctuations within a clay layers could indicate variation in consolidation, which, if too high, prevent the development of quick-clay. As the main difference between normal clay and high-sensitive clay lies in the clay particles bonding difference (weak bonds in case of sensitive clays), slight variation of S-wave velocities is to be expected (lower S-wave velocity for sensitive clays). This weak clay particle bonding could also potentially imply higher S-wave attenuation. Moreover, structural information derived from seismic investigations should help constraining ERT inversions, in order to retrieve resistivity variations within the clay layers alone and therefore, better constrain the resistivity response to salt concentration fluctuation.

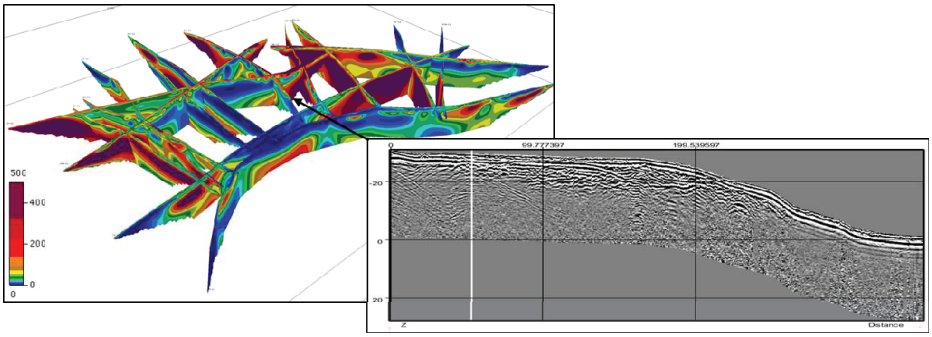

Figure 4 *Rissa site: 3D plot of resistivity profiles and example of one depth-converted GPR profile.*

Conclusions

The study of the genesis of quick clays should allow evaluating the potential of various geophysical methods for their mapping and characterisation. Clays deposited in marine environment exhibit a flocculated structure with high void ratio, which is a pre-requisite for the development of high sensitivity as it allows for high un-remoulded shear strength. As this flocculated structure is necessary but not sufficient for quick-clay formation, we need to discriminate normal-flocculated clays from high-sensitive ones. The extension of the electrical double layers around clay particles should be high enough to prevent the particles to re-flocculate at remoulding. Extension of the double layer is dependent on the ion composition and concentration in the pore water. Therefore, marine clay that has been leached from their salt could potentially become "quick". As shown in the site investigations described above, structural information retrieved from geophysical measurement may help locating preferential leaching paths, depending on bedrock topography, presence of underlying and/or embedded coarse-grained sediments and thickness of the clay layers. Resistivity variations within clay layers could also reflect the variation of salt concentration in the pore water. Moreover, high zeta-potential induces weak bonding of clay particles that could potentially lead to S-wave velocity decrease in leached clays. This study is on-going.

Acknowledgements

The authors thank N. C. Meyer, N. Langet, S. Tissot, C. Maskrey, H. Akerholt, T. Overskeid and K. Petrus for their help in the field, and the University of Oslo for some of the equipment. G. Sauvin thanks the funding partners of his PhD: the Norwegian Public Roads Administration, the Norwegian National Rail Administration, the Norwegian Water Resources and Energy Directorate and the International Centre for Geohazards (ICG). SEG, with its "*Geoscientists-Without -Border*" program, is thanked for funding the Swedish project. This is ICG contribution no. 384.

References

Rankka, K., Andersson-Sköld, Y., Hulten, C., Larsson, R., Leroux, V., and Dahlin, T. [2004] Quick clay in Sweden. *Swedish Geotechnical Institute*, Report 65.

Malehmir, A., [2012] Ultra high-resolution reflection seismic imaging of quick-clay landslides in south-west Sweden. *Extended Abstract, 74$_{th}$ EAGE Conference & Exhibition*, Copenhagen, C037.

Rosenqvist I.T. [1978] A general theory for the sensitivity of clays. *In Proc. Interdisciplinary Conf. Mechanisms of Deformation and Fracture*, Luleå 1, 258-262.

Solberg, I.L., Hansen, L., Rønning, J.S., Haugen, E., Dalseg, E., Tønnesen, J.F. [2011] Combined geophysical and geotechnical approach to ground investigations and hazard zonation of a quick clay area, Mid Norway. *Bull. Eng. Geol. Environ., **71**, 119-133*.